R-1035

AD 607245

# DAVIDSON LABORATORY

DDC
RECEIVED
OCT 26 1964
DDC-IRA B

2 OF 3
COPY $.5.00
FICHE $.1.00
182p

REPORT 1035


STEVENS INSTITUTE OF TECHNOLOGY

CASTLE POINT STATION
HOBOKEN, NEW JERSEY


## ESTIMATION OF STABILITY DERIVATIVES AND INDICES OF VARIOUS SHIP FORMS, AND COMPARISON WITH EXPERIMENTAL RESULTS

by


Winnifred R. Jacobs


September 1964

R-1035

DAVIDSON LABORATORY

REPORT 1035

September 1964

# ESTIMATION OF STABILITY DERIVATIVES AND INDICES OF VARIOUS SHIP FORMS, AND COMPARISON WITH EXPERIMENTAL RESULTS

by

Winnifred R. Jacobs

Prepared for
Bureau of Ships Fundamental Hydromechanics
Research Program (S-R009-01-01)
Administered by David Taylor Model Basin
Contract Nonr 263(57)
DL Project 2803/063



Approved

Stavros Tsakonas

Stavros Tsakonas, Chief
Fluid Dynamics Division

ix + 23 pp.
4 figures
6 appendices (11 tables, 62 figures)

## ABSTRACT

The analytical method of Ref. 1 for estimating stability derivatives, and hence stability on course, which combines Albring's empirical modifications of simplified flow theory with low aspect-ratio wing theory, is extended to take into consideration the effects on course stability of higher aspect-ratio fins as well. The method, which had been applied in the earlier report to a family of eight hulls of 0.5 block coefficient, is tested further by application to eight Series 60 forms differing in block coefficient as well as in beam, draft, and displacement — with and without rudders; to an extreme vee modification of a Series 60 model; and to three other forms — a Mariner Class model, a destroyer, and a hopper dredge. Comparison with experimental results shows that the values of stability derivatives and indices determined by the analytical method are of the right orders of magnitude and indicate correct trends. Application to a variety of ship forms has demonstrated that the method can predict relative effects of changes in the geometry of a ship form, as well as the effects of changes in skeg and rudder area.

Keywords: Hydrodynamics, Maneuvering, Controllability

## TABLE OF CONTENTS


| | |
|---|---|
| Abstract | iii |
| Nomenclature | vii |
| Introduction | 1 |
| The Analytical Method | 4 |
| Assumed Stability Derivatives for Hulls without Deadwood or Fins | 4 |
| Assumed Stability Derivatives for Hulls with Large Areas of Deadwood Aft | 7 |
| Changes in Stability Derivatives Due to Adding or Subtracting Fins of Aspect Ratio Equal to or Greater than Unity | 9 |
| The Stability Indices | 10 |
| Presentation and Discussion of Results | 13 |
| 840 Series Hulls | 13 |
| Series 60 Hulls | 14 |
| Extreme Vee Modification | 15 |
| Mariner Class Hull | 16 |
| Destroyer Model | 16 |
| Hopper-Dredge Models | 17 |
| Course Stability Dependence on Hull Geometry | 17 |
| Conclusion | 20 |
| References | 22 |
| Figures (1 through 4) | |
| Appendix A — 840 Series Hulls | |
| Appendix B — Series 60 Hulls | |
| Appendix C — Extreme Vee Modification of Series 60 Model 1 developed at the University of Michigan | |
| Appendix D — Mariner Class Hull | |
| Appendix E — Destroyer Model | |
| Appendix F — Hopper-Dredge Models | |

## NOMENCLATURE

| | |
|---|---|
| $A$ | profile area of wing or hull, $ft^2$ |
| $AR$ | aspect ratio of wing |
| $B$ | beam, ft |
| $b$ | local beam, ft |
| $C_L$ | lift coefficient based on profile area |
| $C_s$ | two-dimensional lateral added mass coefficient (sectional inertia coefficient) |
| $\bar{C}_s$ | average $C_s$ over the hull |
| $D'_o = \dfrac{R_f + R_r}{\frac{\rho}{2} U^2 \ \ell H}$ | total resistance coefficient of the hull |
| $F$ | force, lb |
| $F'_y = \dfrac{F_y}{\frac{\rho}{2} U^2 \ \ell H}$ | measured lateral force coefficient |
| $g$ | acceleration of gravity |
| $H$ | maximum draft, ft |
| $h$ | local draft, ft |
| $h_f$ | maximum fin height, ft |
| $I_o$ | moment of inertia of hull, $lb\text{-}ft\text{-}sec^2$ |
| $I_z$ | added moment of inertia of entrained water (see text), $lb\text{-}ft\text{-}sec^2$ |
| $k_1$, $k_2$, $k'$ | Lamb's coefficients of accession to inertia; longitudinal, lateral, and rotational |

| | |
|---|---|
| $L$ | lift, lb |
| $L' = \dfrac{L}{\frac{\rho}{2} U^2 \ell H}$ | lift coefficient based on area $\ell \cdot H$ |
| $\ell$ | length, ft |
| $m_o = \dfrac{\Delta}{g}$ | mass of hull, slugs |
| $m_o' = \dfrac{m_o}{\frac{\rho}{2} \ell^2 H}$ | hull mass coefficient |
| $m_1' = k_1 \; m_o'$ | longitudinal added mass coefficient |
| $m_2'$ | lateral added mass coefficient (see text) |
| $m_x' = m_o' + m_1'$ | longitudinal virtual mass coefficient |
| $m_y' = m_o' + m_2'$ | lateral virtual mass coefficient |
| $m_z'$ | rotational added mass coefficient (see text) |
| $N$ | yawing moment, lb-ft |
| $N' = \dfrac{N}{\frac{\rho}{2} U^2 \ell^2 H}$ | yawing moment coefficient |
| $n_z' = \dfrac{I_o + I_z}{\frac{\rho}{2} \ell^4 H}$ | virtual moment of inertia coefficient |
| $R$ | radius of turning circle, ft |
| $R_f$ | frictional resistance, lb |
| $R_r$ | residual resistance, lb |
| $r' = \dfrac{\ell}{R}$ | dimensionless angular velocity |
| $s = \dfrac{Ut}{\ell}$ | dimensionless distance along the path of the center of gravity of the hull |
| $t$ | time, sec |
| $U$ | velocity of the center of gravity of the hull, ft/sec |

| | |
|---|---|
| $x, y, z$ | coordinate axes fixed in the hull with origin at the center of gravity |
| $\bar{x}$ | longitudinal distance from LCG, of center of gravity of lateral added mass, ft |
| $x_p$ | longitudinal distance from LCG, of center of pressure at which lateral force Y acts, ft |
| $x_S$ | assumed longitudinal distance from LCG, of center of pressure of tail surface or skeg, ft |
| $x_s$ , $x_b$ | x-coordinates of stern and bow, respectively |
| $Y$ | lateral hydrodynamic force, lb |
| $Y' = \dfrac{Y}{\frac{\rho}{2} U^2 \ell H}$ | lateral hydrodynamic force coefficient |
| $\beta$ | yaw angle or drift angle |
| $\delta$ | rudder angle |
| $\Delta$ | displacement of hull, lb; also increment |
| $\rho$ | mass density of the fluid, slugs/ft$^3$ |
| $\sigma_{1,2}$ | stability indices |

Subscripts (other than those in above definitions)

| | |
|---|---|
| f | refers to high aspect-ratio fin (skeg or rudder) |
| H | refers to bare hull |
| i | refers to ideal fluid |
| $r'$ | refers to derivative with respect to $r'$ |
| s | refers to derivative with respect to s |
| $\beta$ | refers to derivative with respect to $\beta$ |

BLANK PAGE

## INTRODUCTION

In an earlier report,[1] an analytical method was developed for estimating the first-order stability derivatives (static and rotary lateral-force and yawing-moment rates) which would indicate the course stability and turning or steering qualities of ships. The method was applied to the case of a family of eight hulls of the same length and the same prismatic and block coefficient, but differing in draft, beam, and displacement. The hulls were the 840 Series of the Taylor Standard Series type with the after deadwood (faired-in skeg) removed. Experimentally measured lateral forces and yawing moments, from Davidson Laboratory rotating-arm tests at different turning radii, were available for these hulls and for three of the hulls with flat-plate skegs in the place of the removed deadwood.*

Although the analytical method is based upon simple concepts combining simplified flow theory with low aspect-ratio wing theory and using Albring's[3] empirical modifications for viscid flow, good correlation was attained between the stability derivatives calculated by this method and those determined from experimental data. However, Albring's modification of the rotary moment rate is a function of prismatic coefficient and, since all the hulls of the 840 Series have the same prismatic (0.54), this modification was not fully tested. It was decided, therefore, to extend application of the prediction method to hulls of other prismatic, with and without skegs or deadwood aft, for which experimental data were available.

Fortunately, straight-course and rotating-arm model tests have been concluded on eight members of the Series 60 family of ships,[4] so that the effects on stability of varying block and prismatic coefficients, beam,

*Results of several straight-course tests[2] confirmed previous experience at Davidson Laboratory that entirely reliable static force and moment rates for straight-course motion can be obtained from rotating-arm data at sufficiently large turning radii.

and draft — other form characteristics remaining constant — can be ascertained from the experimental measurements, for comparison with theoretical predictions. These forms were not altered, as were the Standard Series types, by removal of the after deadwood. Tests were made with and without rudder and propeller, and one model was tested with three rudders of differing chord length. In addition, the analytical method was applied to the following four forms: an extreme vee modification of a Series 60 ship,[4] a mariner class vessel,[5] and the widely different destroyer[6] and hopper-dredge[7] forms. Consistent experimental techniques have been used in tests of these forms conducted in recent years at Davidson Laboratory.

With the exception of the hopper dredge, all models had large areas of deadwood (faired-in skeg, including rudder) aft, with maximum height at the stern from extended keel line to load waterline. The aspect ratio of the skeg, equal to the square of the maximum skeg height divided by the skeg area and doubled to take into account the free-surface effect, was, in all these cases, less than unity. The hopper dredge, on the other hand, had a skeg of small area at the stern, masked from the water surface by the broad bottom of the afterbody. The aspect ratio of this skeg, equal to the square of its maximum height divided by its area, was greater than unity. For this form, and for the Series 60 cases where the rudder was removed or rudder area was added, the effects of altering a body by adding or subtracting area having fin effect could not be treated by using low aspect-ratio wing theory.

The method of Ref. 1 was therefore extended by including the technique of Ref. 8 in studying the effect on ship behavior of adding or subtracting fins. The lift on the fin itself is calculated by using aerodynamic wing theory for wings of aspect ratio greater than unity. Then, by assuming that the interference between fin and body is negligible, as in the simplified theory used in Ref. 1, the changes in static and rotary force and moment rates are computed.

Comparison with experimentally derived stability derivatives and indices shows that the theoretically determined values are of the right orders of magnitude and indicate correct trends. The fact that the analytical method has the ability to predict relative effects of changes in the geometry of a ship form, in addition to the effects of changes in rudder and skeg area, makes it an acceptable working tool in designing ships for greater course stability. It is useful not only as an augment to experimentation but also in planning an efficient program of model testing.

This project was sponsored by the Office of Naval Research under Contract Nonr 263(57) and technically administered by David Taylor Model Basin.

## THE ANALYTICAL METHOD

### Assumed Stability Derivatives for Hulls Without Deadwood or Fins

In the potential flow theory the hydrodynamic force and moment rate coefficients, or stability derivatives, of an elongated body of revolution without appendages are defined for the linearized region of small angles of attack and large radii of rotation as:

$$\left.\begin{aligned}
&\text{On straight course, } r' = \frac{\ell}{R} = 0\ . \\
&\qquad L'_{\beta_H} = Y'_{\beta_H} = 0 \\
&\qquad N'_{\beta_H} = m'_2 - m'_1 = N'_{\beta_i} \quad \text{(Munk ideal moment)} \\
&\text{In turn, around } \beta = 0\ , \\
&\qquad Y'_{r_H} = 0 \qquad\qquad N'_{r_H} = 0
\end{aligned}\right\} \quad (1)$$

The notation is that of the Society of Naval Architects and Marine Engineers (see Nomenclature and Fig. 1; the subscript H refers to bare hull). The measured lateral force coefficient is defined as

$$F'_y = Y' - \left(m'_o + m'_1\right) r'$$

and its derivative with respect to $r'$ as

$$\frac{\partial F'_y}{\partial r'} = Y'_{r'} - \left(m'_o + m'_1\right) \qquad (2)$$

where $m'_o$ is the mass coefficient of the hull and $m'_1$ is the longitudinal added mass coefficient. Lamb,[9] considering the added mass term as a hydrodynamic force, defines $Y'_{r'_H} = - m'_1 = - k_1\ m'_o$ where $k_1$ is the coefficient of longitudinal accession to inertia (Fig. 2). Equations 1 are equivalent to those derived by Breslin[10] for a long slender body with tapered or pointed ends, from three-dimensional singularity distributions.

In Albring's[3] modification of potential flow theory for a body of revolution moving in a viscous and eddying fluid, the lift on the bare hull is no longer zero as in potential theory, but the force developed as by "oblique attack under an angle [β] of a correspondingly shaped solid without effect of curvature," which acts at a distance $x_p$ from the center of gravity. In determining this lift force on a surface ship, Ref. 1 follows Fedyaevsky and Sobolev[11] in identifying the bare hull of a ship (i.e., the ship without deadwood, ske , or any other area which has only fin effect) with a low aspect-ratio wing. In this analogy the span of the wing is assumed to be double the draft of the ship, to take into account the action of the free water surface. Tsakonas[2] shows that this "solid wall" method of accounting for free-surface effect is correct for moderate speeds when the influence of wave-making can be neglected.

The dimensionless lift rate per unit lateral area of the hull is assumed as given by Jones' formula for a low aspect-ratio wing, derived from the consideration of elliptic load distributions along the chord and the span of a thin foil. The Jones formula is

$$\frac{\partial C_L}{\partial \beta} = \frac{\pi}{2} \mathit{AR} = \frac{\pi}{2}\left(\frac{2H^2}{A}\right) \tag{3}$$

The total bare-hull lift rate, nondimensionalized on the basis of area $\ell \times H$, is then

$$L'_{\beta_H} = \frac{\pi H}{\ell} \tag{4}$$

On combining low aspect-ratio wing theory with Albring's empirically based formulas, the stability derivatives for a bare ship moving in a viscous fluid are obtained as:

On straight course, $r' = \ell/R = 0$ .

The static force rate $Y'_{\beta_H} = L'_{\beta_H} + D'_o = \frac{\pi H}{\ell} + D'_o$ (5)

The static moment rate $N'_{\beta_H} = N'_{\beta_i} + \frac{x_p}{\ell} L'_{\beta_H} = m'_2 - m'_1 + \left(\frac{x_p}{\ell}\right) \frac{\pi H}{\ell}$ (6)

In turn, around $\beta = 0$ ,

The total rotary force rate $\frac{\partial F'_{y_H}}{\partial r'} = - m'_x + Y'_{r'_H} = - \left(m'_o + m'_1\right) - \frac{x_p}{\ell} L'_{\beta_H}$ (7)

The rotary moment rate $N'_{r'_H} = - m'_z \frac{\bar{x}}{\ell} - \left(\frac{x_o}{\ell}\right)^2 L'_{\beta_H}$ (8)

The various terms are determined as follows:

$H/\ell$ = ratio of maximum draft to length of ship

$D'_o$ = drag coefficient at yaw angle $\beta = 0$ , obtained by experiment or estimated from the Taylor Standard Series curves of resistance[12].

$N'_{\beta_i}$ = Munk's moment rate in an ideal fluid, equal to the difference between the lateral added mass coefficient $m'_2$ and the longitudinal added mass coefficient $m'_1$ of entrained water

$x_p$ = distance from LCG of the center of pressure of lateral force, taken as the center of area of the hull profile (positive if forward of the LCG)

$m'_x = m'_o + m'_1$ = virtual longitudinal mass coefficient

$m'_o = \frac{\Delta}{g \frac{\rho}{2} \ell^2 H}$ , where $\Delta$ is ship displacement in lb

$m'_1 = k_1 m'_o$ , where $k_1$ is Lamb's coefficient of longitudinal accession to inertia for an equivalent ellipsoid with ratio of minor axis to major axis equal to $2H/\ell$

$\frac{x_o}{\ell}$ = half the prismatic coefficient $C_p$ , following Albring

$m_z'$ = the rotary added mass of entrained water acting at the distance $\bar{x}$ from LCG

The terms $m_2'$, $m_z'$, and $\bar{x}$ are estimated as follows, according to the procedure advocated by Martin:[13]

$$m_2' = \frac{m_2}{\frac{\rho}{2} \ell^2 H}$$

where

$$m_2 = k_2 \frac{\rho}{2} \pi \int_{x_s}^{x_b} C_s\ h^2 dx$$

$$m_z' = \frac{k'}{k_2}\ m_2'$$

$k_2$, $k'$ = Lamb's coefficients of accession to inertia, lateral and rotational, for an equivalent ellipsoid (see Fig. 2)

$x_s$, $x_b$ = x-coordinates of the stern, bow

$h$ = local draft at each section

$C_s$ = two-dimensional lateral added-mass coefficient, determined at each section from the curves on two-dimensional forms of Lewis' sections, by Prohaska[14] (see Fig. 3)

$$\bar{x} = \frac{\int_{x_s}^{x_b} C_s\ h^2 x dx}{\int_{x_s}^{x_b} C_s\ h^2 dx}$$ where $x$ is positive forward of LCG

### Assumed Stability Derivatives for Hulls with Large Areas of Deadwood Aft

For hulls with large areas of deadwood or low aspect-ratio skegs aft, extending to the water surface at the stern, and including rudders parallel to the center line (rudder angle $\delta = 0$), simplified theory assumes that there is no interference between the bodies and these surfaces, so that the effects of the skeg area are simply additive. The lift rate per unit skeg area is given by Eq.(3) and, as in Ref. 1, the lift is assumed to act at the after end of the skeg, at $x_s$ the distance of the ship stern from the LCG. Since the length of the deadwood, or skeg, plus rudder is small in comparison with the length of the hull, the distance between the stern and the actual center of pressure of the skeg area is a negligible part of the moment arm about the LCG.

The increments due to deadwood, etc., to be added to the bare hull stability derivatives given by Eq.(5)-(8), are (see Ref. 1)

$$\Delta L'_\beta = \Delta Y'_\beta = \frac{\pi H}{\ell} \tag{9}$$

$$\Delta N'_\beta = \left(\frac{x_s}{\ell}\right)\frac{\pi H}{\ell} \tag{10}$$

$$\Delta Y'_{r'} = -\left(\frac{x_s}{\ell}\right)\frac{\pi H}{\ell} \tag{11}$$

$$\Delta N'_{r'} = -\left(\frac{x_s}{\ell}\right)^2 \frac{\pi H}{\ell} \tag{12}$$

where $x_s$ is negative.

As shown in Ref. 1, these formulas give essentially the same results as those obtained in the procedure suggested by Martin.[13] Martin modified the linearized equations of motion in the horizontal plane, given in Ref. 15, by including terms involving two-dimensional lateral added mass at the stern to account for the sudden change of section of the hull and skeg at $x_s$.

The total values of the static and rotary force and moment rates in the case of hulls with large skeg area aft extending to the load waterline at the stern are:

On straight course, $r' = \ell/R = 0$.

$$Y'_\beta = \frac{2\pi H}{\ell} + D'_o \tag{13}$$

$$N'_\beta = m'_2 - m'_1 + \left(\frac{x_p + x_s}{\ell}\right) \frac{\pi H}{\ell} \tag{14}$$

In turn, around $\beta = 0$ ,

$$\frac{\partial F'_y}{\partial r'} = - m'_x - \left(\frac{x_p + x_s}{\ell}\right) \frac{\pi H}{\ell} \tag{15}$$

$$N'_r = - m'_z \frac{\bar{x}}{\ell} - \left(\frac{x_o^2 + x_s^2}{\ell^2}\right) \frac{\pi H}{\ell} \tag{16}$$

### Changes in Stability Derivatives Due to Adding or Subtracting Fins of Aspect Ratio Equal to or Greater than Unity

In the case of hulls like the hopper dredge, with very little deadwood or skeg area aft (and that masked from the water surface by the hull bottom), a different treatment is required. The bare hull stability derivatives are obtained from Eqs.(5)-(8) as before, but the effect on the derivatives of adding area having fin effect and an aspect ratio which cannot be considered low is determined as in Ref. 8 by using aerodynamic wing theory applicable to wings of higher aspect ratio , equal to or greater than unity. The latter theory is also employed in studying the effects of adding or subtracting rudder area in the hull cases with large deadwood aft.

The dimensionless lift rate per unit of fin area $A_f$ in such case is

$$\frac{\partial C_L}{\partial \beta} = \frac{2\pi}{1 + \frac{2}{AR_f}} \tag{17}$$

Because the skeg or rudder is below the hull bottom and does not extend to the water surface, it is assumed that there are no free-surface effects. Thus the fin aspect ratio $AR_f$ is the ratio of the square of the fin span (maximum height $h_f$ ) to the fin area $A_f$ . The increment or decrement to the static-lateral-force rate, nondimensionalized on the basis of area $\ell \cdot H$ , will be

$$\left(\Delta Y'_\beta\right)_f = \pm\left(\frac{2\pi}{1+\frac{2}{AR_f}}\right)\frac{A_f}{\ell H} = \pm\frac{\pi h_f^2}{\ell H}\left(\frac{1}{1+\frac{AR_f}{2}}\right) \tag{18}$$

where $\left(\Delta Y'_\beta\right)_f < 0$ when subtracting fin area.

Again the assumptions are made that interference between fin and body is negligible and that the center of pressure of the fin is at the stern at a distance $x_s$ aft of the LCG. The other stability-derivative changes are then

$$\left(\Delta N'_\beta\right)_f = \frac{x_s}{\ell}\left(\Delta Y'_\beta\right)_f \tag{19}$$

$$\left(\Delta Y'_{r'}\right)_f = -\frac{x_s}{\ell}\left(\Delta Y'_\beta\right)_f \tag{20}$$

$$\left(\Delta N'_r\right)_f = -\frac{x_s^2}{\ell^2}\left(\Delta Y'_\beta\right)_f \tag{21}$$

Although Eqs.(19)-(21) are derived for fin area at the stern, they are, through substitution of the correct moment arm in place of $x_s$, applicable also to added or subtracted fin area at the bow.

In the case of a ship with small skeg of relatively high aspect ratio at the after end of the underwater hull, the stability derivatives $Y'_\beta$, $N'_\beta$, $(m'_x - Y'_{r'})$, and $N'_{r'}$ are obtained from Eqs.(5)-(8), modified by Eqs.(18)-(21) with $(\Delta Y'_\beta)_f$ positive. When rudders are removed from hulls with large deadwood area aft, the stability derivatives are defined by Eqs.(13)-(16), modified by Eqs.(18)-(21) with $(\Delta Y'_\beta)_f$ negative.

## The Stability Indices

The criteria for inherent dynamic stability of a free body moving on straight course in the horizontal plane are the damping exponents $\sigma_1$

and $\sigma_2$ in the solution

$$\beta = \beta_1 e^{\sigma_1 s} + \beta_2 e^{\sigma_2 s} \quad , \quad r' = r_1' e^{\sigma_1 s} + r_2' e^{\sigma_2 s}$$

of the homogeneous linearized equations of motion[15]

$$\left.\begin{aligned} \left(m_x' - Y_{r'}'\right) r' - m_y'\beta_s - Y_\beta' \beta = 0 \\ n_z' r_s' - N_{r'}' r' - N_\beta' \beta = 0 \end{aligned}\right\} \tag{22}$$

Here $s = Ut/\ell$ . The damping exponents are given by

$$\sigma_{1,2} = \frac{-\left(n_z' Y_\beta' - m_y' N_r'\right) \pm \sqrt{\left(n_z' Y_\beta' - m_y' N_{r'}'\right)^2 + 4 n_z' m_y' \left[N_{r'}' Y_\beta' + \left(m_x' - Y_{r'}'\right) N_\beta'\right]}}{2 n_z' m_y'} \tag{23}$$

where $m_x' = m_o' + m_1'$ , virtual longitudinal mass coefficient

$m_y' = m_o' + m_2'$ , virtual lateral mass coefficient

$n_z' = \dfrac{I_o + I_z}{\frac{\rho}{2} \ell^4 H}$ , virtual moment-of-inertia coefficient

$\dfrac{I_o}{\frac{\rho}{2} \ell^4 H} = \dfrac{m_o'}{16}$ (assuming the radius of gyration is equal to $\frac{\ell}{4}$ )

= moment of inertia of the ship

$I_z = k' \dfrac{\pi\rho}{2} \displaystyle\int_{x_s}^{x_b} C_s h^2 x^2 dx$ (Ref. 13)

= moment of inertia of the entrained mass of water

The derivatives, $Y_\beta'$ , $N_\beta'$ , $\left(m_x' - Y_{r'}'\right)$, and $N_{r'}'$ , are defined for the various configurations as follows:

| | | |
|---|---|---|
| Bare hull (no deadwood) | 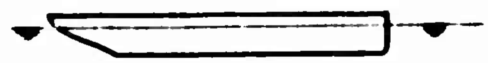 | Eqs.(5)-(8) |
| Hull with large dead-wood and rudder | 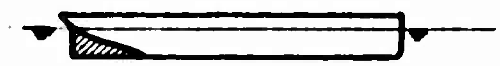 | Eqs.(13)-(16) |
| Hull with small skeg | 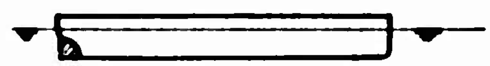 | Eqs.(5)-(8) plus Eqs. (18)-(21) |
| Hull with large dead-wood, rudder removed | 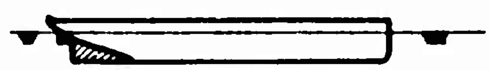 | Eqs.(13)-(16) plus Eqs.(18)-(21) |

The index $\sigma_2$, obtained by using the minus sign in Eq.(23), is always negative. Therefore the stability of the motion depends on the sign of $\sigma_1$ or its real part; the more negative $\sigma_1$, the sooner an initial disturbance will damp out, and hence the greater the stability. If $\sigma_1$ or its real part is positive, the motion is unstable and the hull cannot be kept on straight course without applying a corrective rudder.

The stability criterion $\sigma_1$ is also an index of the turning qualities of a hull in turns that are not too tight, i.e. when nonlinearities can be neglected. A more dynamically stable hull will turn in a larger radius than will a less stable hull with equal rudder force. Conversely, the more stable hull will require greater rudder force than the less stable hull to turn in a given radius. On the other hand, an unstable ship, defined by positive $\sigma_1$, may turn in a direction opposite to that called for by the applied rudder, in which case it will need a large force to bring it around.

## PRESENTATION AND DISCUSSION OF RESULTS

In the appendices, lateral-force and yawing-moment coefficients and stability derivatives determined from experimental measurements are compared graphically with those computed by the linear theory of the present report. Annotations pertaining to the appendices follow.

### 840 Series Hulls

In Appendix A are reproduced the table of particulars and charts of Ref. 1 for three Taylor Standard Series models, with deadwood removed and with flat-plate skegs added in lieu of deadwood. These models had been tested at Davidson Laboratory in 1959 and 1951. The tests were made at Froude numbers of 0.16 and 0.23; hence the assumption that wave-making effects can be neglected is tenable.

Figure A-1 shows the body plan of the parent hull and Fig. A-2 the stern profile with skeg installed. Figure A-3 is a summary chart comparing the calculated $Y'_\beta$ , $N'_\beta$ , $Y'_{r'}$ , $N'_{r'}$ , and $\sigma_1$ with values obtained in 1959 from measurements on the 842 hull,[a] without skeg and with three skegs of different sizes. The calculated and experimentally measured static rates, $Y'_\beta$ and $N'_\beta$ , are identical. The calculated and experimental magnitudes of the rotary derivatives and stability index differ slightly, but the stability predictions err on the conservative side.

It is seen that the analytical method predicts the trends in stability derivatives with increase in profile area. This conclusion is confirmed by Figures A-4 and A-5 for the 846 and 848 models, although these models were tested in 1951 by experimental techniques not quite consistent with those of more recent years. As skeg area is increased and extended farther aft, $Y'_\beta$ and $Y'_{r'}$ become more positive, $N'_{r'}$ more negative, and $N'_\beta$ less positive. All trends are in the direction of greater course stability, as indicated by the progressively more negative value of $\sigma_1$ .

## Series 60 Hulls

In Appendix B are presented the new results for the eight Series 60 models,[4] with and without rudder and propeller. The forces and moments are for zero rudder angle and a Froude number of approximately 0.20.

Table B-1 notes the hull particulars and the various coefficients of added mass and center of pressure computed by the present analytical method. Table B-2 gives the stability derivatives estimated from theory, and also those estimated from a "least squares" fit of the experimental data. In the latter procedure the force and moment coefficients are assumed to be of the following polynomial form:

$$\left\{\begin{matrix} Y' = F_y' + m_o' r' \\ \\ N' \end{matrix}\right\} = c_o + c_1\beta + c_2 r' + c_3\beta^2 r' + c_4\beta r'^2 + c_5\beta^3 + c_6 r'^3 \tag{24}$$

Each model is designated by a sequence of three digits. The first signifies change in hull; the second signifies presence, 1, or absence, 0, of propeller; the third signifies presence, 1, or absence, 0, of design rudder. The digit 2 or 3 in third place refers to rudder with larger or smaller chord, respectively, than the original rudder.

For the models labeled (-,1,1), with rotating propeller and design rudder, Eqs.(13)-(16) are used for the theoretical derivatives with $D_o' = 0$, since the propeller revolutions are adjusted to obtain zero drag condition. The tests of Models 6,1,1 and 7,1,1 in both clockwise and counterclockwise turns showed practically no asymmetry in the data with change in angular velocity from negative to positive. Therefore lift due to propeller operation can be assumed negligible. For models labeled (-,0,0), without propeller or rudder, Eqs.(13)-(16) are modified by Eqs.(18)-(21). In these cases $D_o'$ is the experimentally measured drag coefficient at zero yaw angle. Models 2,1,2 and 2,1,3 with rotating propeller and larger or smaller rudder chord, respectively, than the original 2,1,1 are treated by subtracting the lift due to the original rudder and adding that due to the replacement.

Appendix B includes typical planforms (Figs. B-1,2,3) and a plan of the design rudder in location (Fig. B-4). Figure B-5 is a summary chart for all eight models, with and without rudder and propeller, showing analytically calculated and experimentally derived stability index $\sigma_1$ versus ship-mass coefficient $m_o' = 2\ C_B B/\ell$ . Figure B-6 shows $\sigma_1$ versus rudder area for Model 2 with rudders of varying chord, again comparing theoretical values with those obtained from a "least squares" fit of the experimental data. The remaining figures (B-7 to B-40) are graphs of lateral-force and yawing-moment coefficients versus yaw angle $\beta$ and angular velocity $r'$ for individual models, showing the experimental data and values computed on the basis of the linear theory, i.e. first order variation with $\beta$ and $r'$ .

The correlation between theoretical and experimental derivative estimates is seen to be good for the hulls with rudder and propeller, slightly less good for the hulls without rudder and propeller. The discrepancies are for the most part within the experimental error.

## Extreme Vee Modification

Appendix C compares the theoretical and experimental results for an extreme vee modification[4] of Series 60 Model 1 (Fig. C-1), which was developed at the University of Michigan. Table C-1 tabulates particulars of this hull (Model 9), with and without propeller and design rudder, the calculated added mass and center of pressure coefficients, and the stability index $\sigma_1$ as computed from theoretical derivatives and from experimentally measured rates. Figures C-2 to C-5 are graphs of the lateral-force and yawing-moment coefficients for models 9,1,1 and 9,0,0, similar to those for the Series 60 hulls.

While the calculated static and rotary lateral force derivatives apply as well to the experimental data, the discrepancies between calculated and experimentally measured moment derivatives are larger than for the normal Series 60 forms. However, the contrary effects of lower static instability and lower rotary stability, predicted by theory, appear to cancel each other in the calculations of the stability index. The experimental and theoretical estimates of $\sigma_1$ are close.

It is suspected that because of the extreme fineness at the bow (the bow sections of the Series 60 model have been pared to fine vee forms while the profile remains the same), there is some vibration at the bow in yawed motion. Such a condition would affect the measured moments.

## Mariner Class Hull

Appendix D treats the Mariner class hull (Table D-1, Fig. D-1) reported in Ref. 5. After that note was published, however, it was found that the calibrations used to reduce the test data were in error. The data have since been revised, with correct calibrations, and are shown on Figs. D-2,3,4, for the hull without propeller, with rudder amidship.

The tests had been conducted on the rotating arm at Davidson Laboratory in 1963. The model was run at a Froude number around 0.20, so that for this model, also, the effects of wave-making can be neglected.

The charts show that the theoretical derivatives obtained by using Eqs.(13)-(16) fit the experimental data reasonably well. Table D-2 gives a comparison of the stability derivatives and indices derived here and the results of Ref. 16 as obtained by an oscillator technique.

## Destroyer Model

Appendix E presents the results for the DD692 destroyer model (Fig. E-1, Table E-1), with twin rudders and propellers, tested on the rotating arm at Davidson Laboratory[6] in 1963. The coefficients of measured forces and moments at three turning diameters for zero rudder angle and Froude number of 0.155 are presented in Figs. E-2,3.

Equations (13)-(16) are used for the theoretical derivatives, and it is assumed that the effects of the off-center twin rudders at zero angle and of the propellers are negligible additions to the effect of the skeg at the stern. The calculated static rates on straight course seem reasonable extrapolations of the rotating-arm data. The calculated rotary rates are close to the measured slopes, certainly within the experimental error.

### Hopper-Dredge Models

The results for the hopper-dredge model (Fig. F-1 of Appendix F), under two displacement conditions, are presented in Figs. F-2,3,4,5. This model was tested on the rotating arm at Davidson Laboratory in 1960,[7] at Froude numbers of 0.12 and 0.20 for the heavy displacement case and 0.155 for the light case.

The theoretical derivatives shown on the charts were calculated from Eqs.(5)-(8) for bare hull, modified by Eqs.(18)-(21) for the small skeg-plus-rudder at the stern. The pertinent characteristics of the models are given in Table F-1. Table F-2 compares the theoretical values of stability index $\sigma_1$ with those calculated from the measurements and reported in Ref. 7.

Although the theoretical estimates are on the average 18% less than the experimental, both indicate an extremely unstable vessel. The theory and results of this report underline the recommendations of Ref. 7, viz., to increase the deadwood forward of the rudder stock and to increase the chord of the rudder aft for stability.

## COURSE STABILITY DEPENDENCE ON HULL GEOMETRY

An analysis of the assumed expressions for ship lateral-force and yawing-moment derivatives will be made in the light of the results presented, to discover the major form-parameters on which course stability depends. It is well known, and further proof has been added here, that low aspect-ratio skegs or deadwood at the afterbody are essential for minimum stability. It has also been demonstrated that increasing skeg area aft by widening the chord of skeg or rudder improves the stability, and that removing area with fin effect at the stern lowers the stability. But aside from such fin areas, how can one tell by the dimensions and body lines of a ship whether the design will lead to greater or less stability? The answer lies in the make-up of the various terms involved in Eqs.(5)-(16). These will be examined now.

For practical ships, the longitudinal coefficient of accession to inertia $k_1$ is close to zero, so that the longitudinal added-mass coefficient $m_1'$ is negligible. The lateral and rotational coefficients of accession to inertia, $k_2$ and $k'$, are approximately equal, and therefore $m_2'$ can be substituted for $m_z'$ . The virtual moment-of-inertia coefficient $n_z'$ is close to $(m_o' + m_2')/16$ for the variety of hull forms treated here. In general, variations in $x_p$ and $\bar{x}$ (the centers of pressure of the lift and lateral added mass, respectively) and in position of longitudinal center of gravity are minor in their influence on the stability derivatives of hulls with deadwood aft. The lift coefficient varies inversely with length-draft ratio. The less important drag coefficient depends, as is known, on block coefficient and beam-draft ratio, and hence on $m_o'$ , which is a function of block coefficient and beam-length ratio, and on $\ell/H$ . The major factors influencing the derivatives and stability index $\sigma_1$ are thus seen to be $m_o'$ , $m_2'$ , and $\ell/H$ .

The dependence of $\sigma_1$ on $x_o/\ell$ , which under Albring's assumption is equal to half the prismatic coefficient, is implicit in its dependence on $m_o'$ and $m_2'$ . The ship-mass coefficient is

$$m_o' \equiv 2\, C_B \frac{B}{\ell} \tag{25}$$

The lateral added-mass coefficient formula

$$m_2' = \frac{k_2 \pi}{\ell^2 H} \int_{x_s}^{x_b} C_s\, h^2\, dx$$

with $k_2 \sim 1$, and $h = H$ , maximum draft, for almost the entire length of commercial and naval vessels, can be written approximately as

$$m_2' \approx \frac{\pi H}{\ell}\, \bar{C}_s \tag{26}$$

where $\bar{C}_s = \frac{1}{\ell} \int_{x_s}^{x_b} C_s\, dx$ , an average sectional inertia coefficient for the hull.

$C_s$ is a function of section beam-draft ratio and section-area coefficient, depending more heavily on the latter (see Fig. 3). Thus prismatic, which is the quotient of block coefficient by midship section-area coefficient, is involved in both $m_o'$ and $m_2'$.

On substituting the approximations noted above in Eq.(23), it can be shown that $\sigma_1$ is some function of the inverse of $(m_o' + m_2')\ \ell/H$. A graph of $\sigma_1$ versus $(m_o' + m_2')\ \ell/H$ for the stable hulls, with low aspect-ratio skegs, or deadwood plus rudder, to the stern, shows clearly that the major form factors have been well explored. On Fig. 4 are plotted the experimentally derived values for hulls tested in recent years at Davidson Laboratory with consistent experimental techniques. The hulls vary in block coefficient from 0.50 to 0.80, in length-draft ratio from 14.5 to 27.40, in length-beam ratio from 6 to 9.45, and in beam-draft ratio from 2.50 to 3.28. The average sectional inertia coefficients $\bar{C}_s$ are tabulated below:

| Model | $C_B$ | $\bar{C}_s$ |
|---|---|---|
| 842 | 0.50 | 0.83 |
| | 0.60 | 1.02 |
| Series 60 | 0.70 | 1.07 |
| | 0.80 | 1.16 |
| Extreme vee | 0.60 | 0.93 |
| Mariner | 0.61 | 0.92 |
| Destroyer | 0.57 | 0.76 |

The curve on Fig. 4 is represented by the formula

$$\sigma_1 = -\left[\frac{5H}{(m_o' + m_2')\ \ell}\right]^{2.5} \tag{27}$$

and is seen to fit the data very well. By making use of Eqs.(25) and (26), course stability is shown to vary inversely as

$$-\left[2\ C_B \frac{B}{H} + \pi \bar{C}_s\right]^{2.5}$$

which may be easily computed from the ship lines and with the aid of Fig. 3. This relationship shows that stability will be increased for hulls with low aspect-ratio skegs to the stern by decreasing one or more of these three form factors: block coefficient, beam-draft ratio, and average sectional inertia coefficient.

## CONCLUSION

The analytical method of Ref. 1 for estimating force and moment rates in yawing motion and stability on course, which combines Albring's empirical modifications of simplified flow theory with low aspect-ratio wing theory, has been extended here to take into consideration the effects on course stability of higher aspect-ratio fins. The method had been applied in Ref. 1 to eight 840 Series hulls, of 0.5 block coefficient and varying beam, draft, and displacement. The hulls were Taylor Standard Series forms with the after deadwood removed, but three of the hulls had also been tested with low-aspect-ratio flat-plate skegs in the place of the removed deadwood. The extended method has now been applied to 12 other ships: six Series 60 forms of 0.6 block coefficient and varying beam, draft, and displacement; two Series 60 forms of 0.7 and 0.8 block; an extreme vee modification of a Series 60, 0.6 block form; and three other widely different forms — a Mariner Class ship, a destroyer, and a hopper dredge at two displacements. All had large areas of deadwood aft, except the hopper dredge, which had a small skeg at the stern. The Series 60 cases without rudders, and the case of one model with rudders of larger and smaller chord, have also been treated, making 24 cases in all.

Good correlation is shown between the values of stability derivatives calculated by this method and those based on experimental measurements, despite the variety in ship design. It has been shown that low aspect-ratio skegs or deadwood at the afterbody are essential for minimum stability and that additional skeg area or an extension of rudder area aft increases stability. For the stable ship with large skegs to the stern, the major form factors influencing course stability are demonstrated to be the coefficients of ship mass and lateral added mass of entrained water and the length-draft ratio, or, as a corollary, the block coefficient, beam-draft ratio, and average sectional inertia coefficient. The functional relationship is expressed by the empirical formula

$$\sigma_1 = - \left[ \frac{5H}{(m_o' + m_2')\,\ell} \right]^{2.5} \approx - \left[ \frac{5}{2\,C_B \frac{B}{H} + \pi \bar{C}_s} \right]^{2.5}$$

The results of this report show that the values of stability derivatives and indices determined by the analytical method are of the right orders of magnitude and indicate correct trends. Application to a variety of ship forms has demonstrated that the method can predict relative effects of changes in the geometry of a ship form, as well as the effects of changes in skeg and rudder area. The analytical method has thus been proved an effective tool to be used in designing ships for greater course stability and in planning an economical program of model testing.

## REFERENCES

1. JACOBS, W.R., "Method of Predicting Course Stability and Turning Qualities of Ships," DL Report 945, March 1963.

2. TSAKONAS, S., "Effect of Appendage and Hull Form on the Hydrodynamic Coefficients of Surface Ships," DL Report 740, May 1959.

3. ALBRING, W., "Summary Report of Experimental and Mathematical Methods for the Determination of Coefficients of Turning of Bodies of Revolution," CONLAN 2.

4. CRANE, C.L., JR., "Research on Ship Controllability," DL Quarterly Progress Report, 1 June 1964.

5. SUAREZ, A., "Rotating Arm Experimental Study of a Mariner Class Vessel," DL Note 696, June 1963. (Measurements revised using correct calibration, April 1964).

6. SUAREZ, A., DL Confidential Letter Report 1012, February 1964.

7. SUAREZ, A., "Stability Analysis of SS Sandcaptain," DL Letter Report 786, March-May 1960.

8. GIMPRICH, M. and JACOBS, W.R., "The Effect of Fins on the Behavior of Free Bodies," ETT DL Report 361, February 1950. CONFIDENTIAL.

9. LAMB, H., Hydrodynamics, Dover Publications, 6th ed., New York, 1945.

10. BRESLIN, J.P., "Derivation of Slender-Body Approximations for Force and Moment Derivatives from Three-Dimensional Singularity Distributions," DL TM 134, January 1963.

11. FEDYAEVSKY, K.K. and SOBOLEV, G.V., "Application of the Results of Low Aspect-Ratio Wing Theory to the Solution of Some Steering Problems," Proc., Netherlands Ship Model Basin Symposium on the Behavior of Ships in a Seaway, Wageningen, September 1957.

12. GERTLER, M., "A Reanalysis of the Original Test Data for the Taylor Standard Series," DTMB Report 806, March 1954.

13. MARTIN, M., "Analysis of Lateral Force and Moment Caused by Yaw During Ship Turning," DL Report 792, March 1961.

14. PROHASKA, C.W., "The Vertical Vibration of Ships," Shipbuilder and Marine Engine-Builder, October-November 1947.

15. DAVIDSON, K.S.M. and SCHIFF, L.I., "Turning and Course-Keeping Qualities," Transactions SNAME, 1946.

16. PAULLING, J.R. and WOOD, L.W., "The Dynamic Problem of Two Ships Operating on Parallel Courses in Close Proximity," University of California Series No. 189, 18 July 1963.

BLANK PAGE

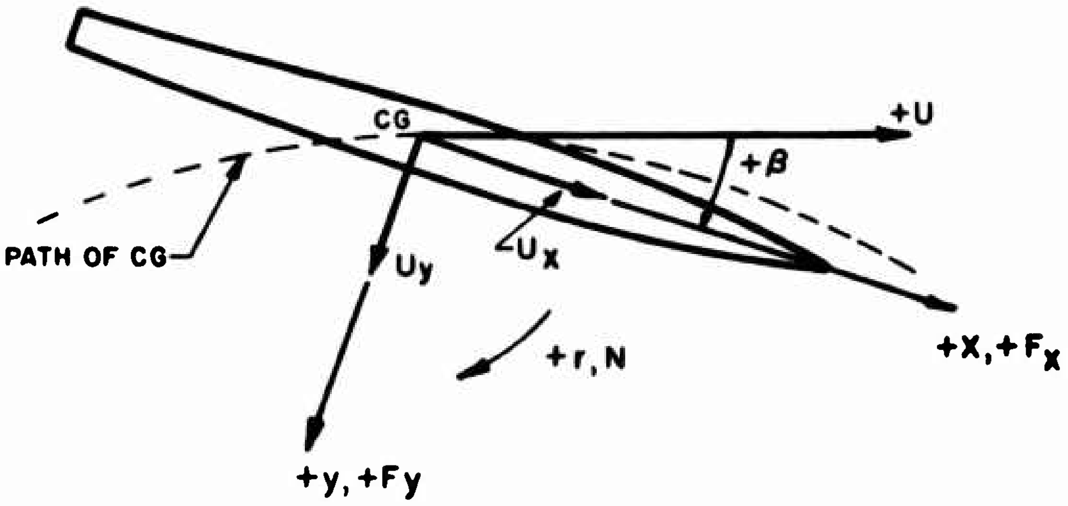


FIGURE I. MODEL ORIENTATION IN X-Y PLANE

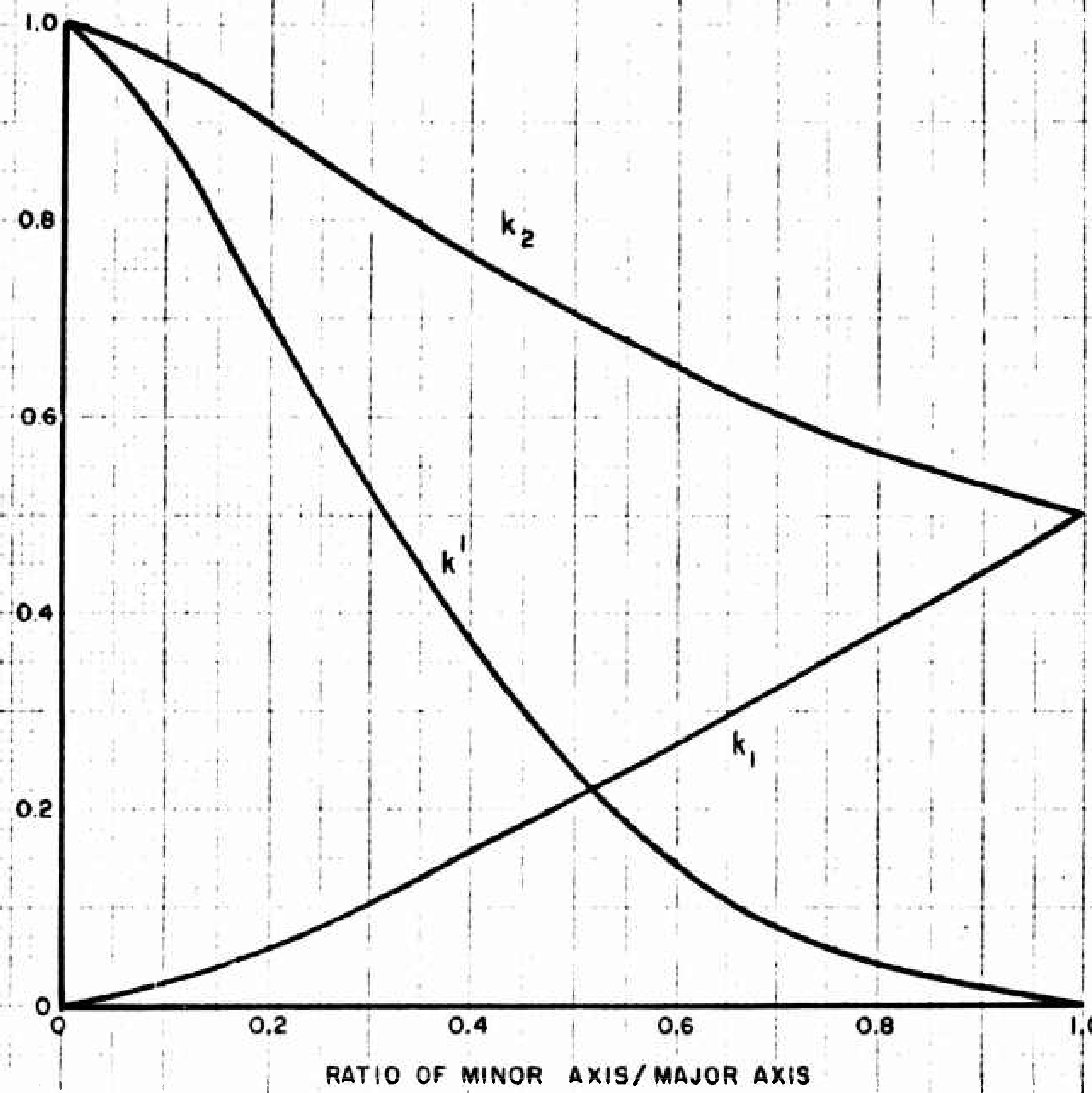


FIGURE 2. COEFFICIENTS OF ACCESSION TO INERTIA FOR PROLATE SPHEROIDS (FROM H. LAMB'S HYDRODYNAMICS)

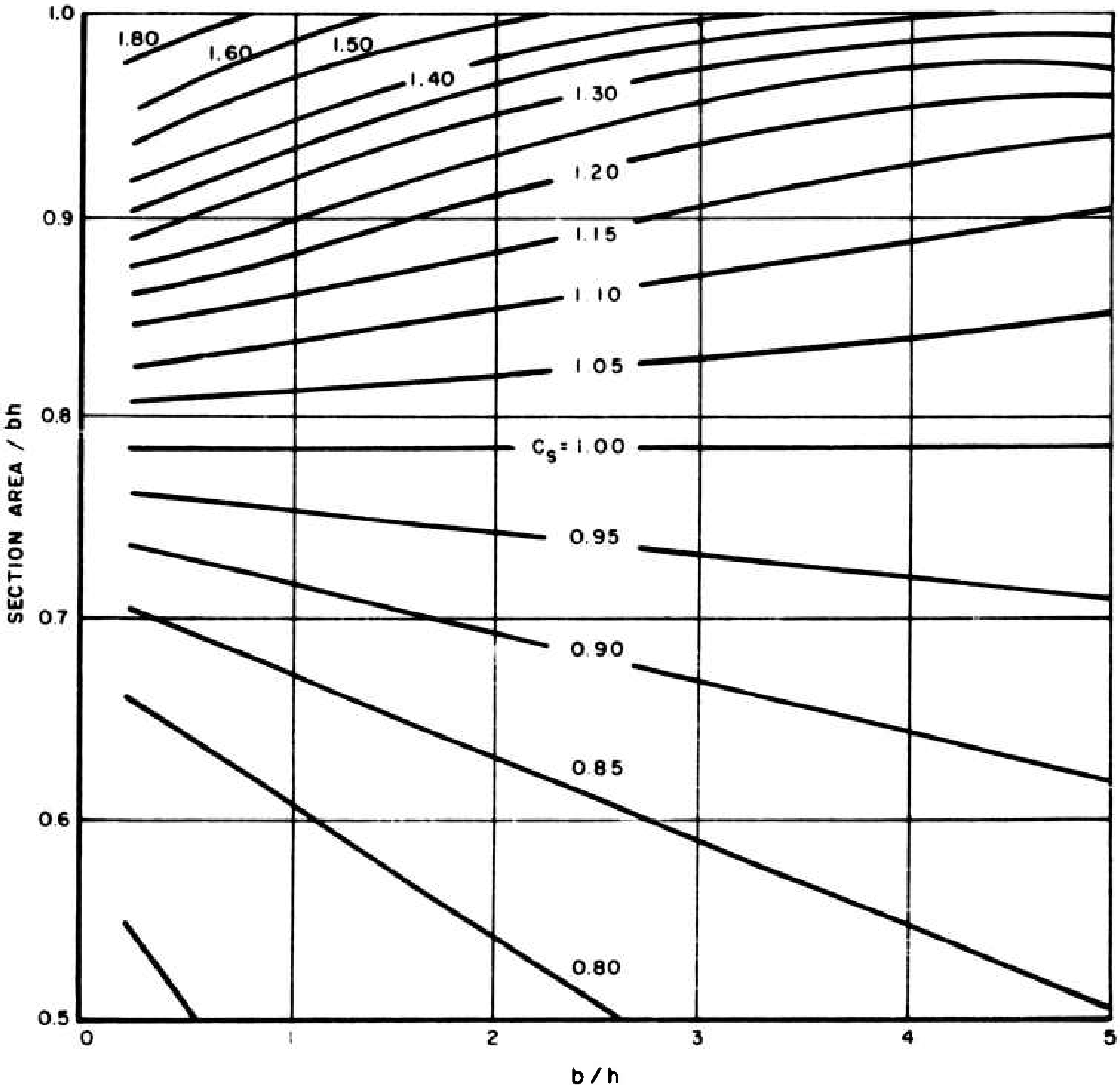


FIGURE 3. SECTIONAL INERTIA COEFFICIENTS $C_s$ AS FUNCTIONS OF THE LOCAL BEAM-DRAFT RATIO b/h AND SECTION AREA COEFFICIENT, FROM PROHASKA

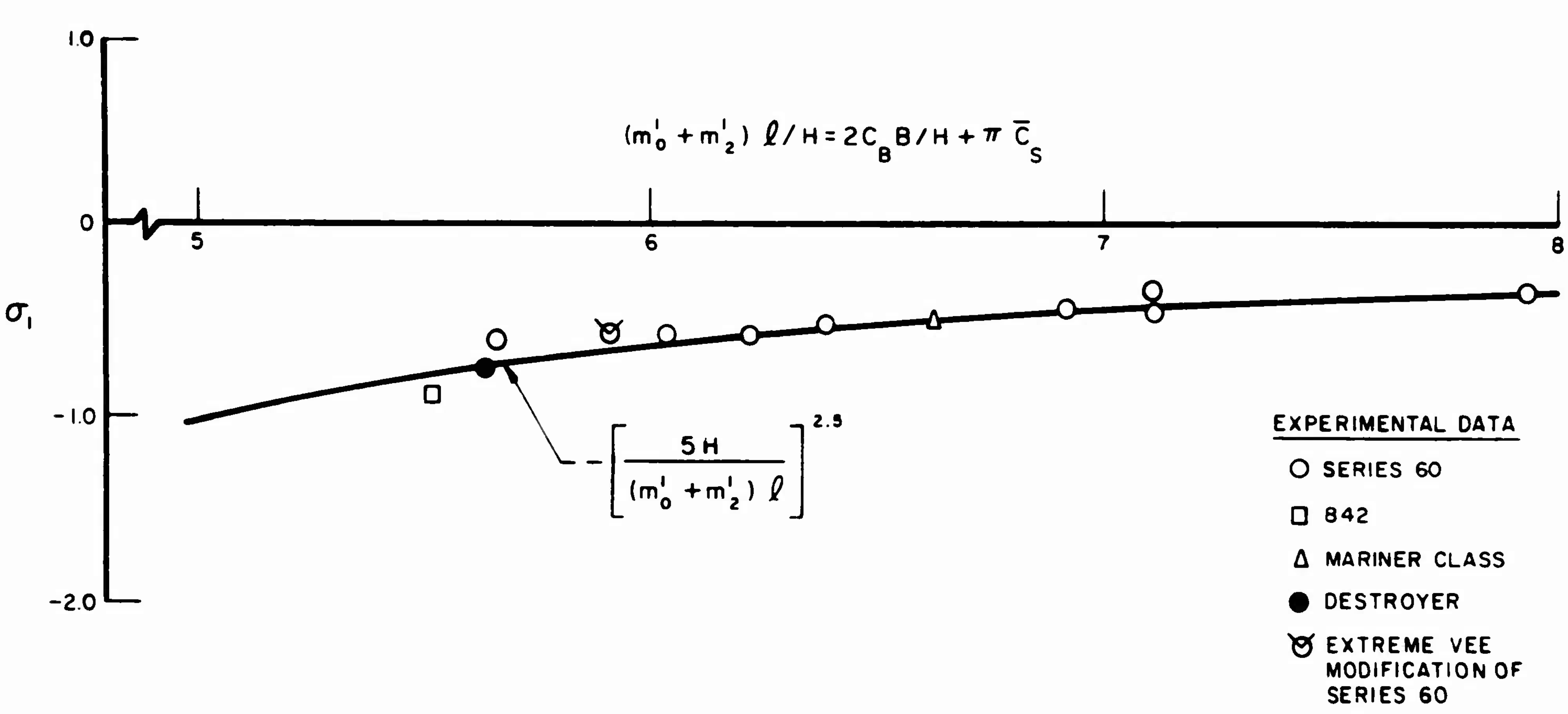


FIGURE 4. STABILITY INDEX $\sigma_1$ FOR HULLS WITH LOW ASPECT-RATIO SKEGS (DEADWOOD) TO STERN.

# APPENDIX A

## 840 SERIES HULLS

(Reference 1)

## TABLE A-1

## PERTINENT CHARACTERISTICS OF THE 840 SERIES HULLS (Taylor Standard Series)

| Model No. | 842 | 846 | 848 |
|---|---|---|---|
| Length $\ell$, ft | 6.0 | 6.0 | 6.0 |
| Beam B, ft | 0.870 | 0.870 | 0.691 |
| Draft H, ft | 0.298 | 0.188 | 0.236 |
| Displacement $\Delta$, lb | 48.40 | 30.50 | 30.50 |
| Prismatic coefficient $C_p$ (= $^{2x}0/\ell$) | 0.54 | 0.54 | 0.54 |
| Block coefficient $C_B$ | 0.50 | 0.50 | 0.50 |
| LCG/$\ell$, from bow | 0.520 | 0.481 | 0.481 |
| B/H | 2.92 | 4.62 | 2.92 |
| $\ell$/B | 6.90 | 6.90 | 8.68 |
| $\ell$/H | 20.13 | 31.90 | 25.42 |

### Lamb's Coefficients of Accession to Inertia for Equivalent Ellipsoids

| | 842 | 846 | 848 |
|---|---|---|---|
| Major axis/minor axis, $\ell$/2H | 10.06 | 15.95 | 12.71 |
| $k_1$ (longitudinal) | .020 | .012 | .017 |
| $k_2$ (lateral) | .960 | .978 | .967 |
| $k'$ (rotational) | .885 | .935 | .902 |

### Other Physical Characteristics

| | 842 | 846 | 848 |
|---|---|---|---|
| $m_o'$, mass coefficient | .145 | .145 | .115 |
| $m_1'$, longitudinal added-mass coefficient | .003 | .002 | .002 |
| $m_2'$, lateral added-mass coefficient | .129 | .084 | .103 |
| $m_z'$, rotational added-mass coefficient | .119 | .080 | .096 |
| $n_z'$, virtual moment-of-inertia coefficient | .0165 | .0141 | .0132 |
| $\bar{x}/\ell$, CG of lateral added mass from LCG | .110 | .070 | .070 |
| $x_p/\ell$, center of area of profile from LCG | .091 | .052 | .052 |
| $D_o'$ (estimated drag coefficient at $\beta$ = 0) | .014 | .018 | .014 |

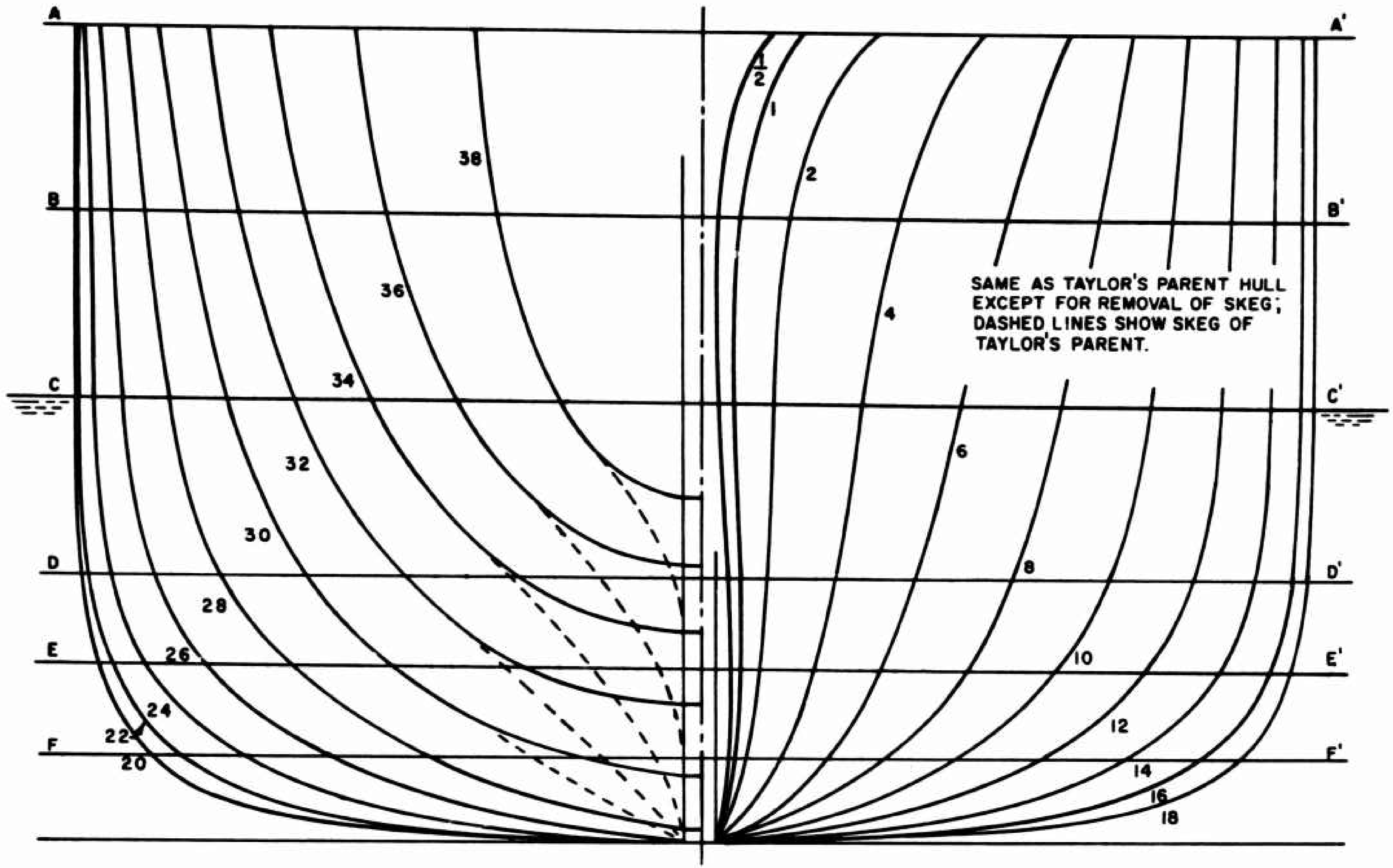


FIGURE A-1. BODY PLAN OF MODEL PARENT (840 SERIES)

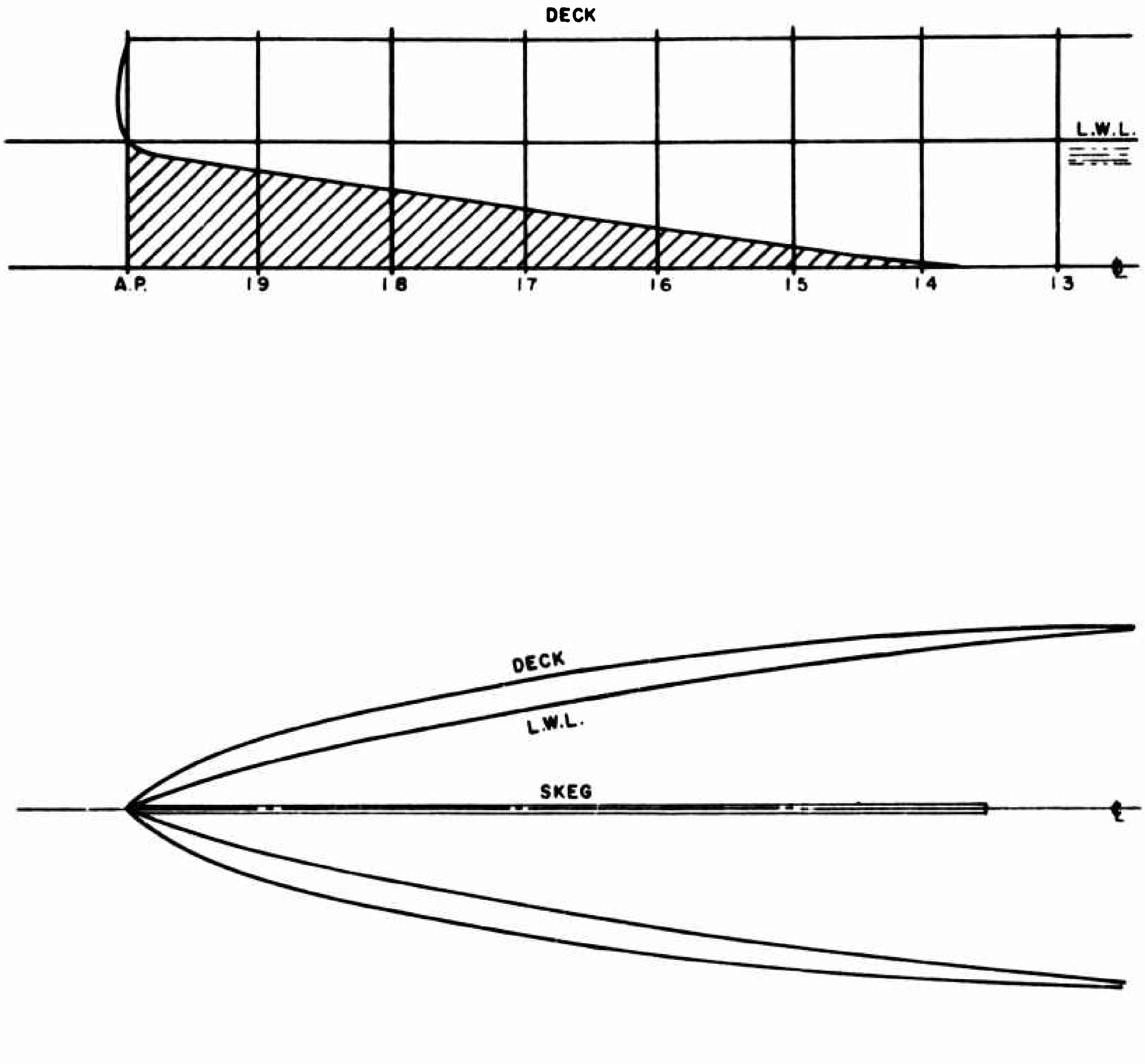


FIGURE A-2. SKEG 20 INSTALLED ON MODEL

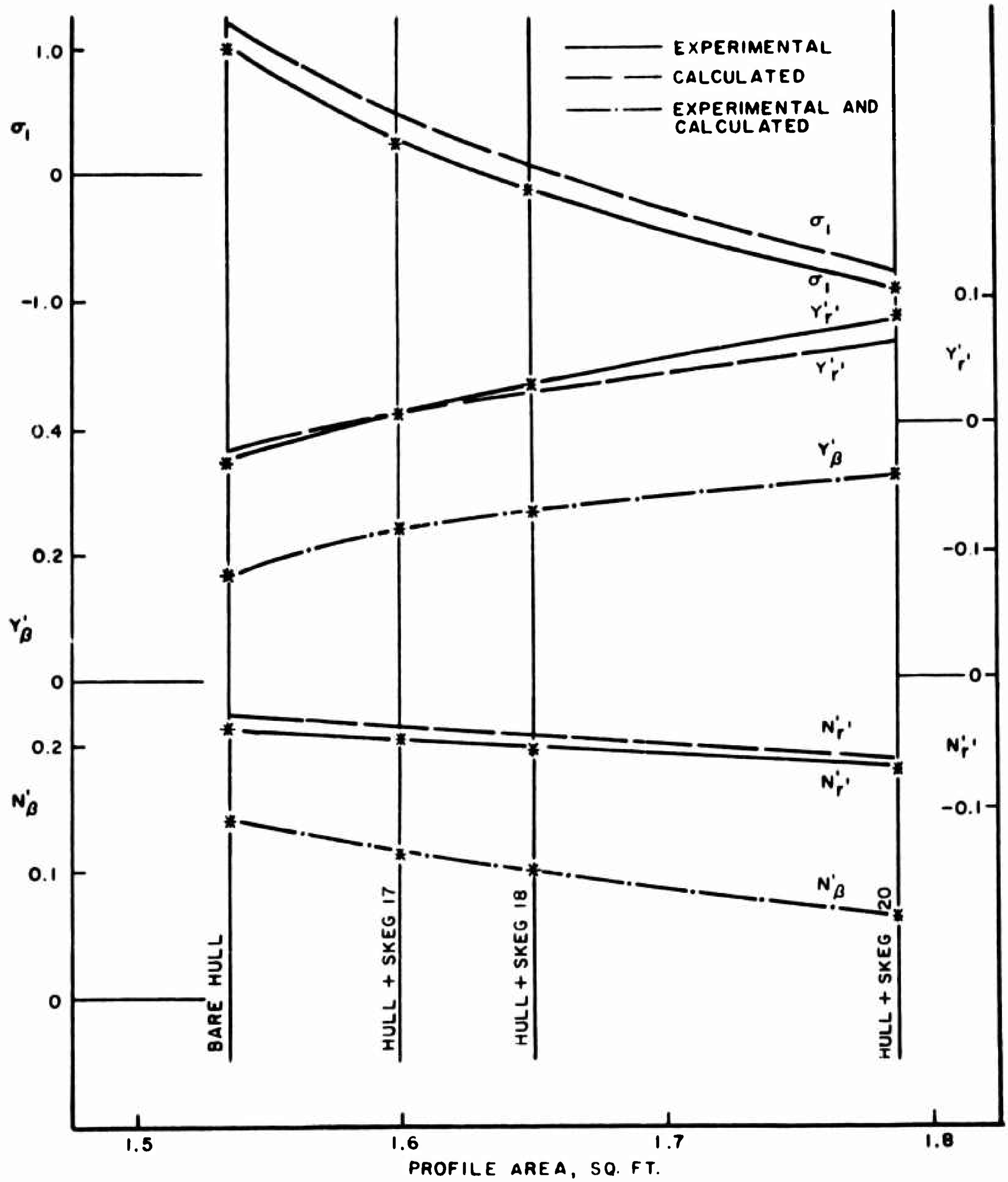


FIGURE A-3. COMPARISON OF CALCULATED AND EXPERIMENTAL STABILITY DERIVATIVES AND INDICES FOR 842 HULL WITH VARIOUS SKEGS

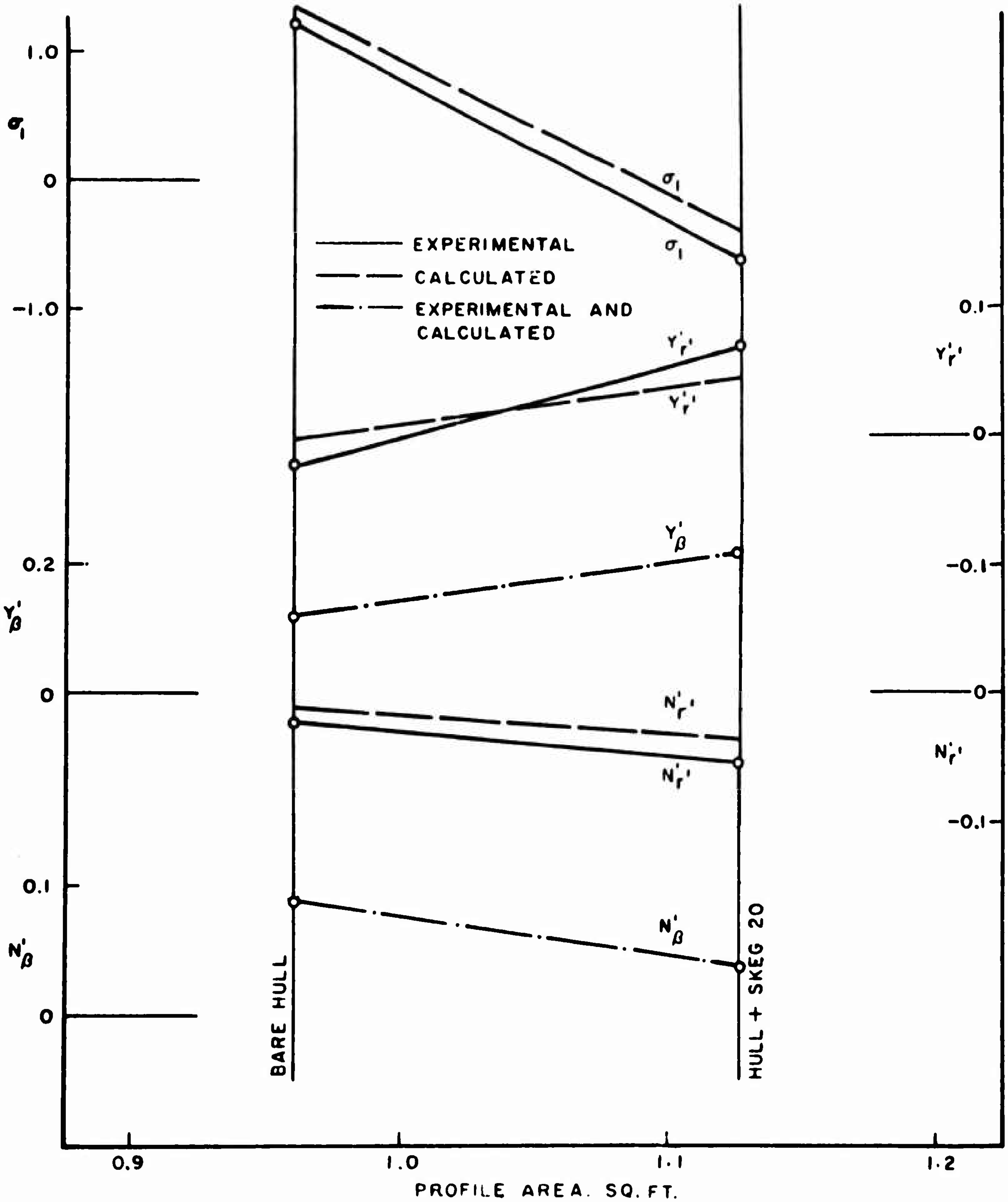


FIGURE A-4. COMPARISON OF CALCULATED AND EXPERIMENTAL STABILITY DERIVATIVES AND INDICES FOR 846 HULL WITHOUT AND WITH SKEG

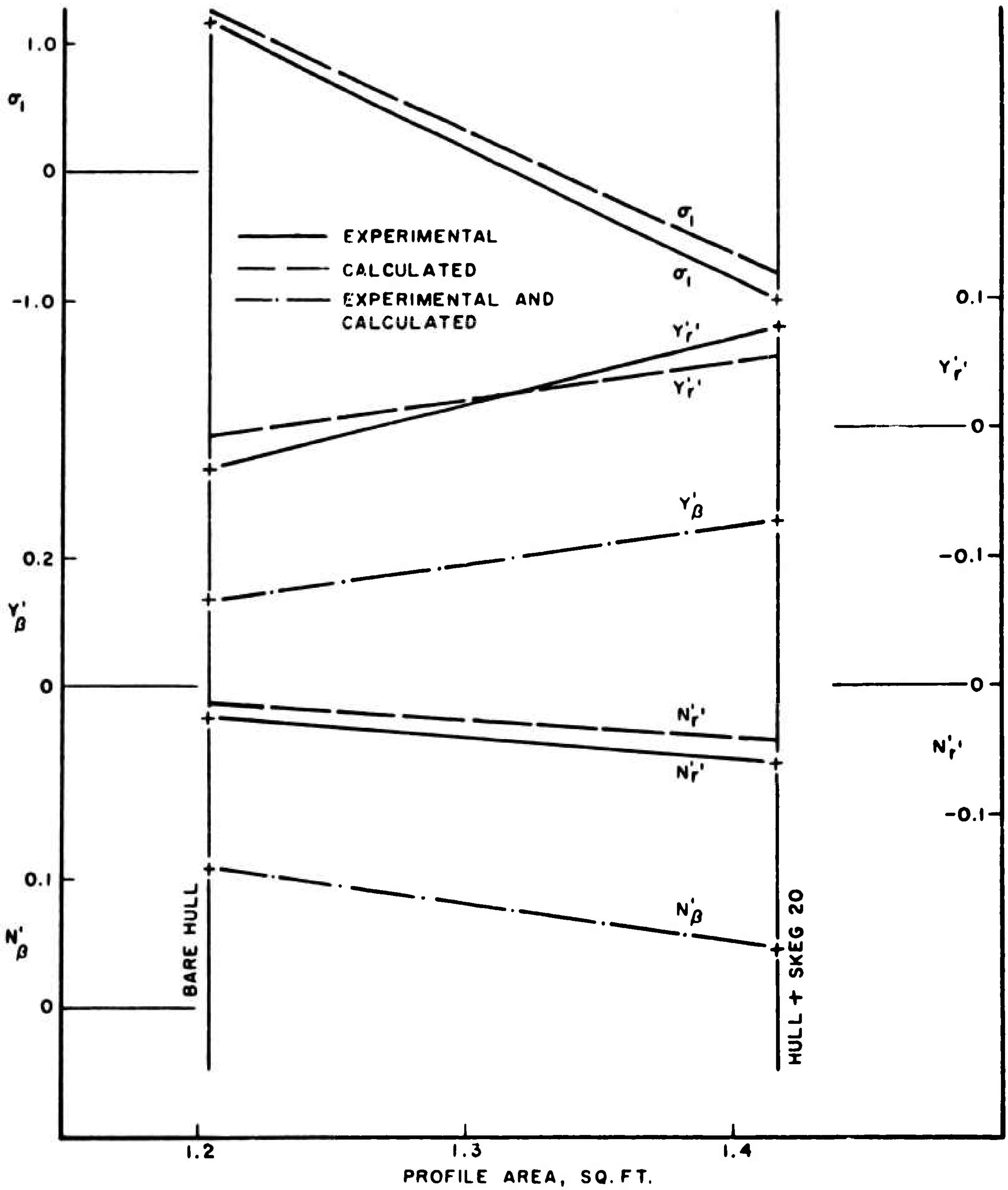


FIGURE A-5. COMPARISON OF CALCULATED AND EXPERIMENTAL STABILITY DERIVATIVES AND INDICES FOR 848 HULL WITHOUT AND WITH SKEG

BLANK PAGE

# APPENDIX B

## SERIES 60 HULLS

(Reference 4)

## TABLE B-1

## PERTINENT CHARACTERISTICS OF THE SERIES 60 HULLS

| Model | 1,1,1 | 2,1,1 | 2,1,2 | 2,1,3 | 3,1,1 | 4,1,1 | 5,1,1 | 6,1,1 | 7,1,1 | 8,1,1 |
|---|---|---|---|---|---|---|---|---|---|---|
| Length $\ell$, ft (LBP) | 5.0 | → | → | → | → | → | → | → | → | → |
| Beam B, ft | 0.667 | 0.714 | → | → | 0.833 | 0.625 | 0.714 | → | → | → |
| Draft H, ft | 0.267 | → | → | → | → | → | 0.2175 | 0.345 | 0.267 | → |
| Displacement $\Delta$, lb | 33.27 | 35.63 | → | → | 41.56 | 31.19 | 29.10 | 46.07 | 41.64 | 47.50 |
| Prismatic coefficient, $C_p = 2x_o/\ell$ | 0.614 | → | → | → | → | → | 0.616 | 0.614 | 0.713 | 0.807 |
| Block coefficient $C_B$ | 0.6 | → | → | → | → | → | → | → | 0.7 | 0.8 |
| LCG/$\ell$ from bow | 0.515 | → | → | → | → | → | → | → | 0.505 | 0.475 |
| B/H | 2.50 | 2.68 | → | → | 3.12 | 2.34 | 3.28 | 2.07 | 2.68 | 2.68 |
| $\ell$/B | 7.5 | 7.0 | → | → | 6.0 | 8.0 | 7.0 | 7.0 | 7.0 | 7.0 |
| $\ell$/H | 18.75 | → | → | → | → | → | 23.00 | 14.50 | 18.75 | → |
| Rudder span, ft | 0.200 | → | → | → | → | → | 0.164 | 0.258 | 0.200 | 0.200 |
| Rudder chord, ft | 0.105 | 0.105 | 0.167 | 0.080 | 0.105 | → | → | → | → | → |
| **Lamb's Coefficients of Accession to Inertia for Equivalent Ellipsoids** | | | | | | | | | | |
| Minor axis/major axis, 2H/$\ell$ | 0.1067 | → | → | → | → | → | 0.0870 | 0.0690 | 0.1067 | → |
| $k_1$ (longitudinal) | 0.022 | → | → | → | → | → | 0.019 | 0.033 | 0.022 | → |
| $k_2$ (lateral) | 0.957 | → | → | → | → | → | 0.968 | 0.940 | 0.957 | → |
| $k'$ (rotational) | 0.875 | → | → | → | → | → | 0.903 | 0.820 | 0.875 | → |
| **Other Physical Characteristics** | | | | | | | | | | |
| $m'_o$, mass coefficient | 0.160 | 0.171 | → | → | 0.200 | 0.150 | 0.171 | 0.171 | 0.200 | 0.229 |
| $m'_1$, longitudinal added-mass coefficient | 0.003 | 0.004 | → | → | 0.004 | 0.003 | 0.004 | 0.006 | 0.004 | 0.005 |
| $m'_a$, lateral added-mass coefficient | 0.171 | 0.170 | → | → | 0.169 | 0.172 | 0.138 | 0.220 | 0.180 | 0.194 |
| $m'_z$, rotational added-mass coefficient | 0.153 | 0.152 | → | → | 0.151 | 0.154 | 0.127 | 0.192 | 0.165 | 0.175 |
| $n'_z$, virtual moment-of-inertia coefficient | 0.0213 | 0.0219 | → | → | 0.0237 | 0.0206 | 0.0202 | 0.0239 | 0.0237 | 0.0271 |
| $\bar{x}/\ell$, CG of lateral added mass from LCG | 0.048 | 0.049 | → | → | 0.048 | 0.049 | 0.048 | 0.049 | 0.039 | 0.005 |
| $x_p/\ell$, center of area of profile from LCG | 0.028 | → | → | → | → | → | 0.033 | 0.028 | 0.026 | -0.016 |
| $D'_o$ (estimated drag coefficient at $\beta$=0) | 0.015 | → | → | → | 0.017 | 0.014 | 0.017 | 0.015 | 0.019 | 0.021 |

## TABLE B-2

## STABILITY DERIVATIVES FOR THE SERIES 60 HULLS

| a) Models with Rudder and Propeller* | 1,1,1 | 2,1,1 | 2,1,2 | 2,1,3 | 3,1,1 | 4,1,1 | 5,1,1 | 6,1,1 | 7,1,1 | 8,1,1 |
|---|---|---|---|---|---|---|---|---|---|---|
| **Estimated from Theory** | | | | | | | | | | |
| $Y'_\beta = L'_\beta$ | 0.335 | 0.335 | 0.347 | 0.329 | 0.335 | 0.335 | 0.273 | 0.434 | 0.335 | 0.335 |
| $N'_\beta$ | 0.088 | 0.086 | 0.080 | 0.089 | 0.085 | 0.089 | 0.071 | 0.114 | 0.097 | 0.095 |
| $m'_x - Y'_{r'}$ | 0.083 | 0.095 | 0.089 | 0.098 | 0.124 | 0.083 | 0.110 | 0.077 | 0.125 | 0.140 |
| $N'_{r'}$ | -0.066 | -0.066 | -0.069 | -0.065 | -0.066 | -0.066 | -0.054 | -0.081 | -0.068 | -0.077 |
| $\sigma_1$ | -0.59 | -0.55 | -0.64 | -0.49 | -0.41 | -0.61 | -0.33 | -0.76 | -0.35 | -0.33 |
| **Estimated from "Least Squares" Fit of Experimental Data** | | | | | | | | | | |
| $Y'_\beta$ | 0.255 | 0.305 | 0.311 | 0.293 | 0.308 | 0.283 | 0.260 | 0.387 | 0.335 | 0.323 |
| $N'_\beta$ | 0.110 | 0.095 | 0.081 | 0.100 | 0.089 | 0.091 | 0.075 | 0.132 | 0.096 | 0.086 |
| $m'_x - Y'_{r'}$ | 0.040 | 0.081 | 0.075 | 0.089 | 0.111 | 0.062 | 0.077 | 0.077 | 0.127 | 0.125 |
| $N'_{r'}$ | -0.080 | -0.070 | -0.076 | -0.073 | -0.075 | -0.066 | -0.057 | -0.081 | -0.068 | -0.070 |
| $\sigma_1$ | -0.57 | -0.52 | -0.62 | -0.45 | -0.42 | -0.56 | -0.45 | -0.60 | -0.34 | -0.34 |

*Propeller revolutions adjusted to obtain zero drag condition.

| b) Models without Rudder or Propeller | 1,0,0 | 2,0,0 | 3,0,0 | 4,0,0 | 5,0,0 | 6,0,0 | 7,0,0 | 8,0,0 |
|---|---|---|---|---|---|---|---|---|
| **Estimated from Theory** | | | | | | | | |
| $Y'_\beta = L'_\beta + D'_o$ | 0.303 | 0.303 | 0.305 | 0.302 | 0.247 | 0.395 | 0.306 | 0.309 |
| $N'_\beta$ | 0.112 | 0.110 | 0.109 | 0.113 | 0.092 | 0.140 | 0.121 | 0.121 |
| $m'_x - Y'_{r'}$ | 0.108 | 0.119 | 0.148 | 0.108 | 0.131 | 0.103 | 0.149 | 0.165 |
| $N'_{r'}$ | -0.055 | -0.055 | -0.055 | -0.055 | -0.043 | -0.068 | -0.056 | -0.064 |
| $\sigma_1$ | -0.20 | -0.15 | -0.027 | -0.20 | +0.075 | -0.38 | +0.32 | +0.005 |
| **Estimated from "Least Squares" Fit of Experimental Data** | | | | | | | | |
| $Y'_\beta$ | | 0.245 | 0.237 | 0.260 | 0.217 | 0.315 | 0.287 | 0.256 |
| $N'_\beta$ | | 0.114 | 0.134 | 0.116 | 0.097 | 0.140 | 0.121 | 0.093 |
| $m'_x - Y'_{r'}$ | | 0.101 | 0.134 | 0.081 | 0.100 | 0.103 | 0.149 | 0.154 |
| $N'_{r'}$ | | -0.055 | -0.054 | -0.059 | -0.045 | -0.068 | -0.056 | -0.052 |
| $\sigma_1$ | | -0.09 | +0.19 | -0.26 | 0 | -0.22 | +.067 | +0.033 |

BLANK PAGE

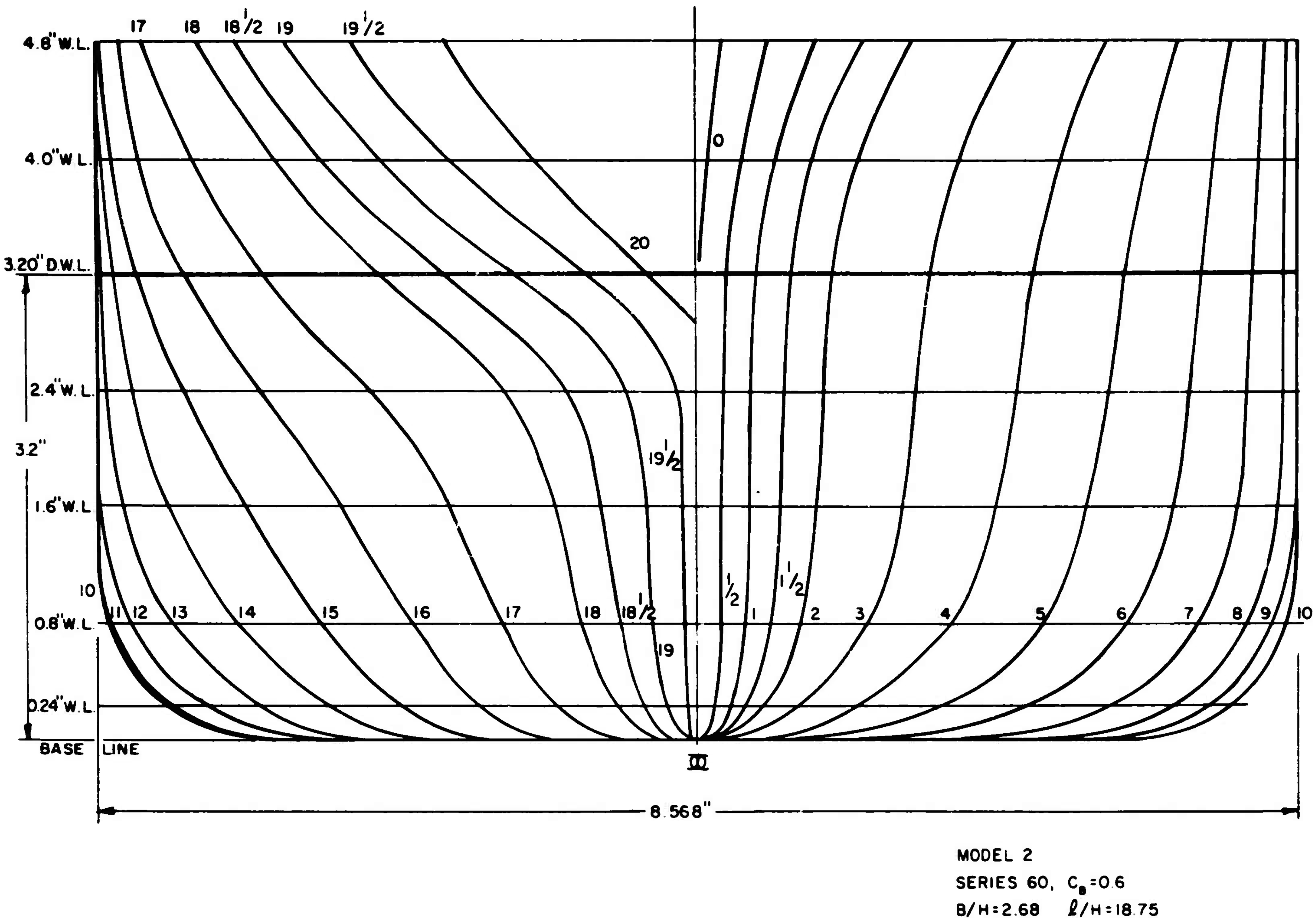


FIGURE B-1. BODY PLAN OF SERIES 60 MODEL 2

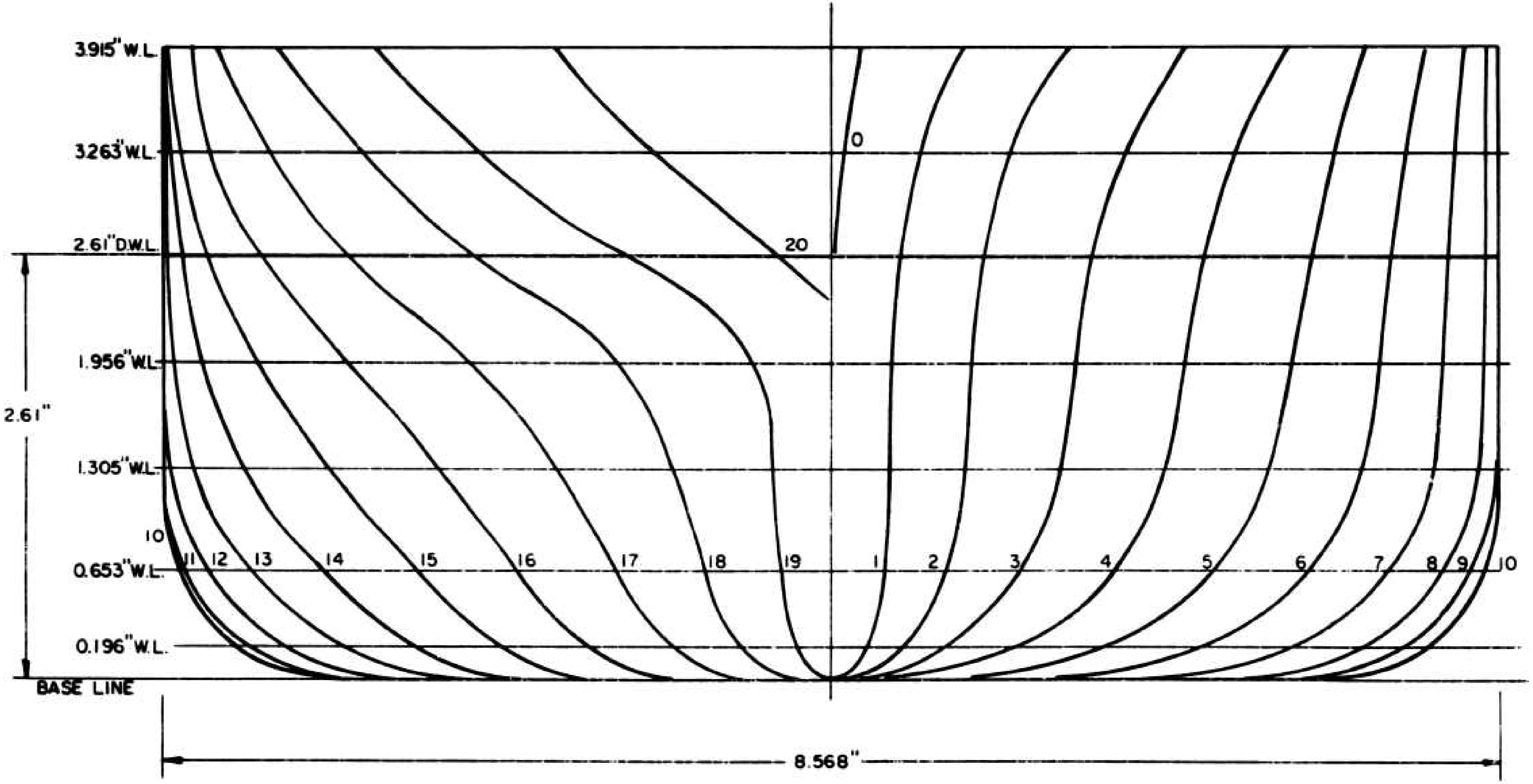


MODEL 5
SERIES 60, $C_B = 0.6$
$B/H = 3.28$, $\ell/H = 23.0$

FIGURE B-2. BODY PLAN OF SERIES 60 MODEL 5

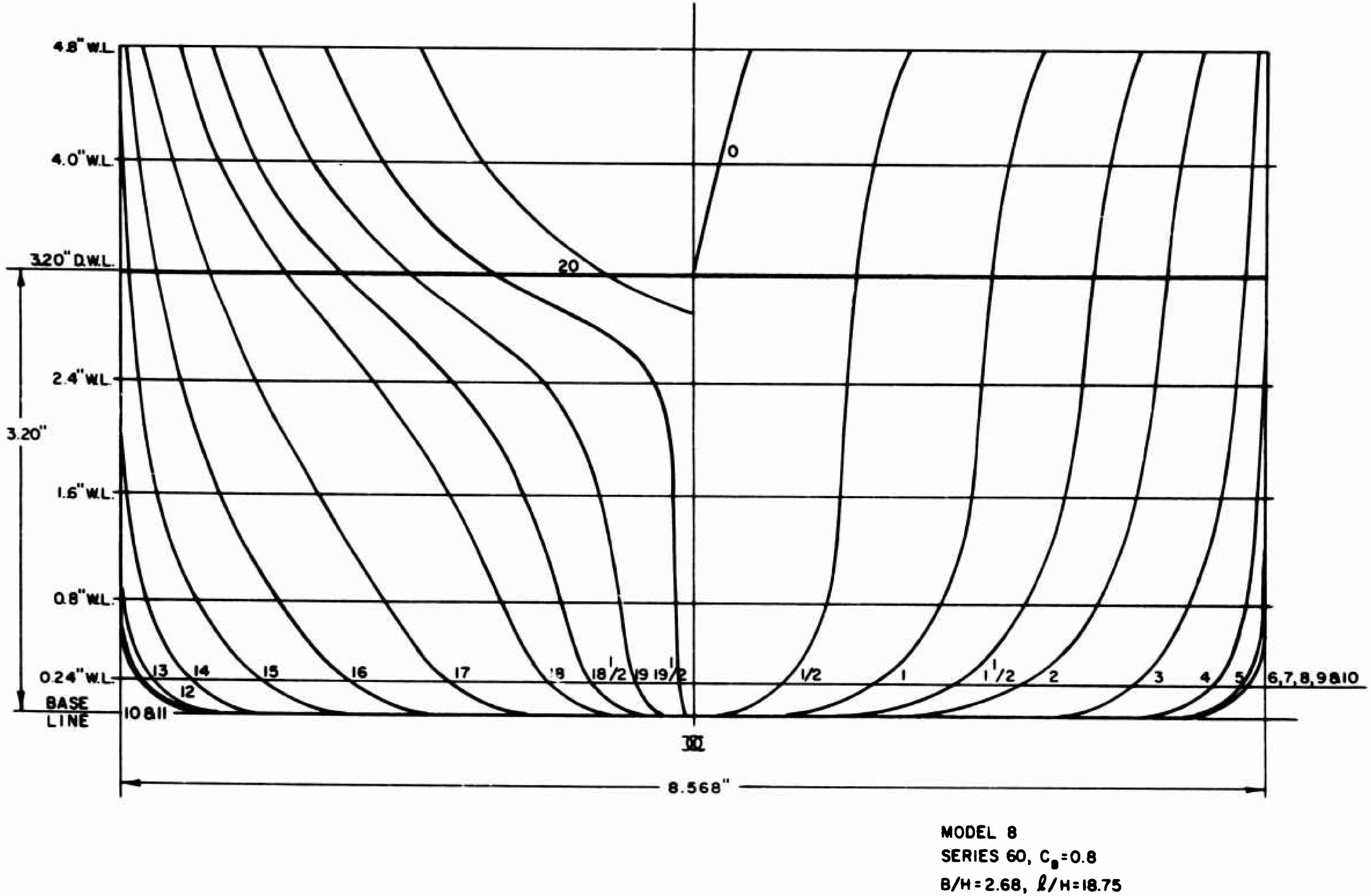


FIGURE B-3. BODY PLAN OF SERIES 60 MODEL 8

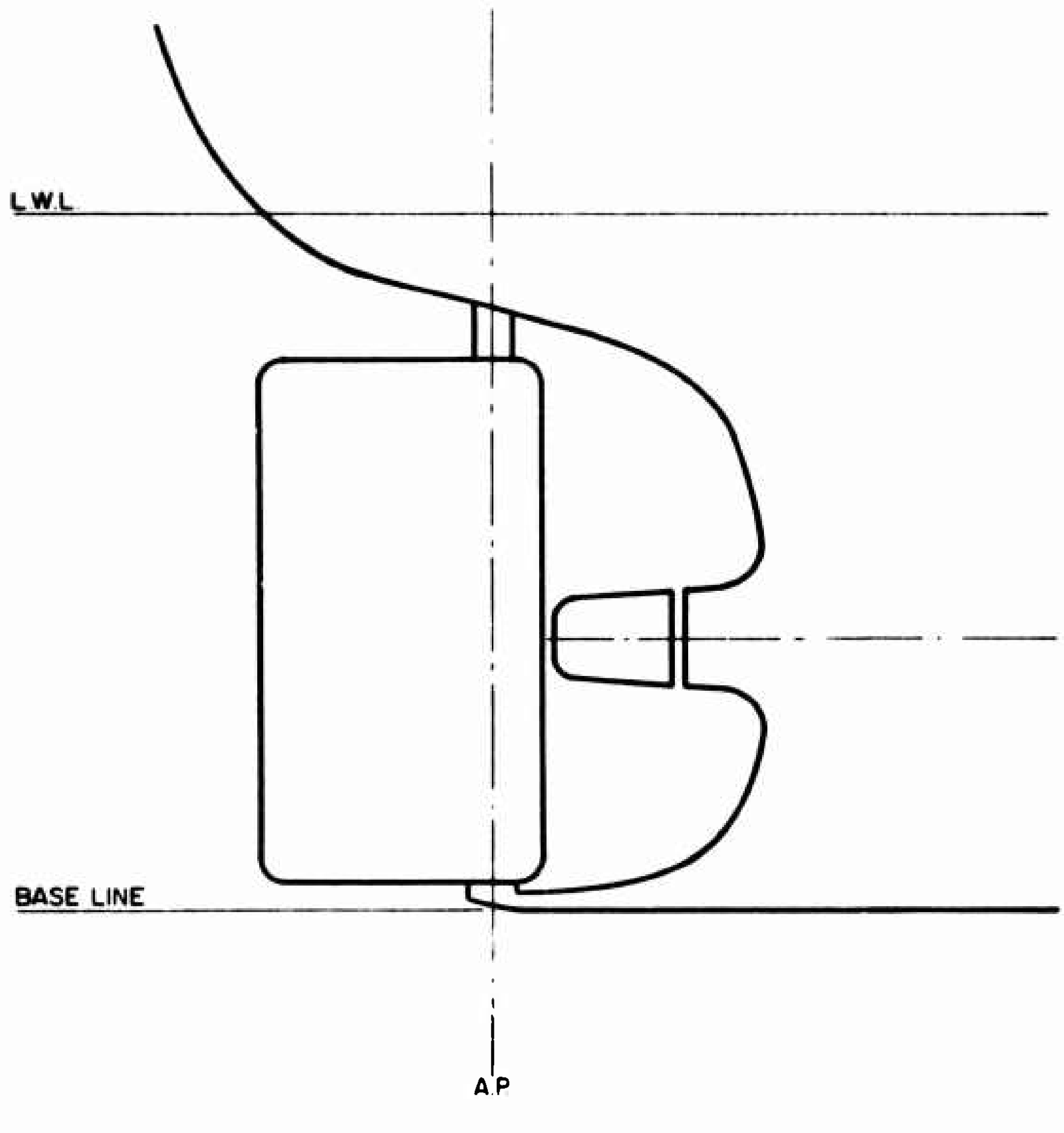


FIGURE B-4. SERIES 60, STERN PROFILE OF MODELS 1,2,3,4,7,8 WITH DESIGN RUDDER

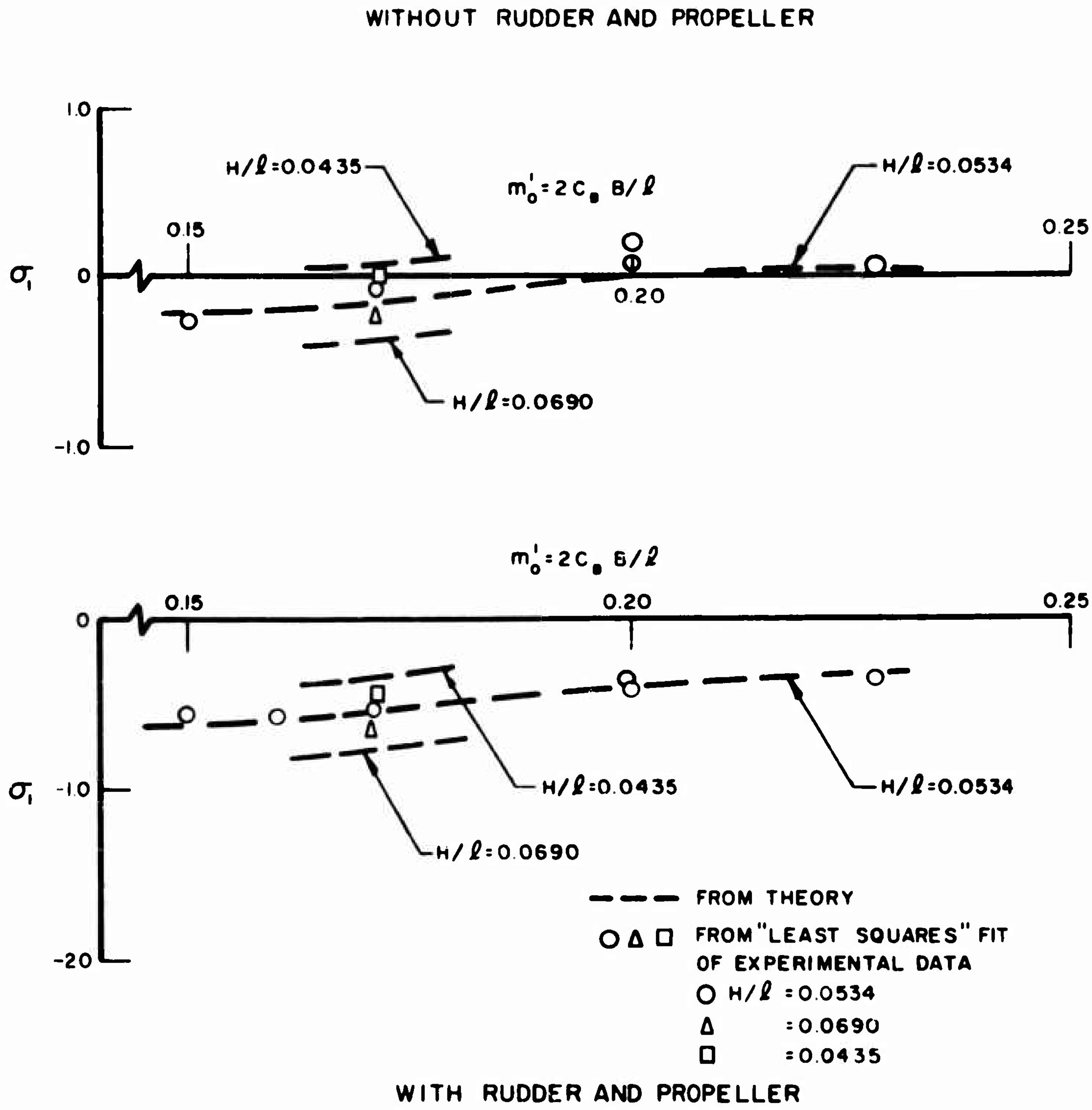


FIGURE B-5. STABILITY INDEX $\sigma_1$, FOR SERIES 60 HULLS

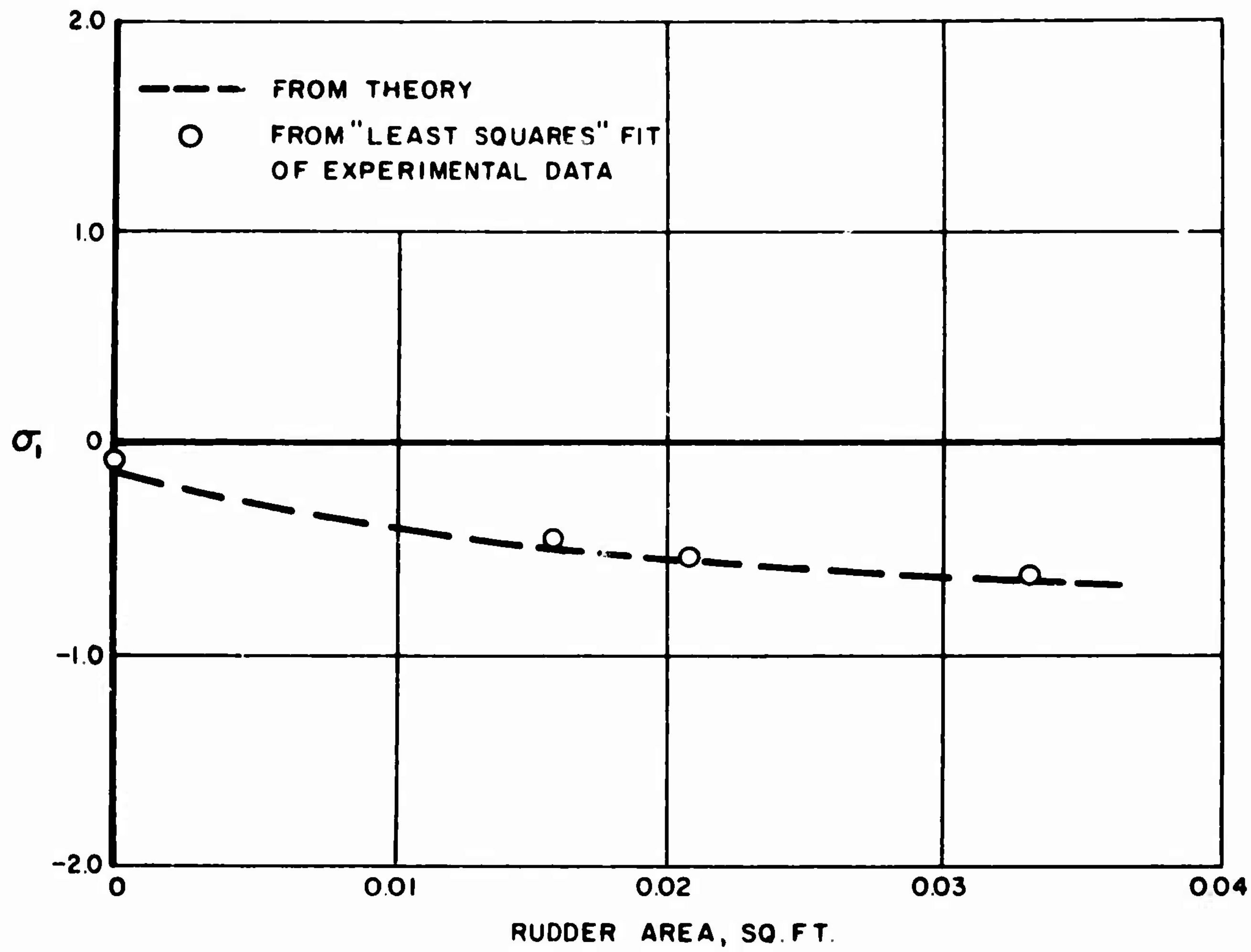


FIGURE B-6. STABILITY INDEX $\sigma_1$ FOR MODEL 2, SERIES 60, WITH RUDDERS OF VARYING CHORD

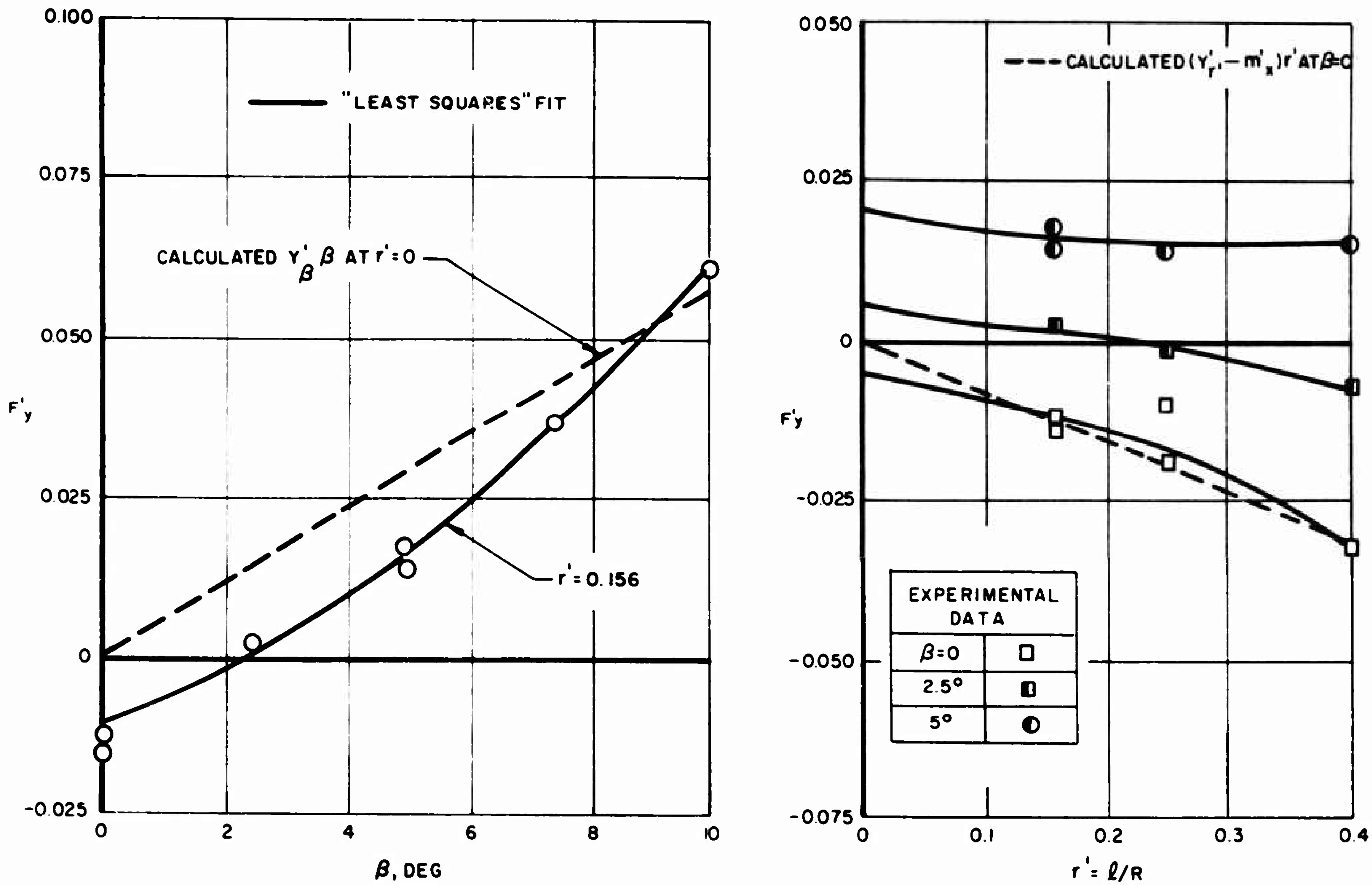


FIGURE B-7. SERIES 60, MODEL 1,1,1. TOTAL LATERAL FORCE COEFFICIENT

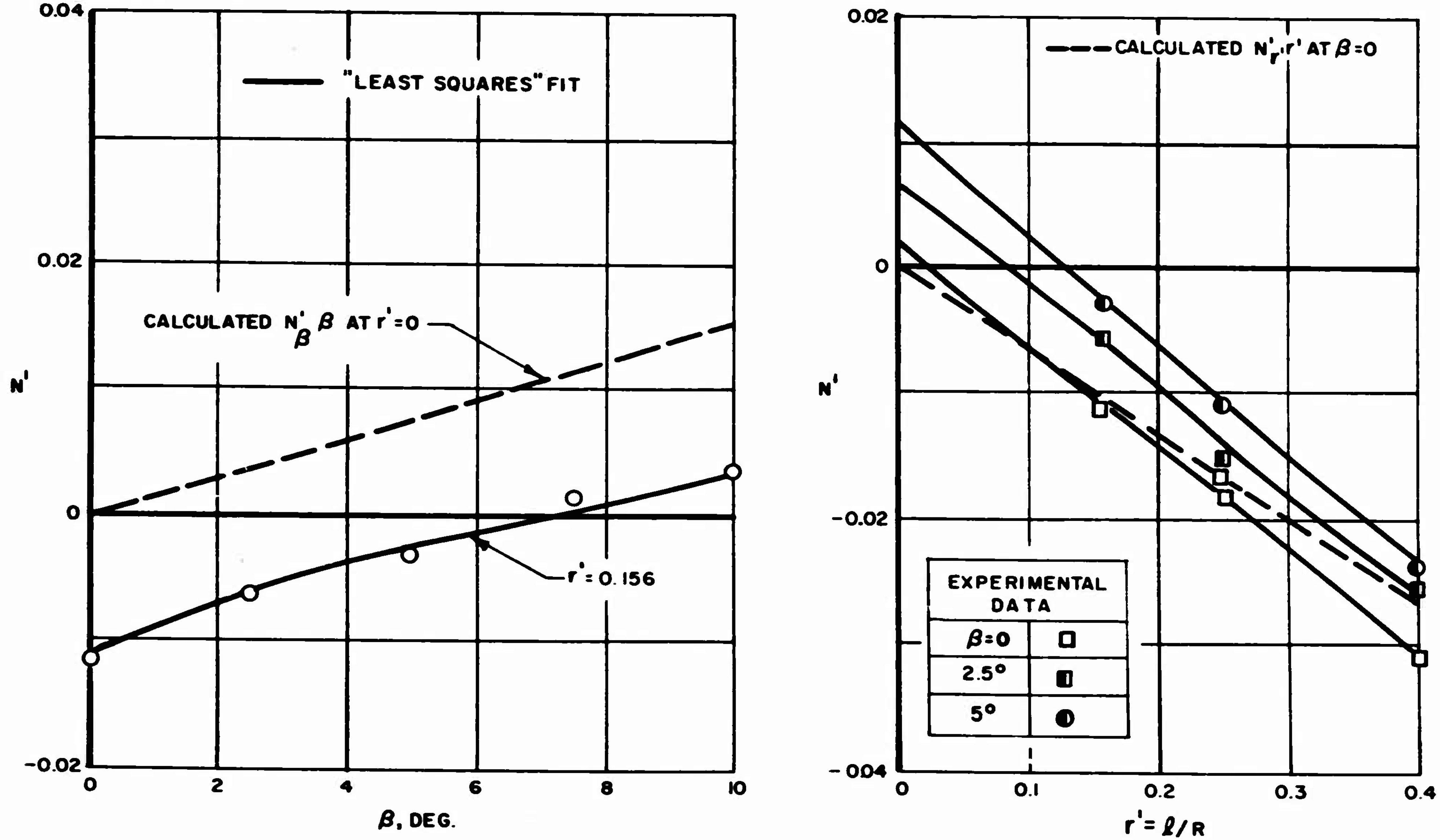


FIGURE B-8. SERIES 60, MODEL 1,1,1. YAWING MOMENT COEFFICIENT

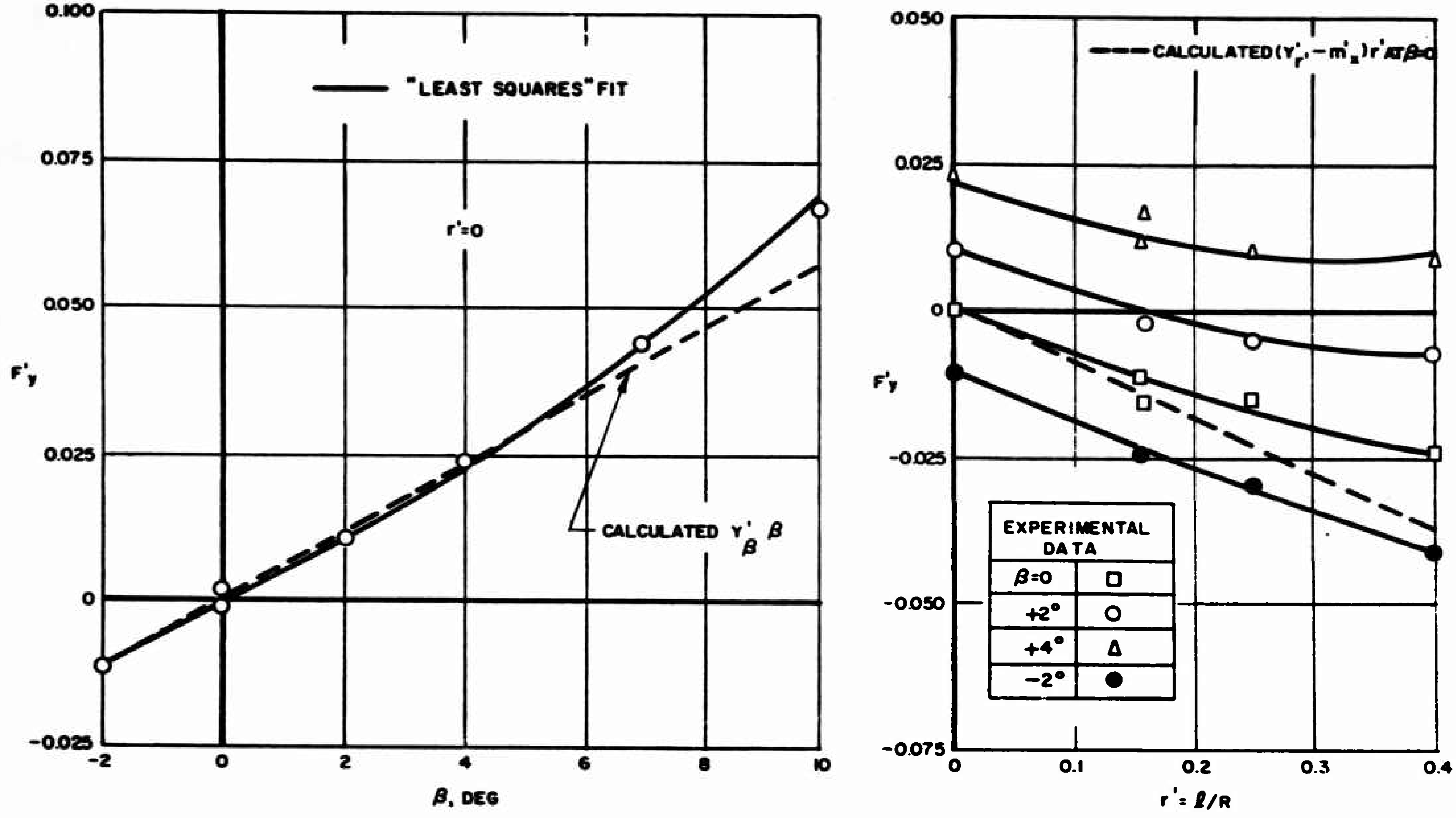


FIGURE B-9. SERIES 60, MODEL 2,1,1. TOTAL LATERAL FORCE COEFFICIENT

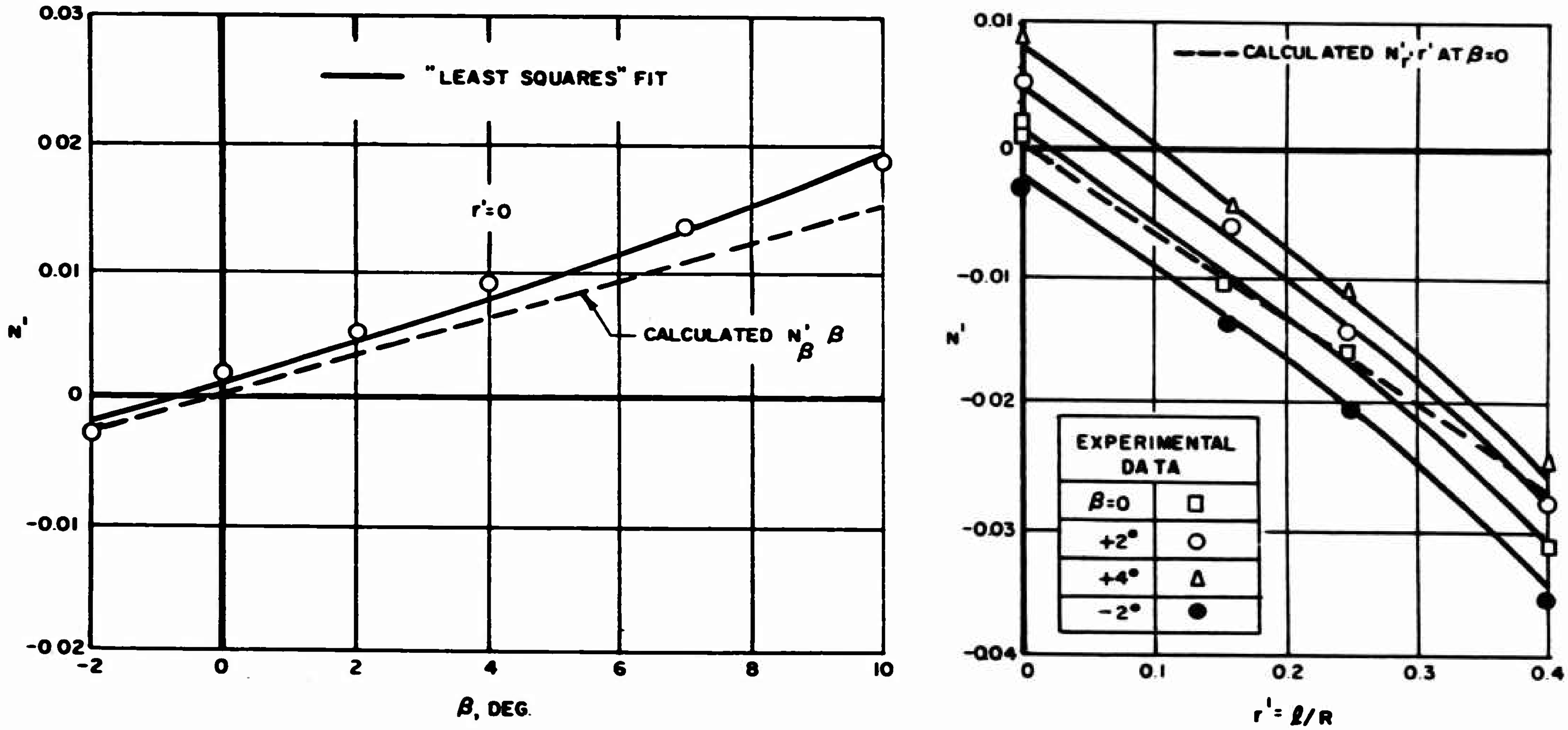


FIGURE B-10. SERIES 60, MODEL 2,1,1. YAWING MOMENT COEFFICIENT

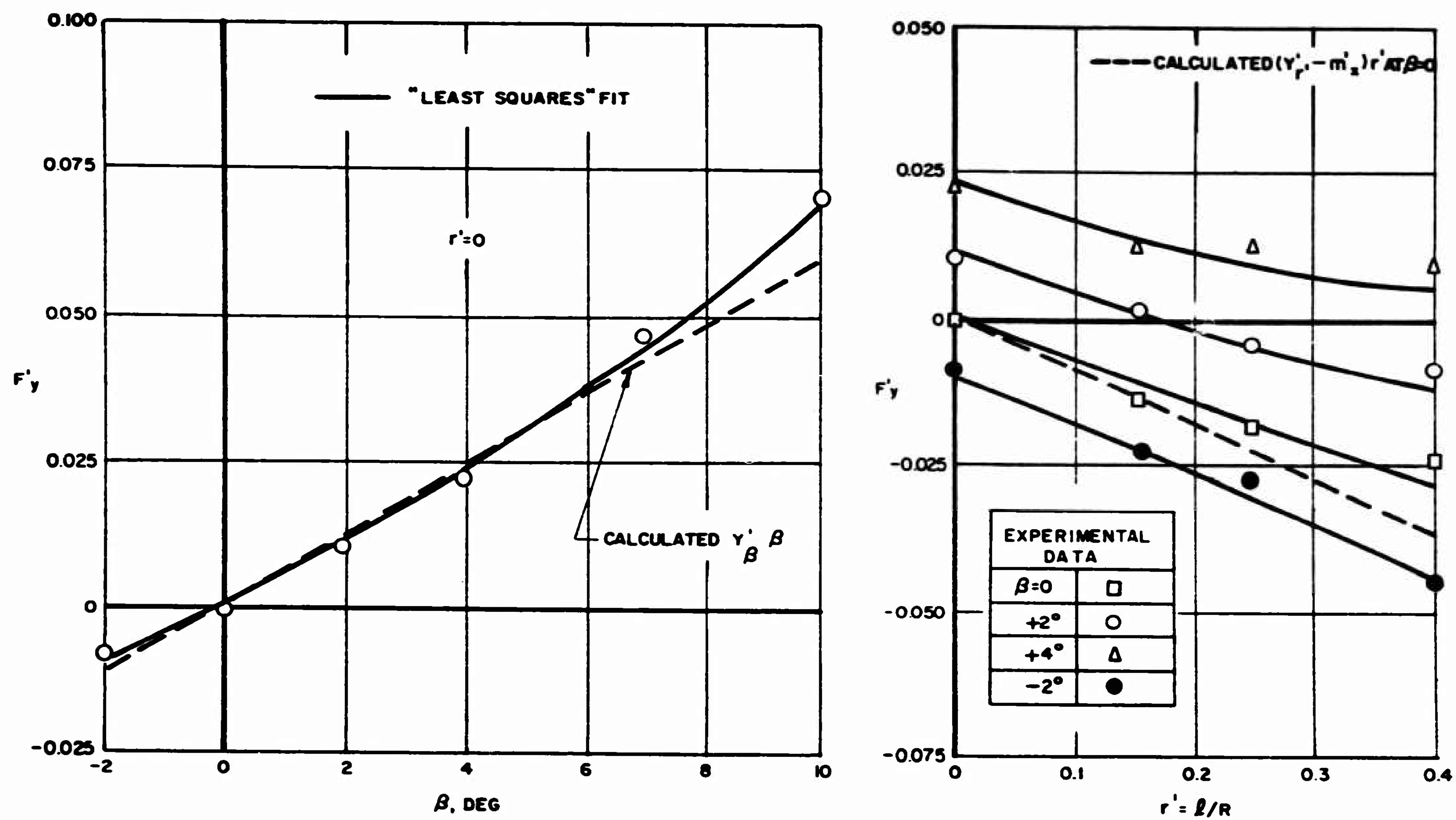


FIGURE B-11. SERIES 60, MODEL 2,1,2. TOTAL LATERAL FORCE COEFFICIENT

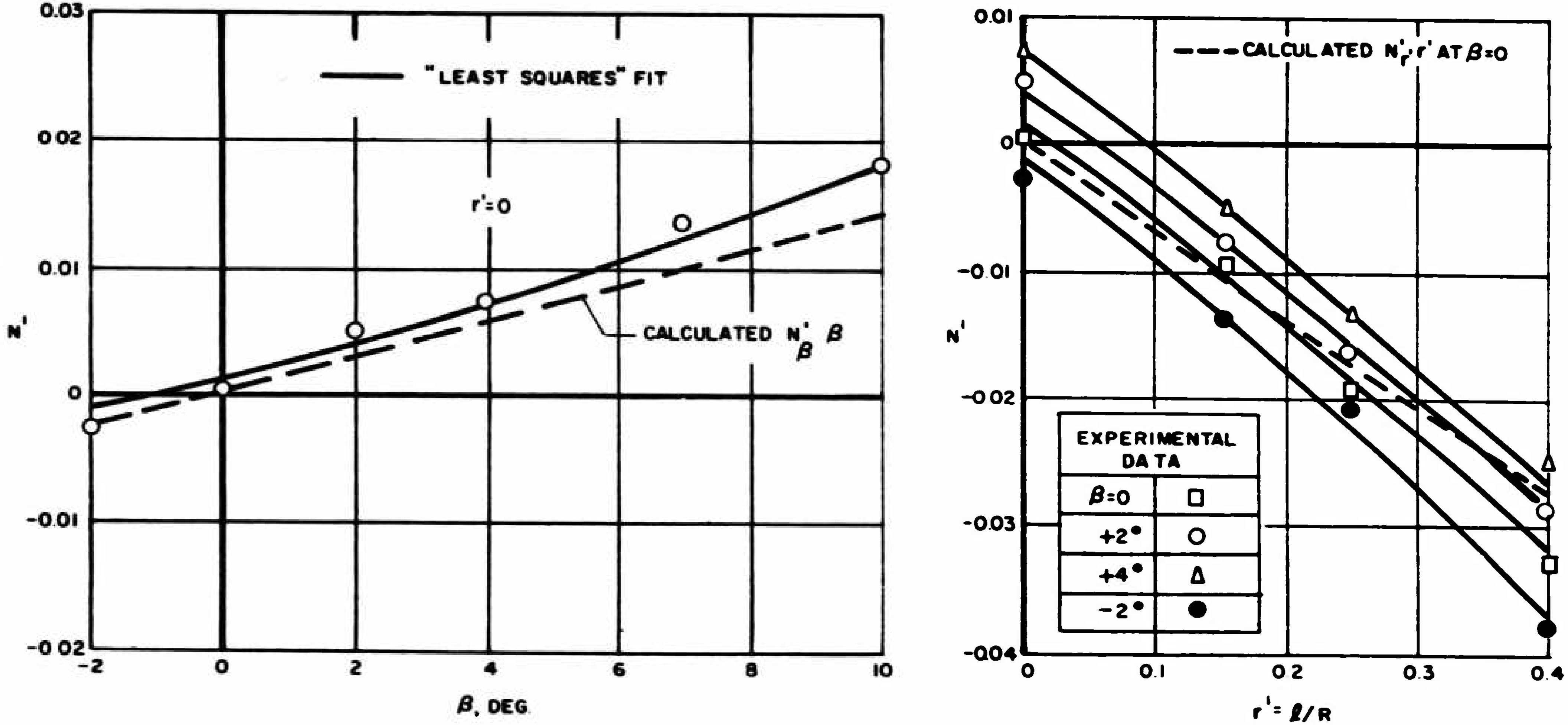


FIGURE B-12. SERIES 60, MODEL 2,1,2. YAWING MOMENT COEFFICIENT

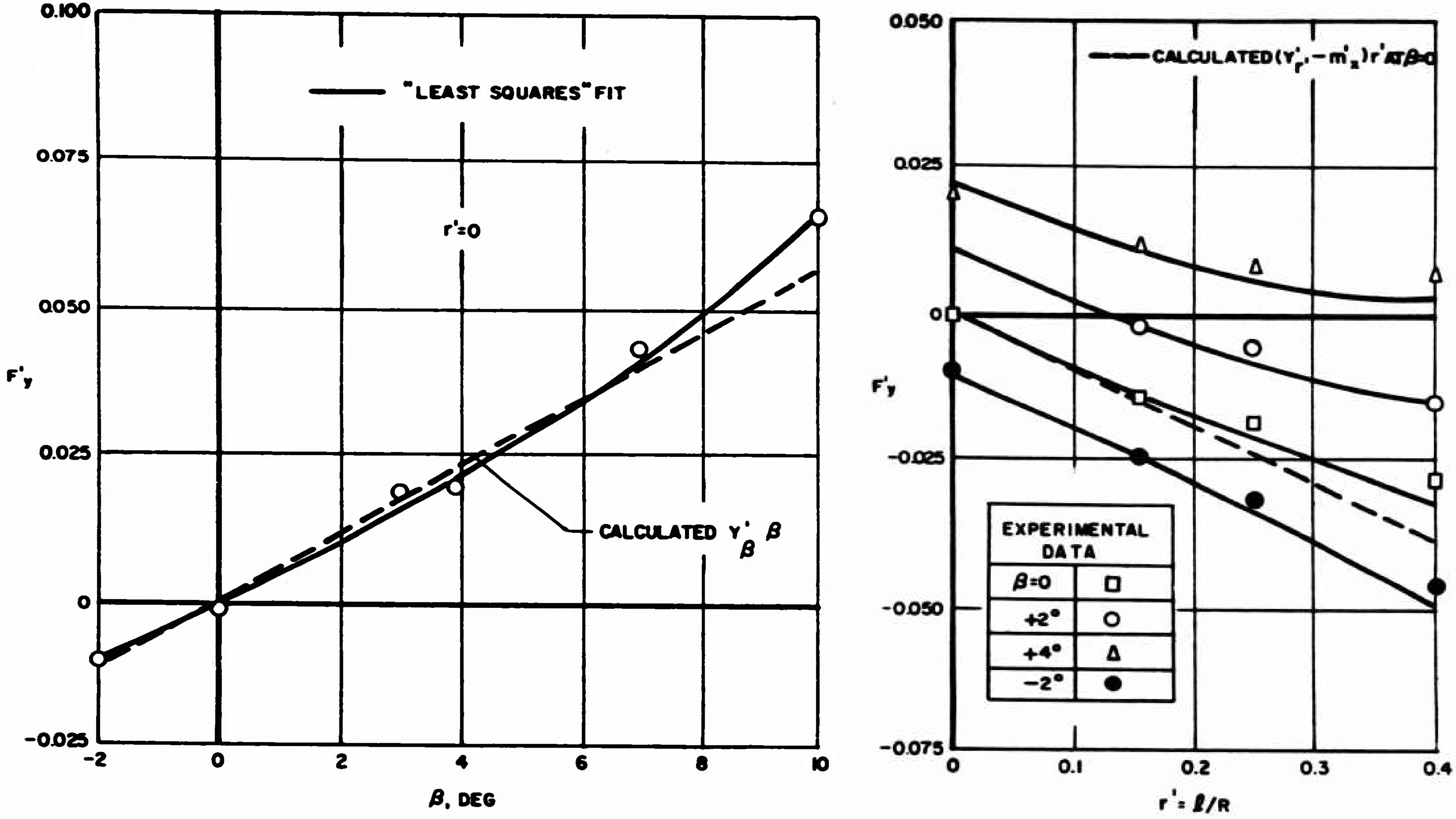


FIGURE B-13. SERIES 60, MODEL 2,1,3. TOTAL LATERAL FORCE COEFFICIENT

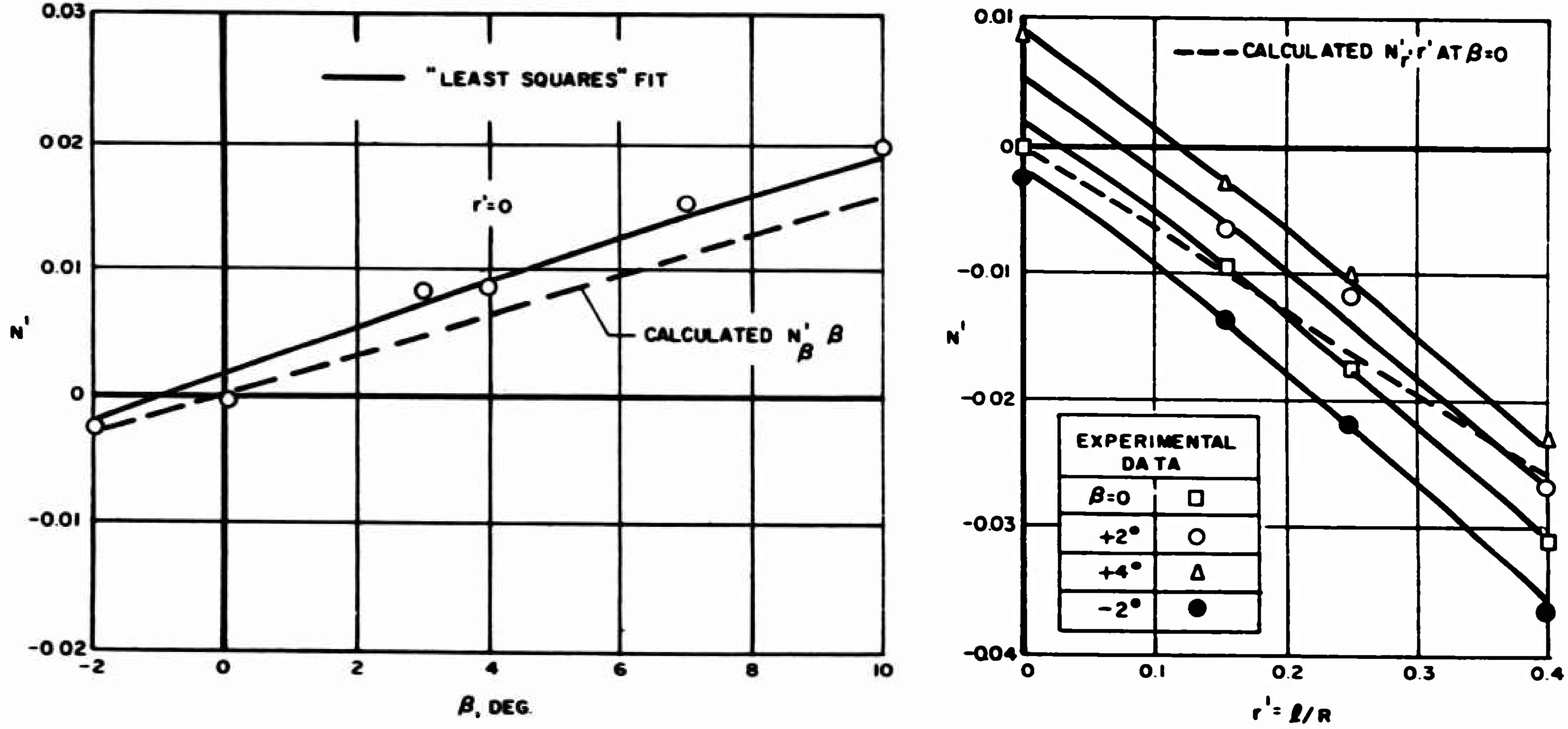


FIGURE B-14. SERIES 60, MODEL 2,1,3. YAWING MOMENT COEFFICIENT

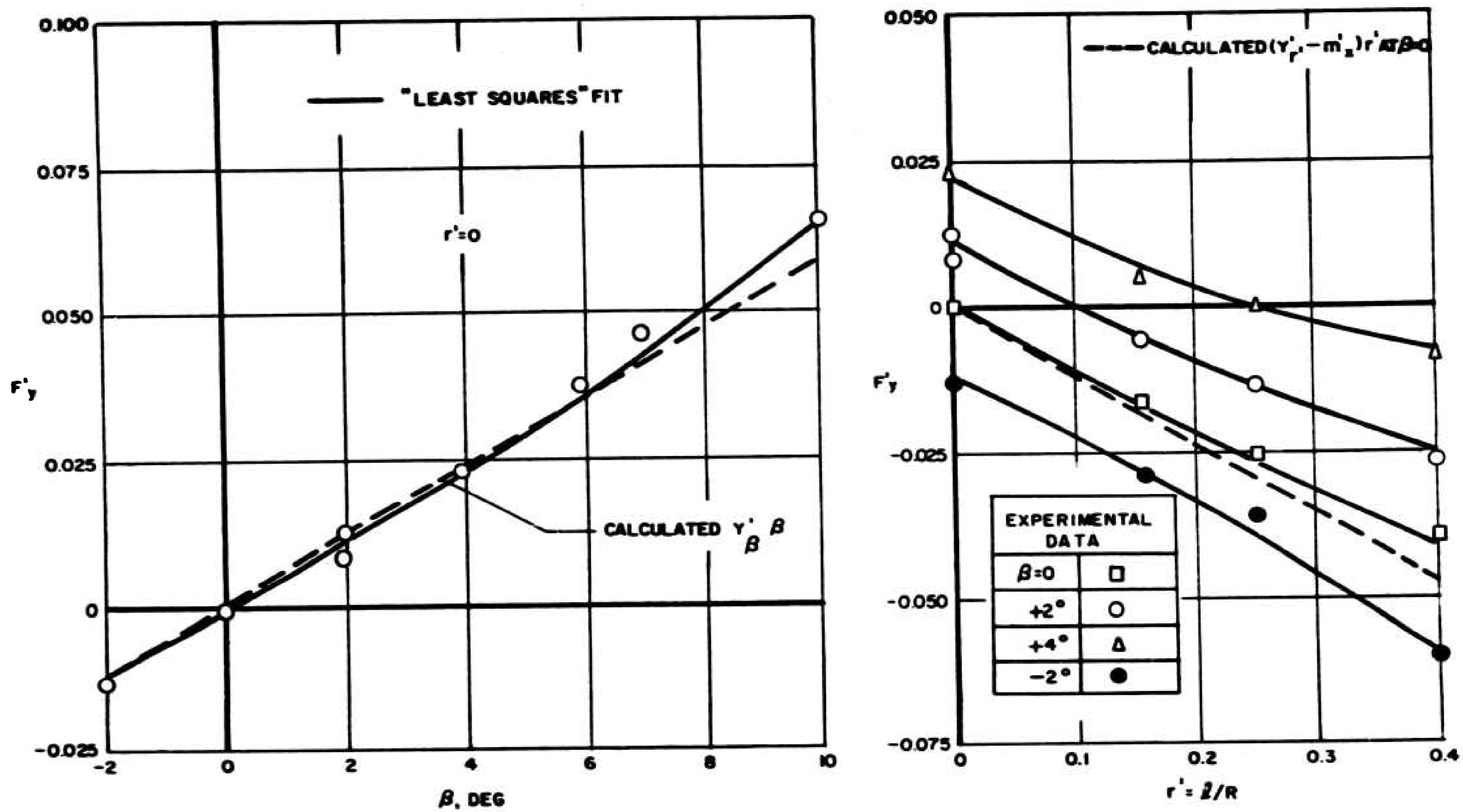


FIGURE B-15. SERIES 60, MODEL 3,1,1. TOTAL LATERAL FORCE COEFFICIENT

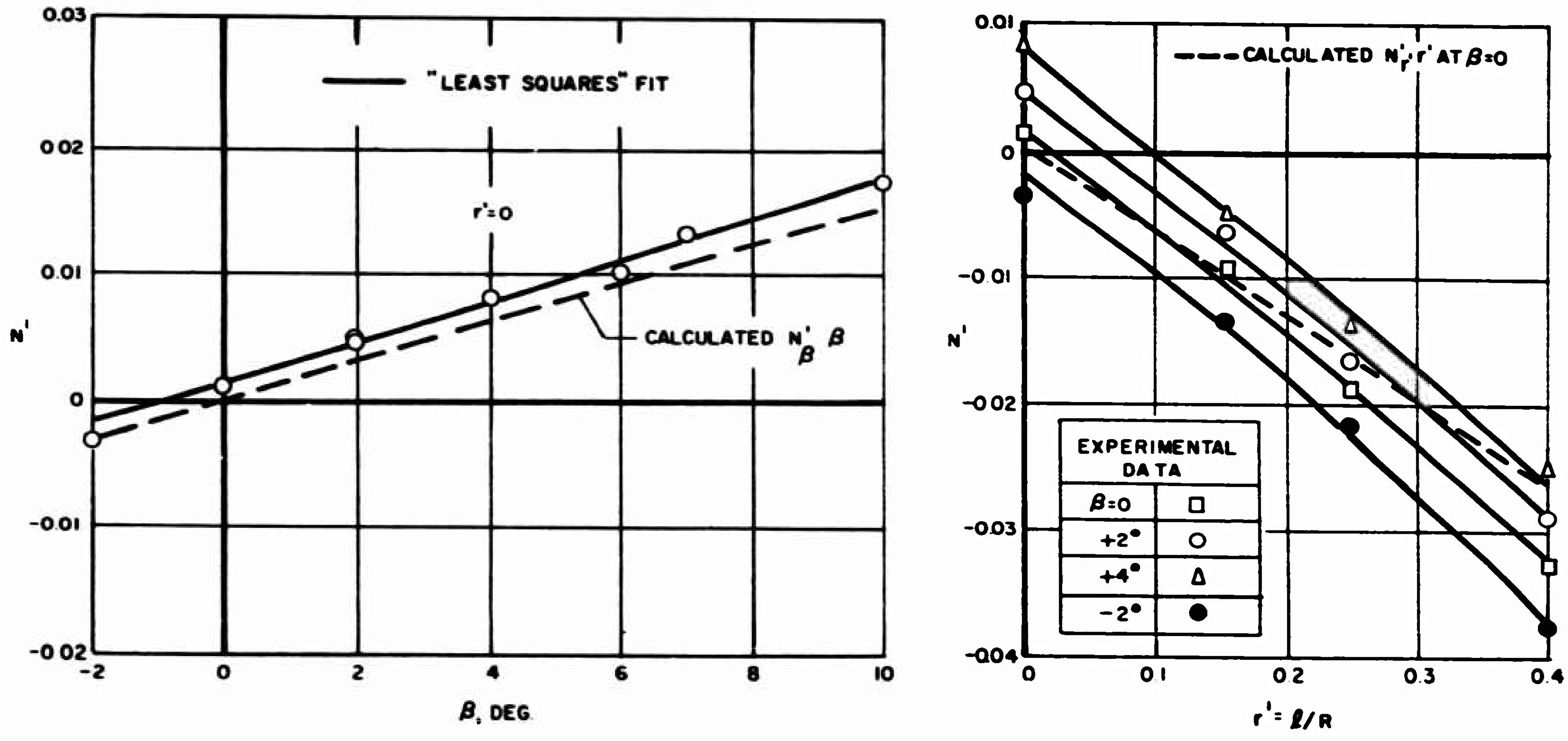


FIGURE B-16. SERIES 60, MODEL 3,1,1. YAWING MOMENT COEFFICIENT

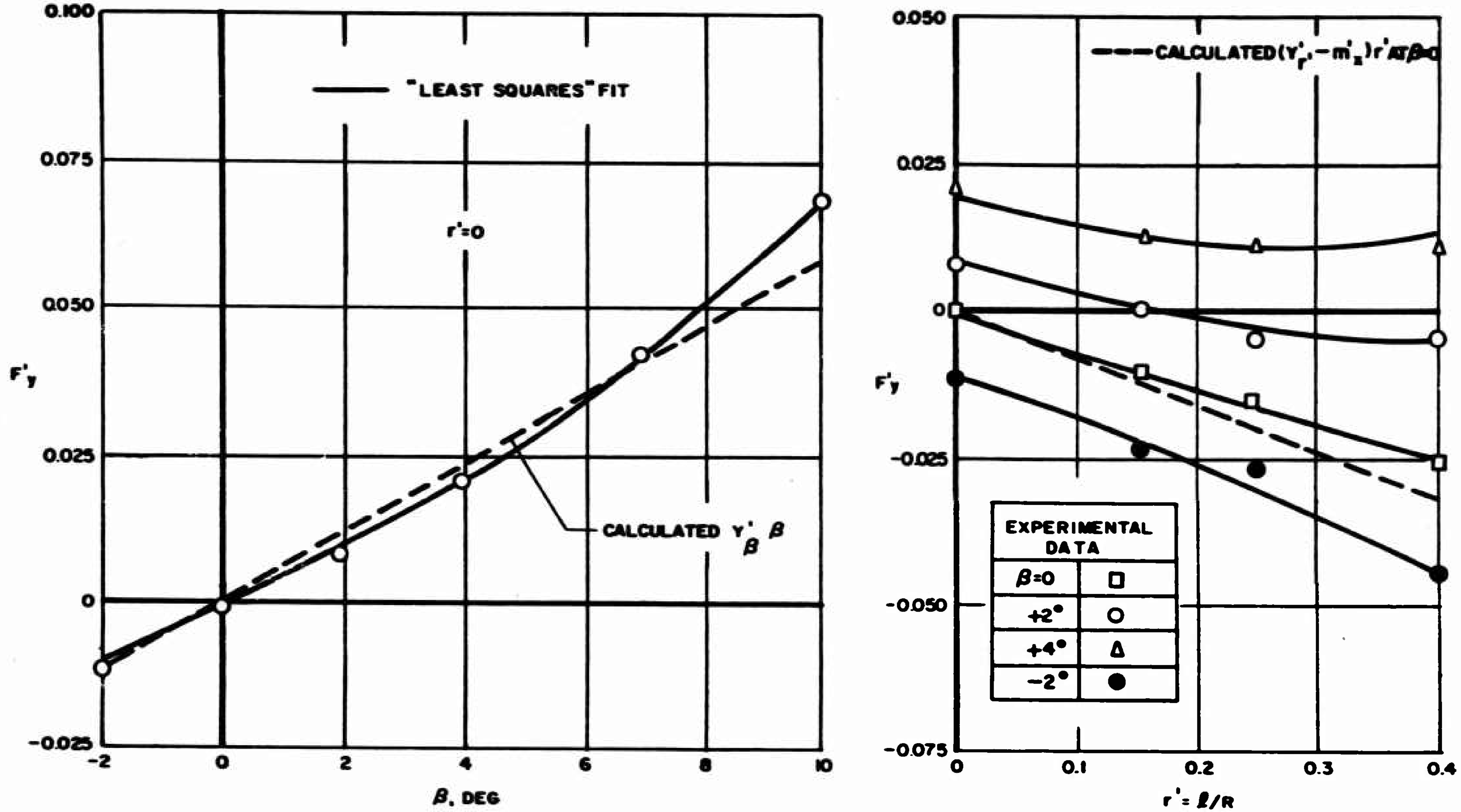


FIGURE B-17. SERIES 60, MODEL 4,1,1. TOTAL LATERAL FORCE COEFFICIENT

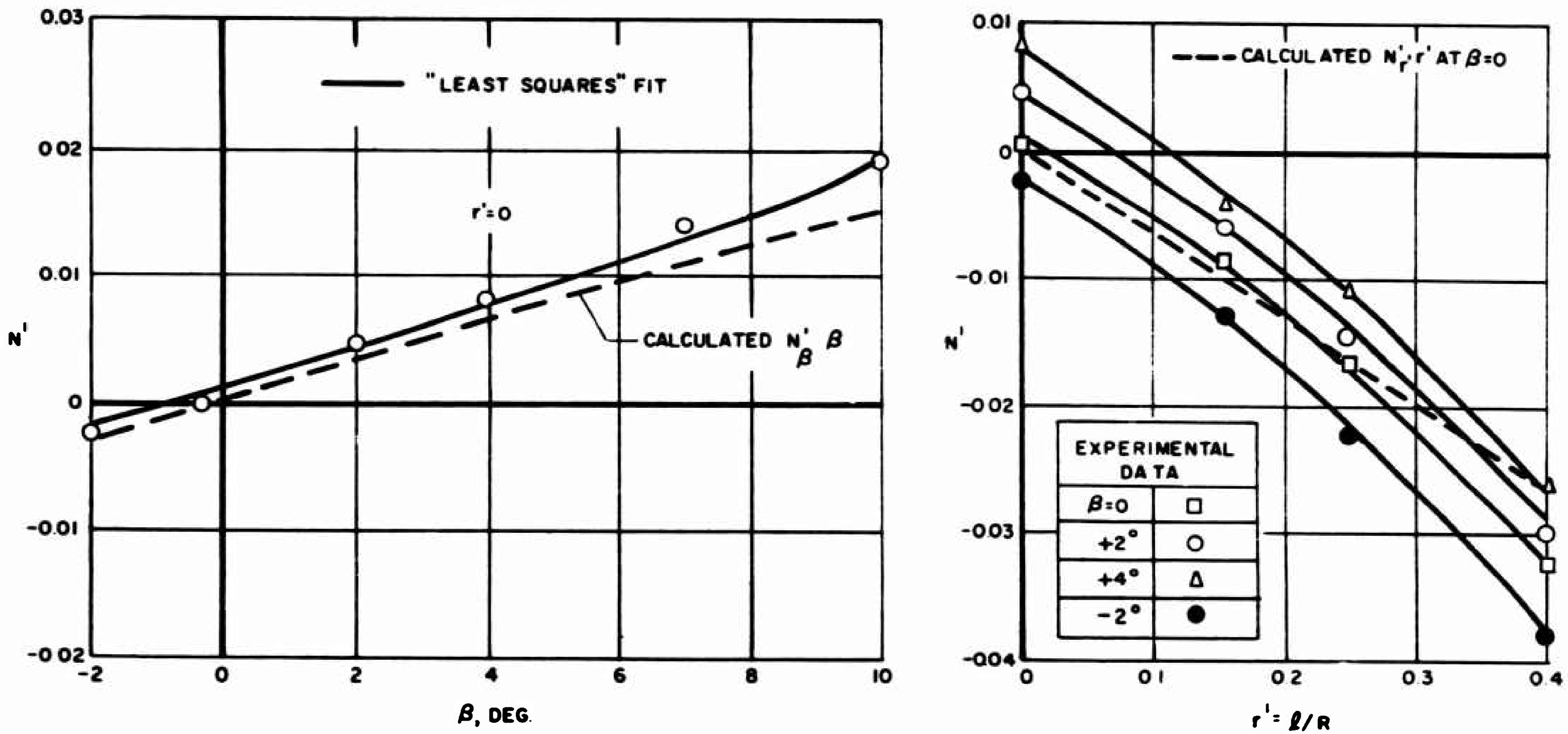


FIGURE B-18. SERIES 60, MODEL 4,1,1. YAWING MOMENT COEFFICIENT

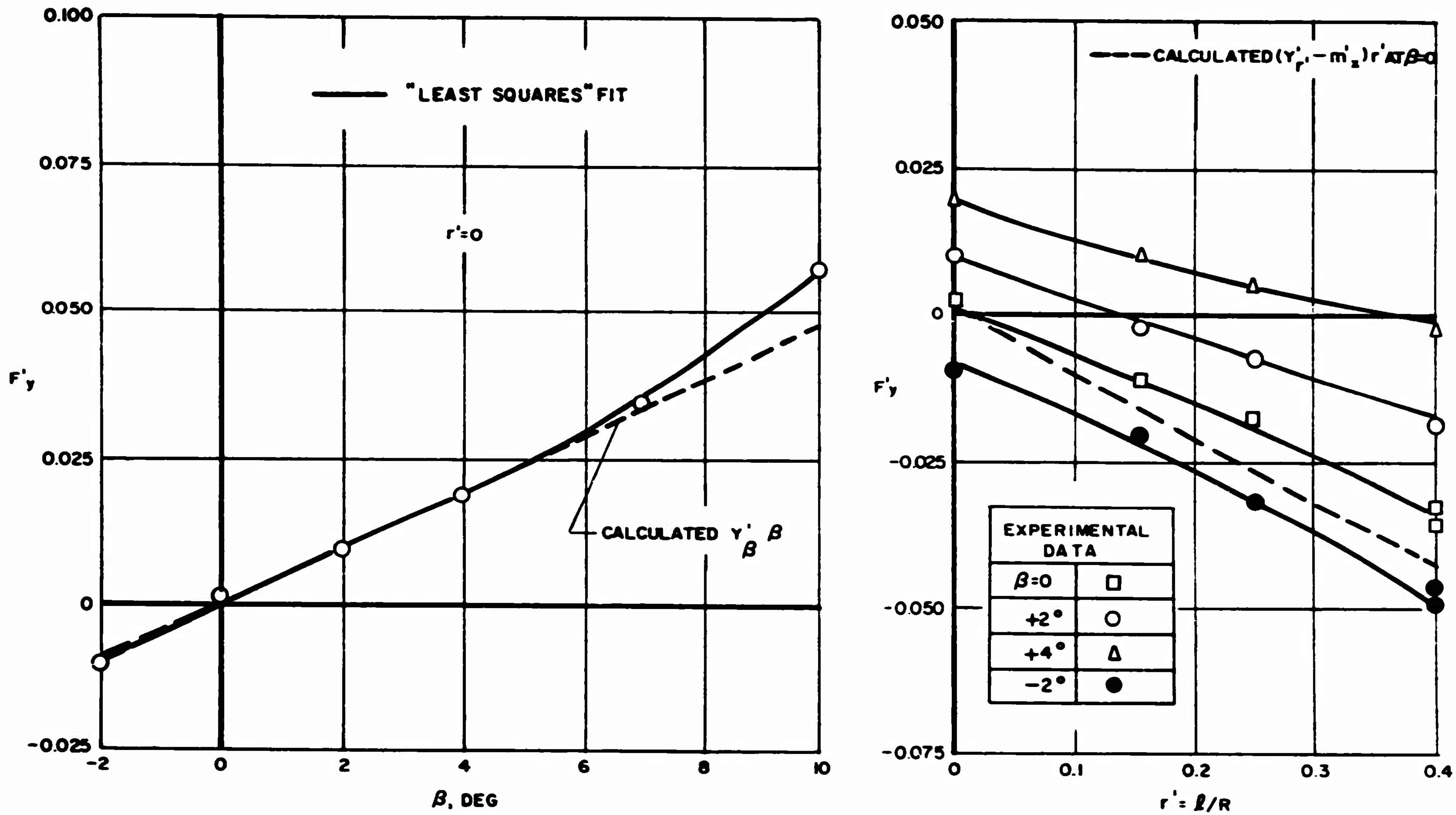


FIGURE B-19. SERIES 60, MODEL 5,1,1. TOTAL LATERAL FORCE COEFFICIENT

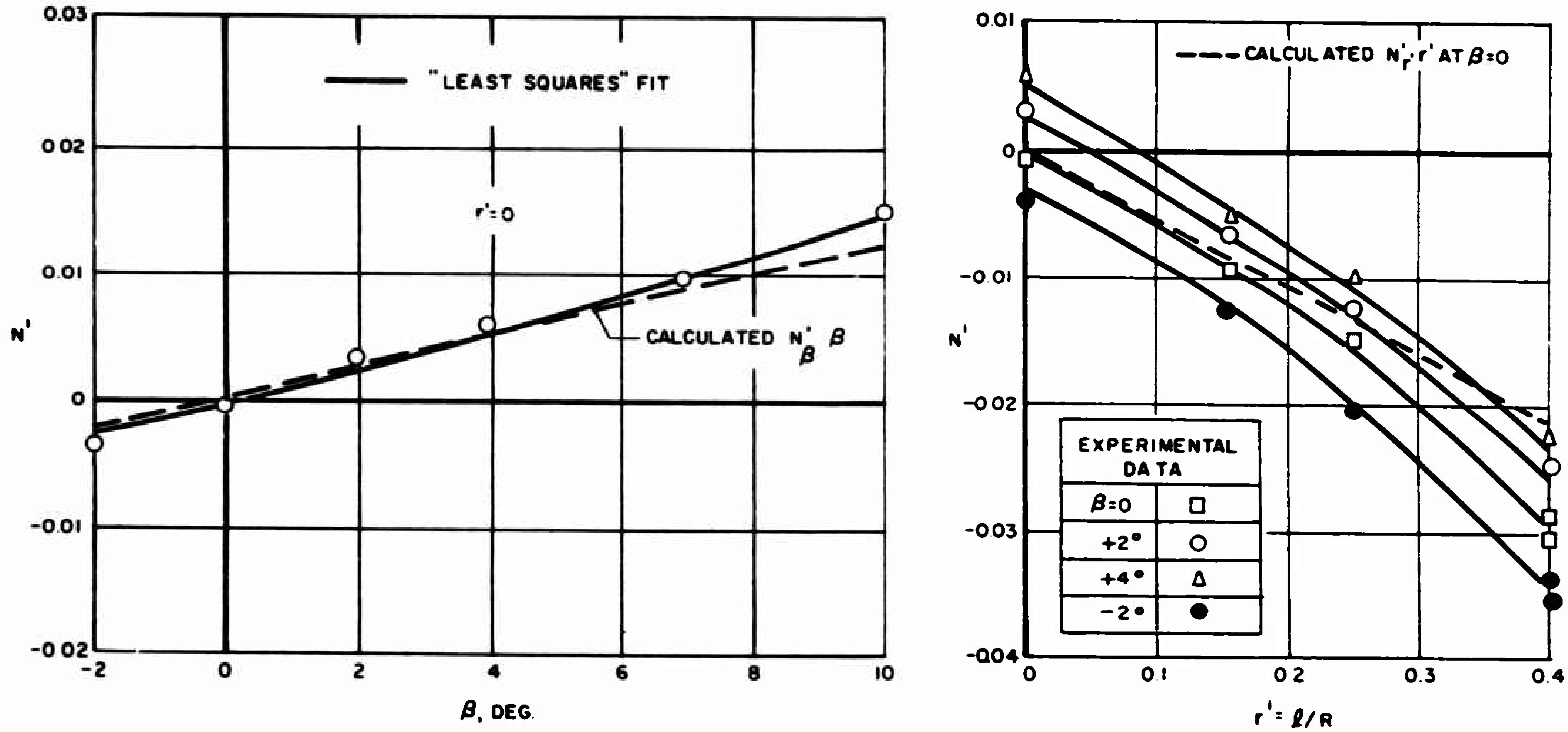


FIGURE B-20. SERIES 60, MODEL 5,1,1. YAWING MOMENT COEFFICIENT

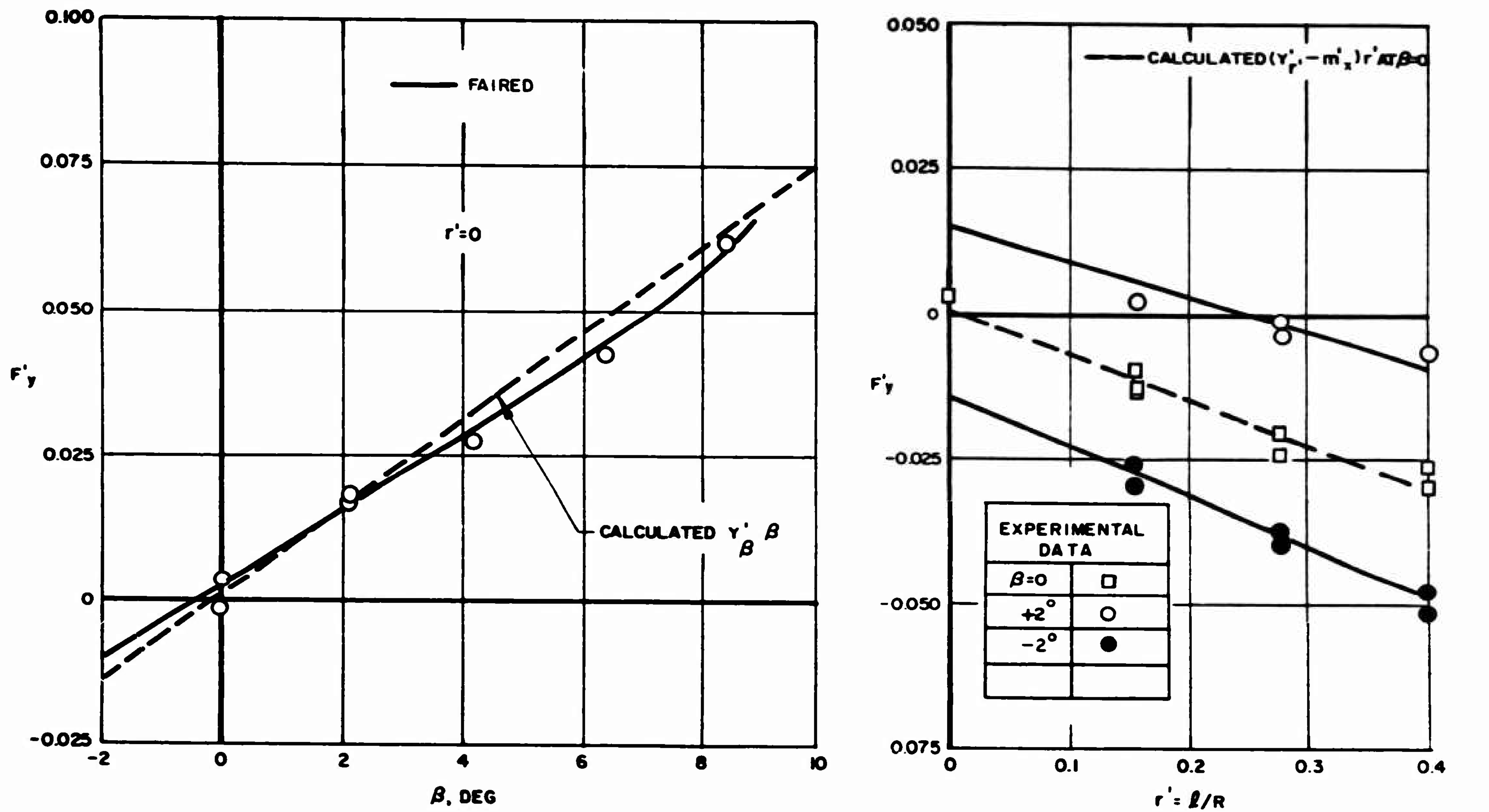


FIGURE B-21. SERIES 60, MODEL 6,1,1. TOTAL LATERAL FORCE COEFFICIENT

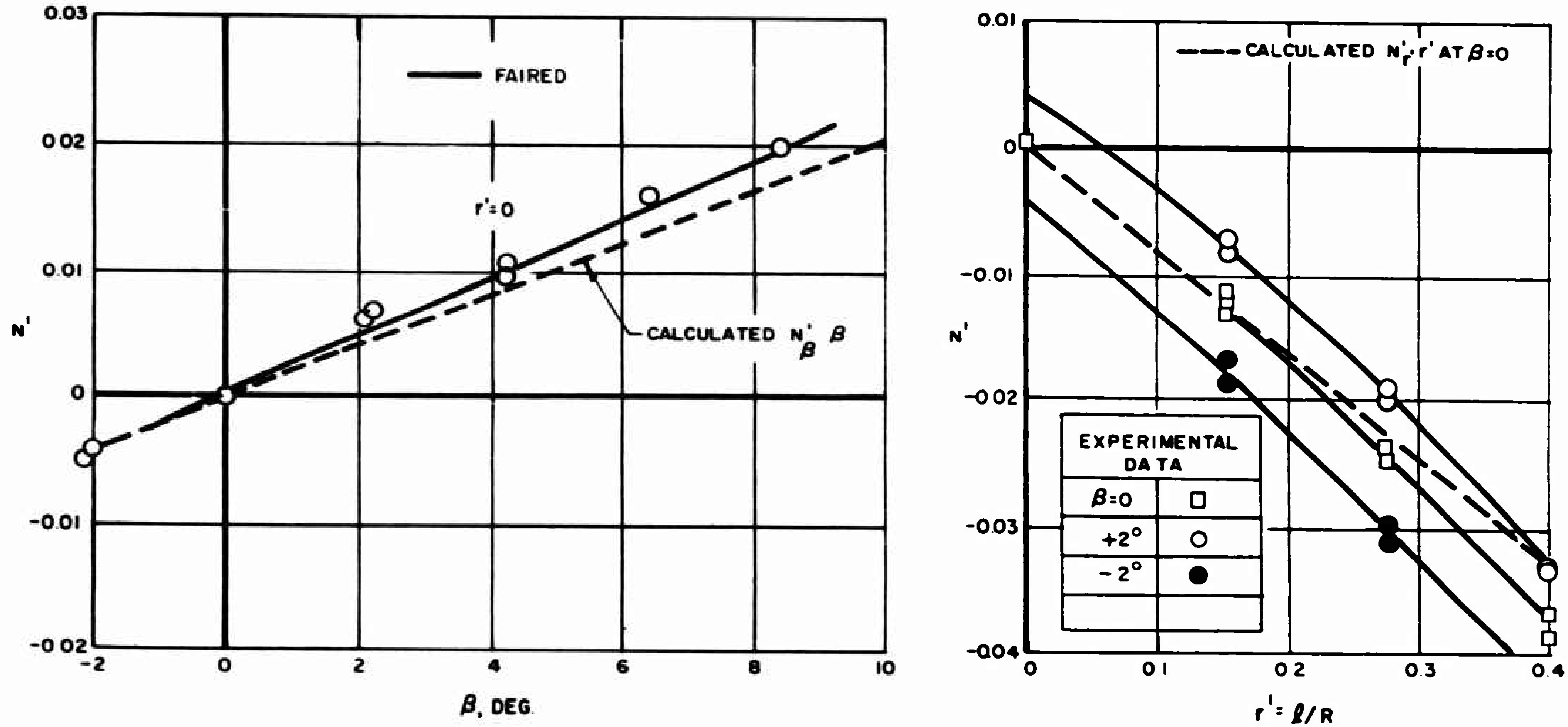


FIGURE B-22. SERIES 60, MODEL 6,1,1. YAWING MOMENT COEFFICIENT

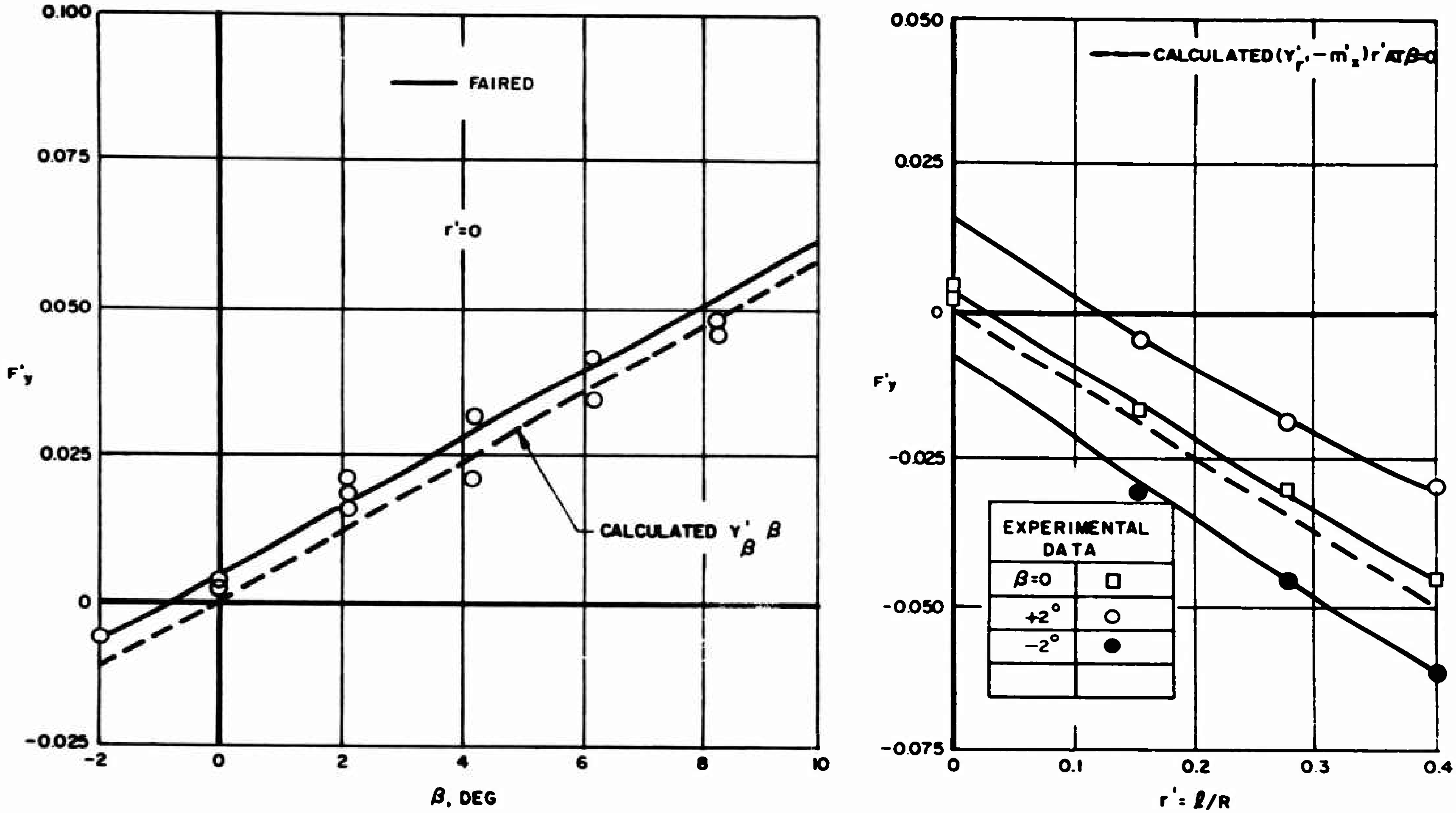


FIGURE B-23. SERIES 60, MODEL 7,1,1. TOTAL LATERAL FORCE COEFFICIENT

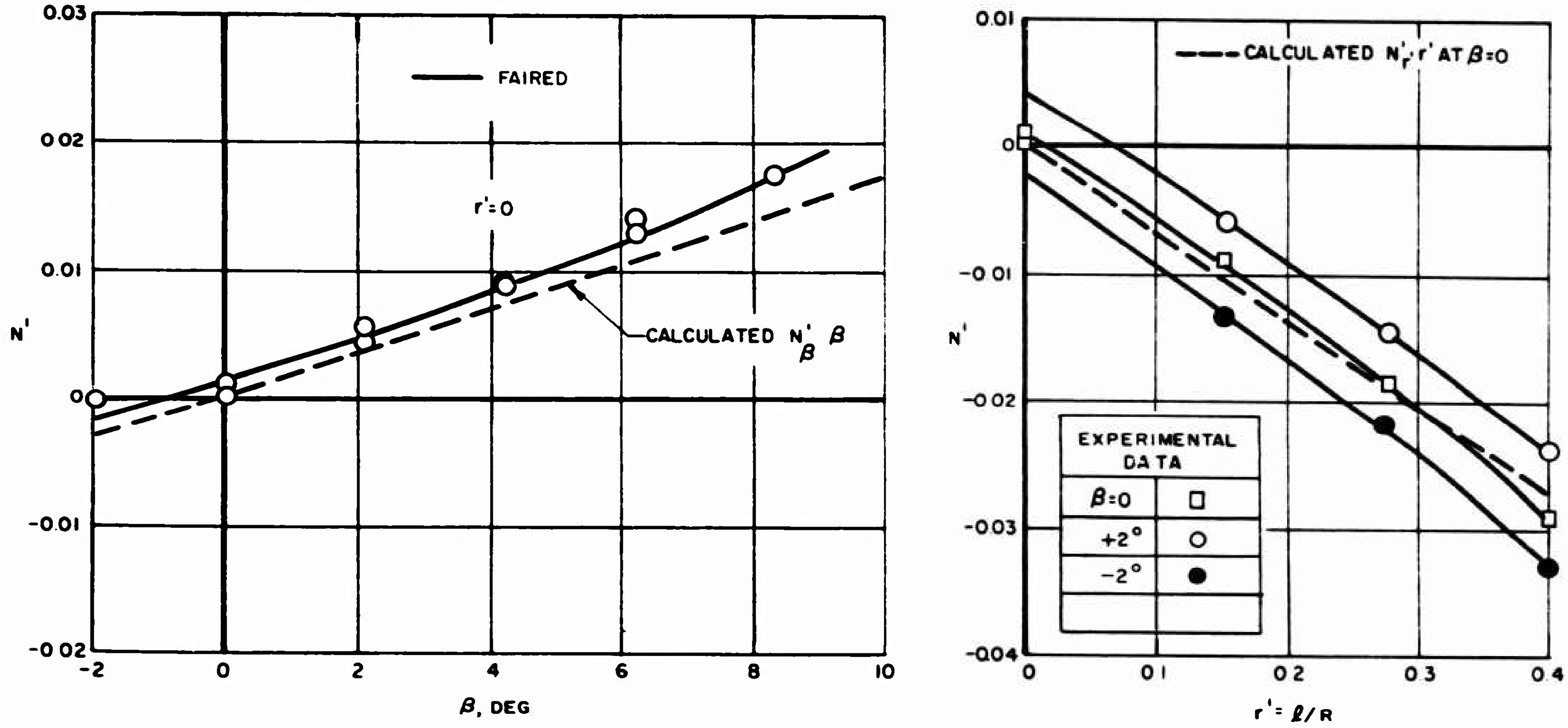


FIGURE B-24. SERIES 60, MODEL 7,1,1. YAWING MOMENT COEFFICIENT

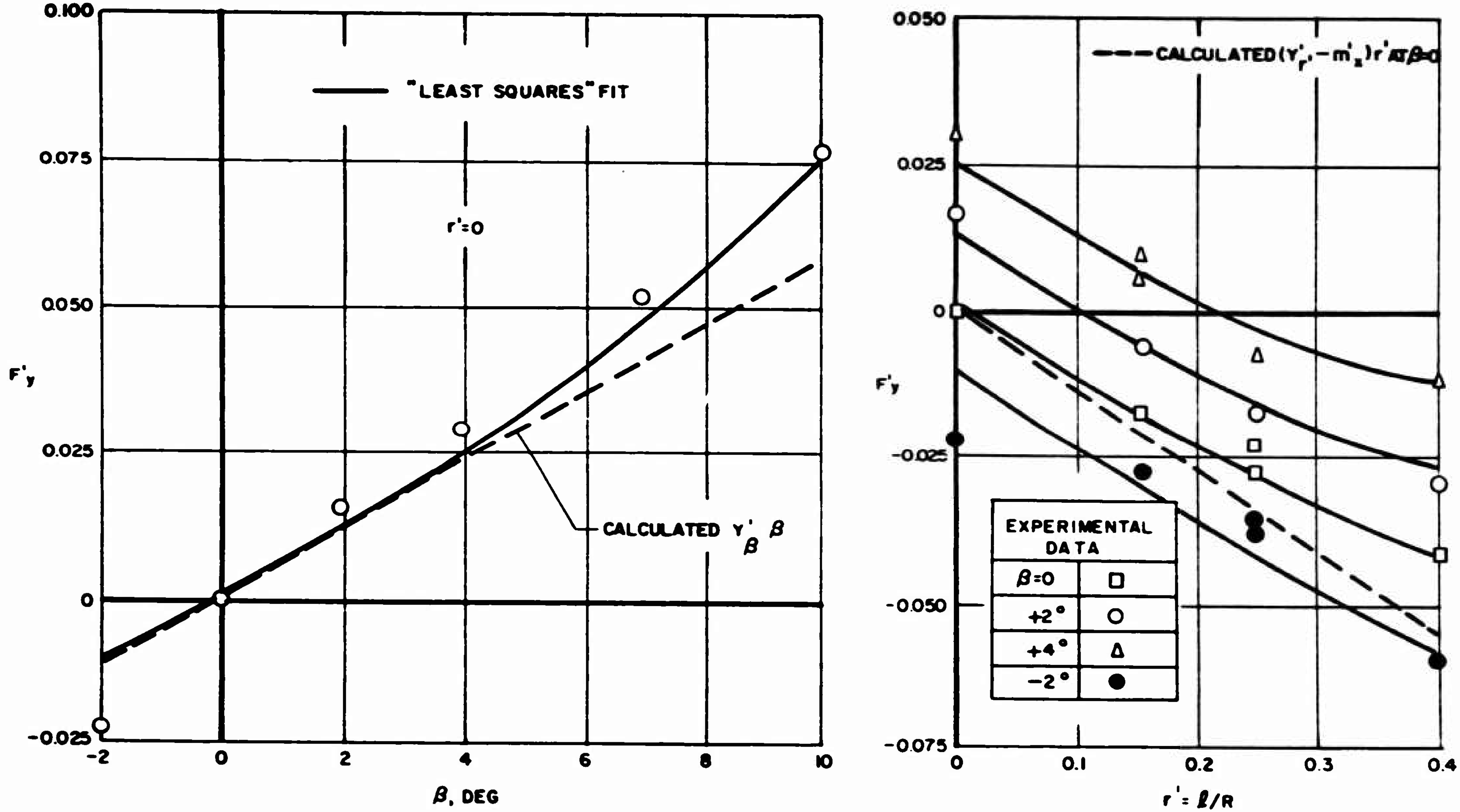


FIGURE B-25. SERIES 60, MODEL 8,1,1. TOTAL LATERAL FORCE COEFFICIENT

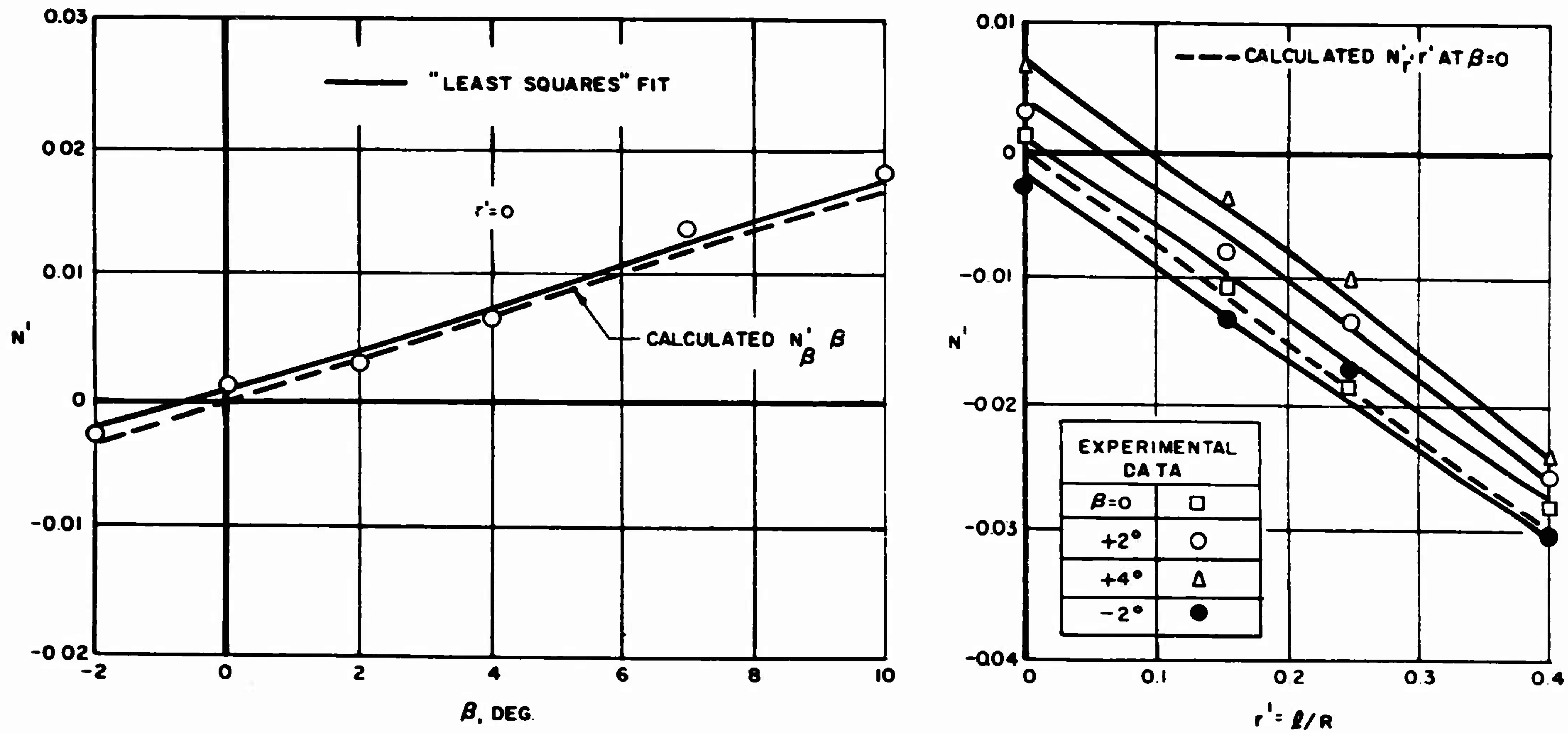


FIGURE B-26. SERIES 60, MODEL 8,1,1. YAWING MOMENT COEFFICIENT

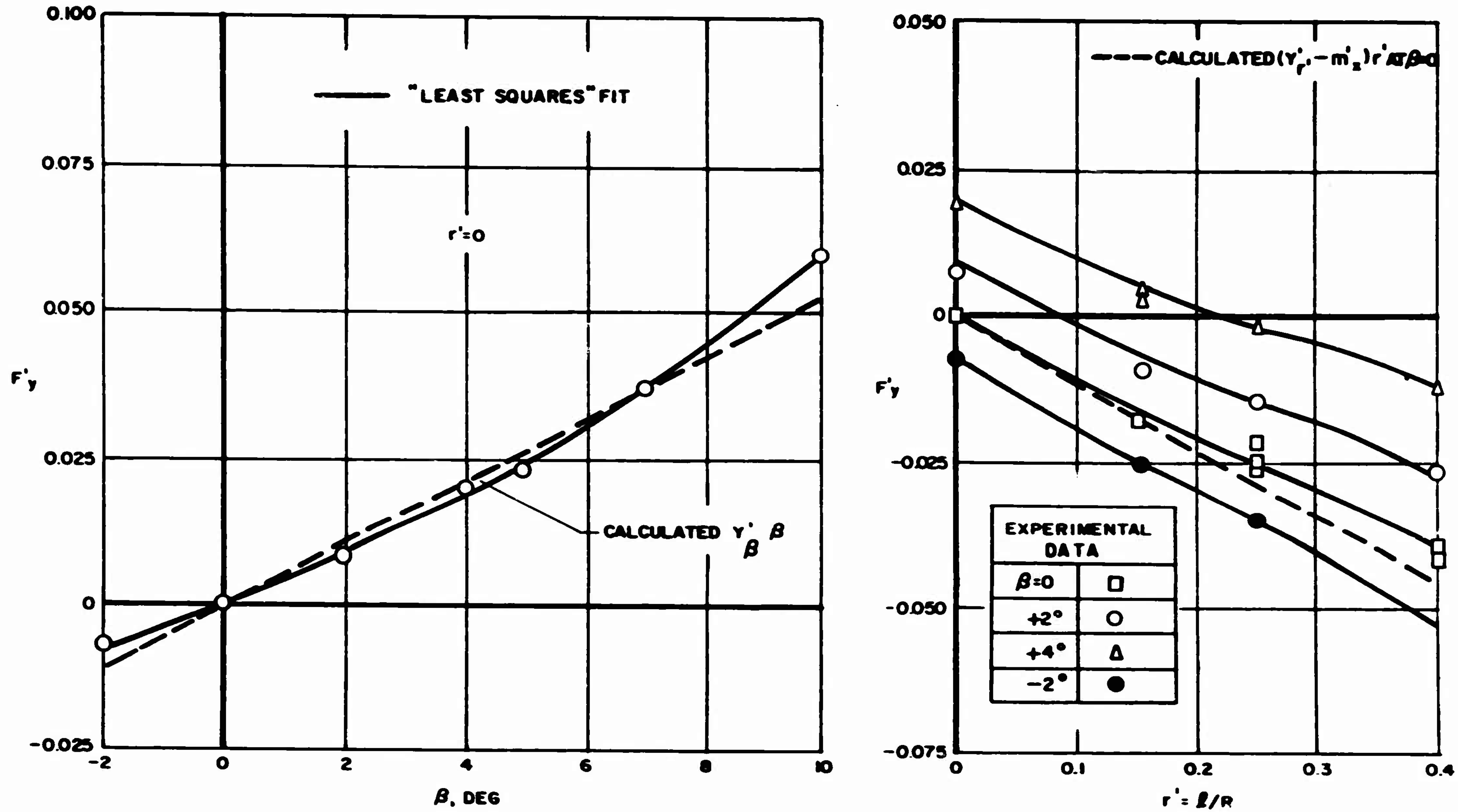


FIGURE B-27. SERIES 60, MODEL 2,0,0. TOTAL LATERAL FORCE COEFFICIENT

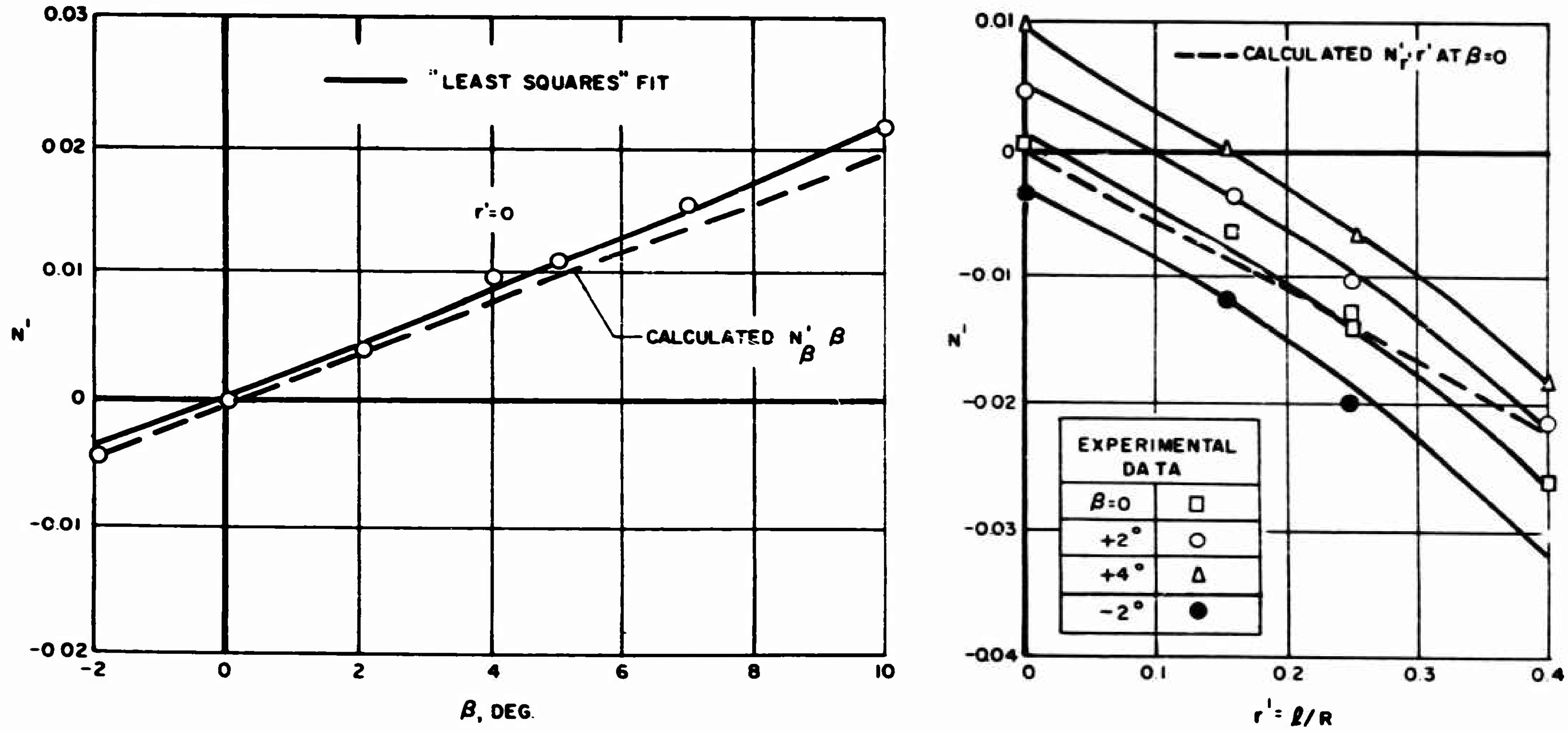


FIGURE B-28. SERIES 60, MODEL 2,0,0. YAWING MOMENT COEFFICIENT

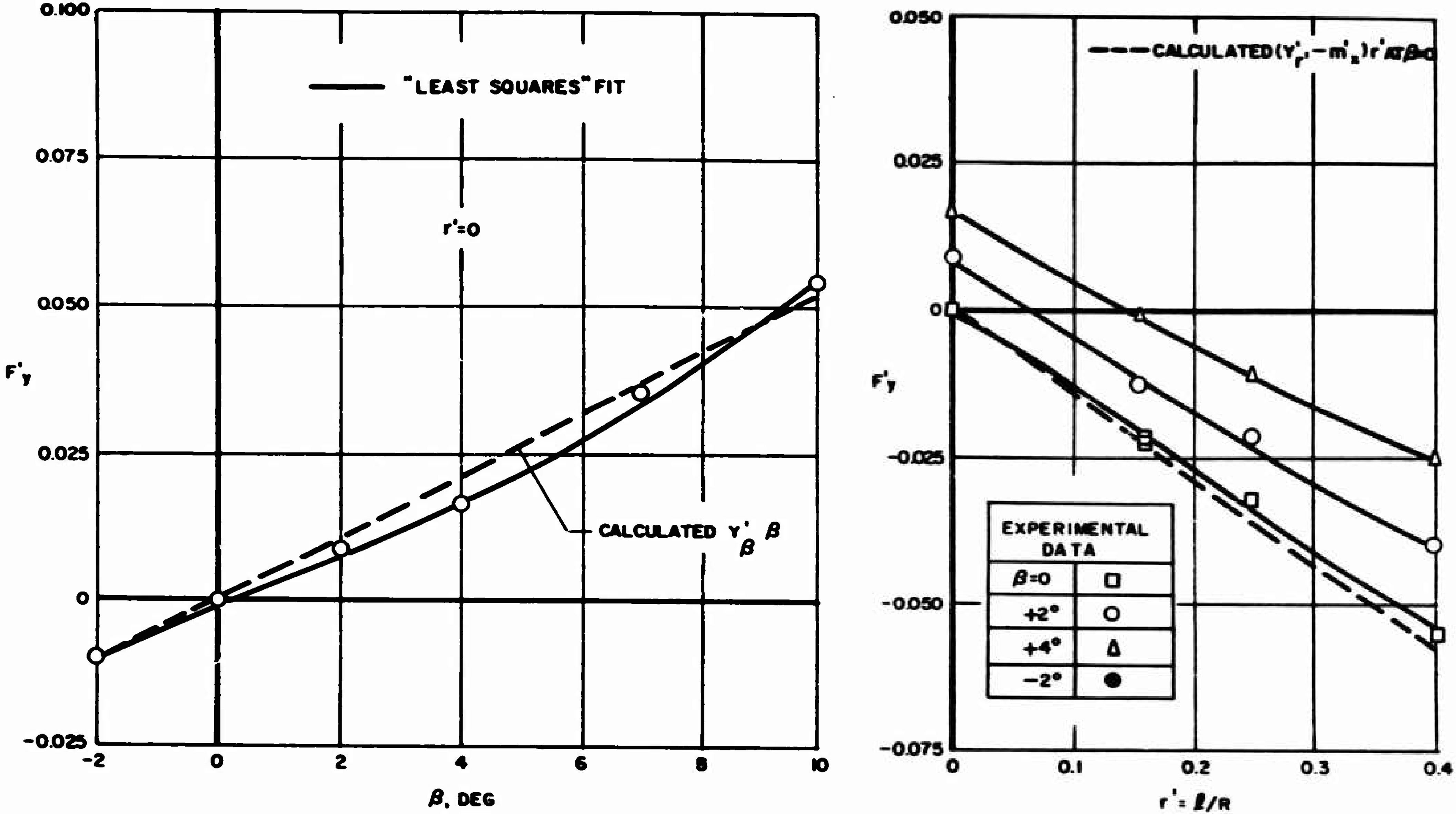


FIGURE B-29. SERIES 60, MODEL 3,0,0. TOTAL LATERAL FORCE COEFFICIENT

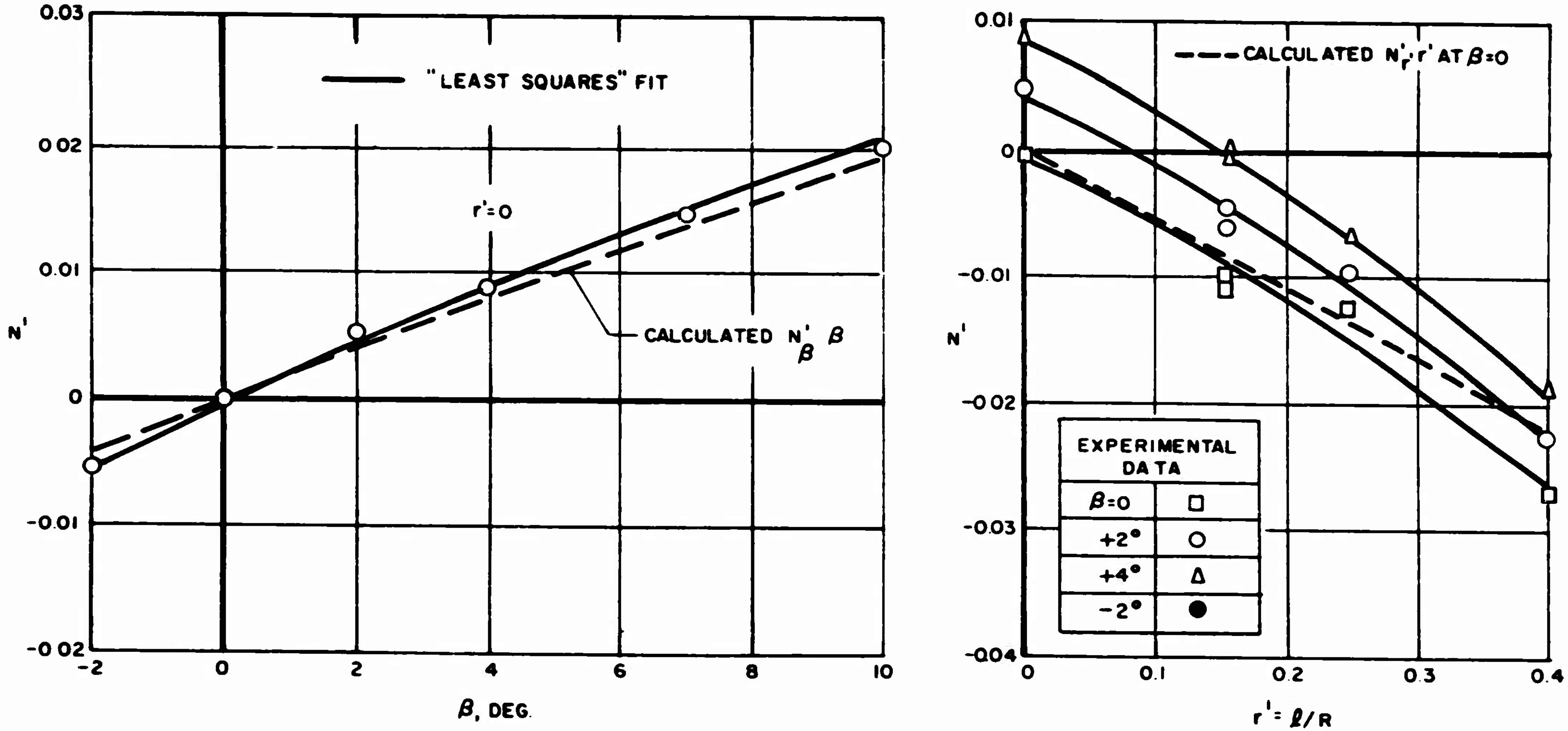


FIGURE B-30. SERIES 60, MODEL 3,0,0. YAWING MOMENT COEFFICIENT

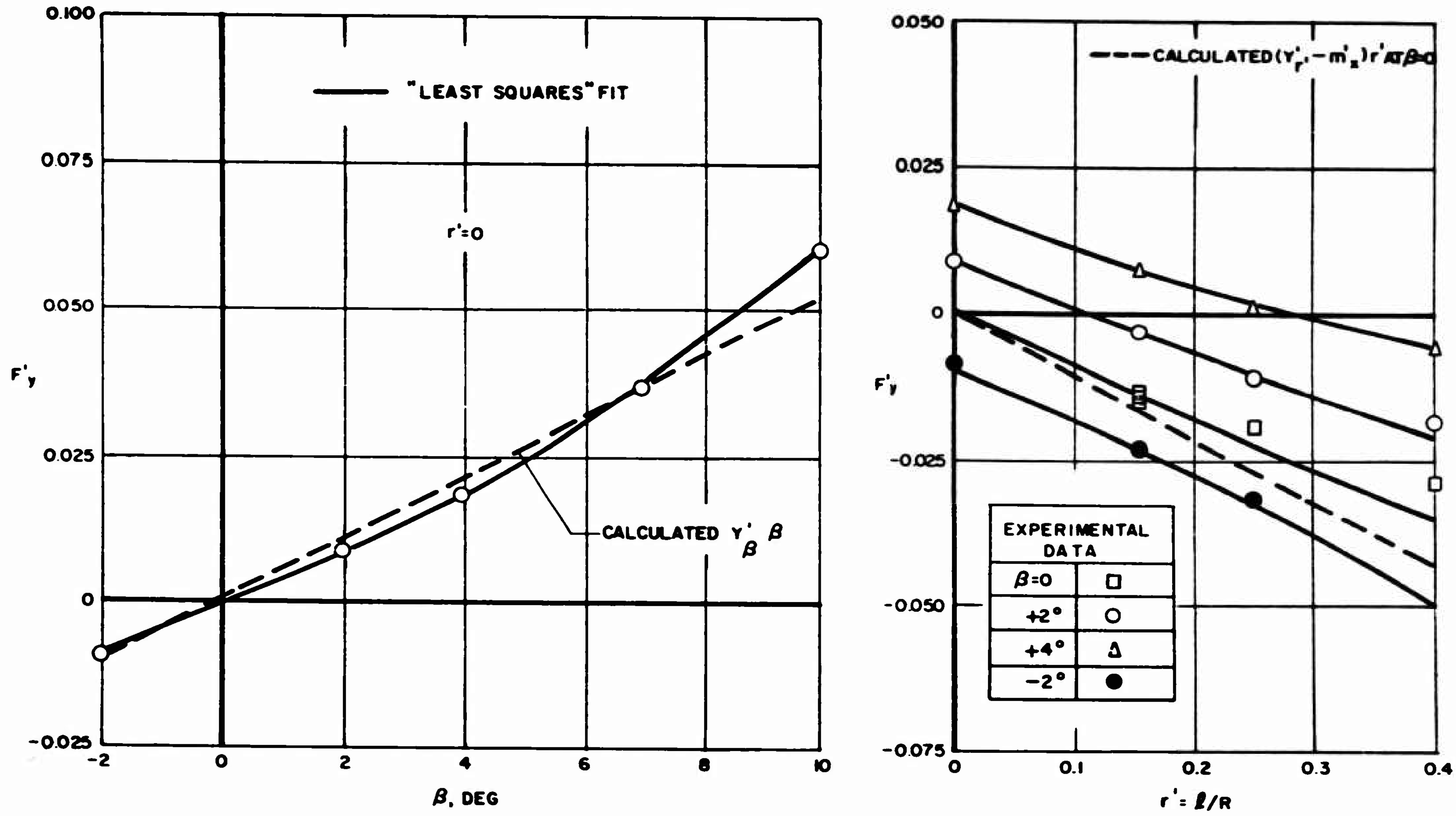


FIGURE B-31. SERIES 60, MODEL 4,0,0. TOTAL LATERAL FORCE COEFFICIENT

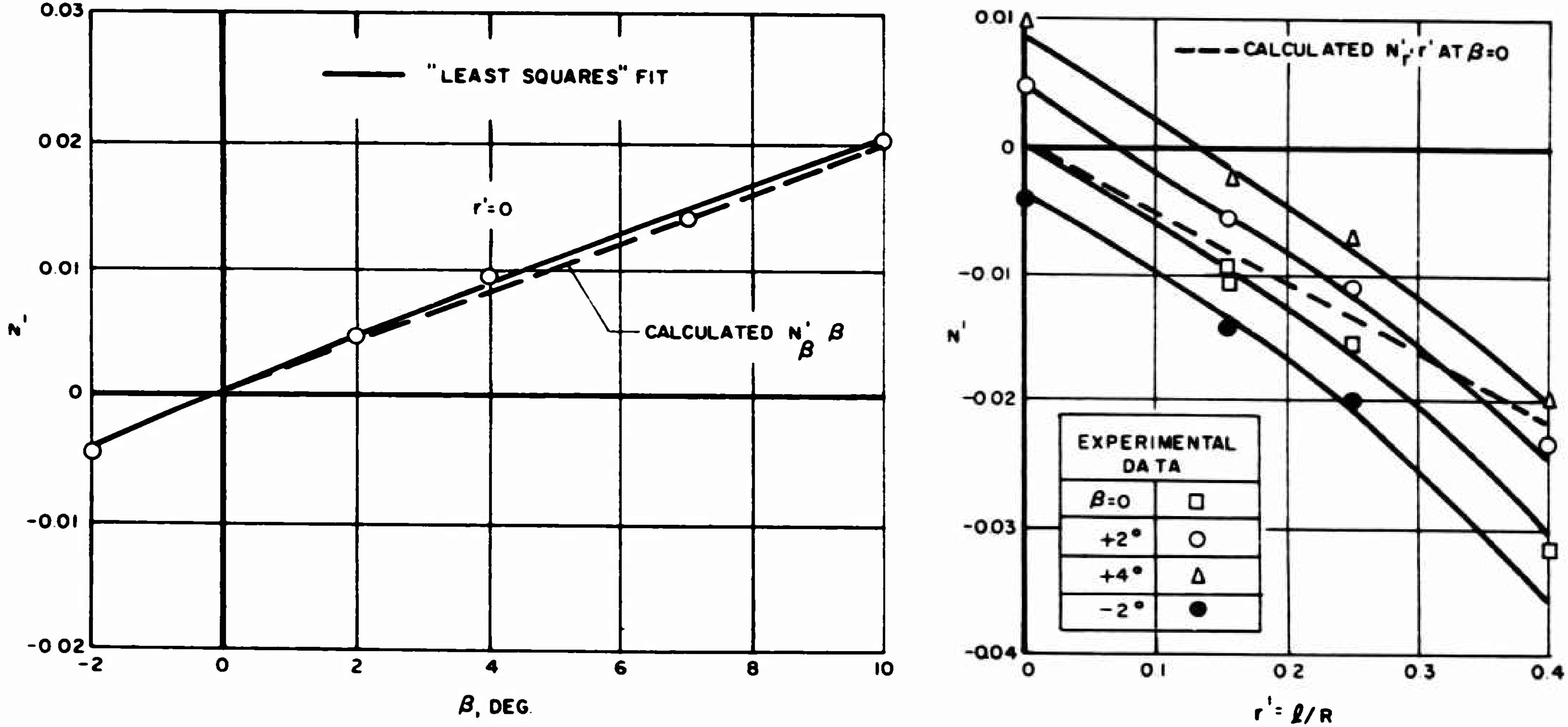


FIGURE B-32. SERIES 60, MODEL 4,0,0. YAWING MOMENT COEFFICIENT

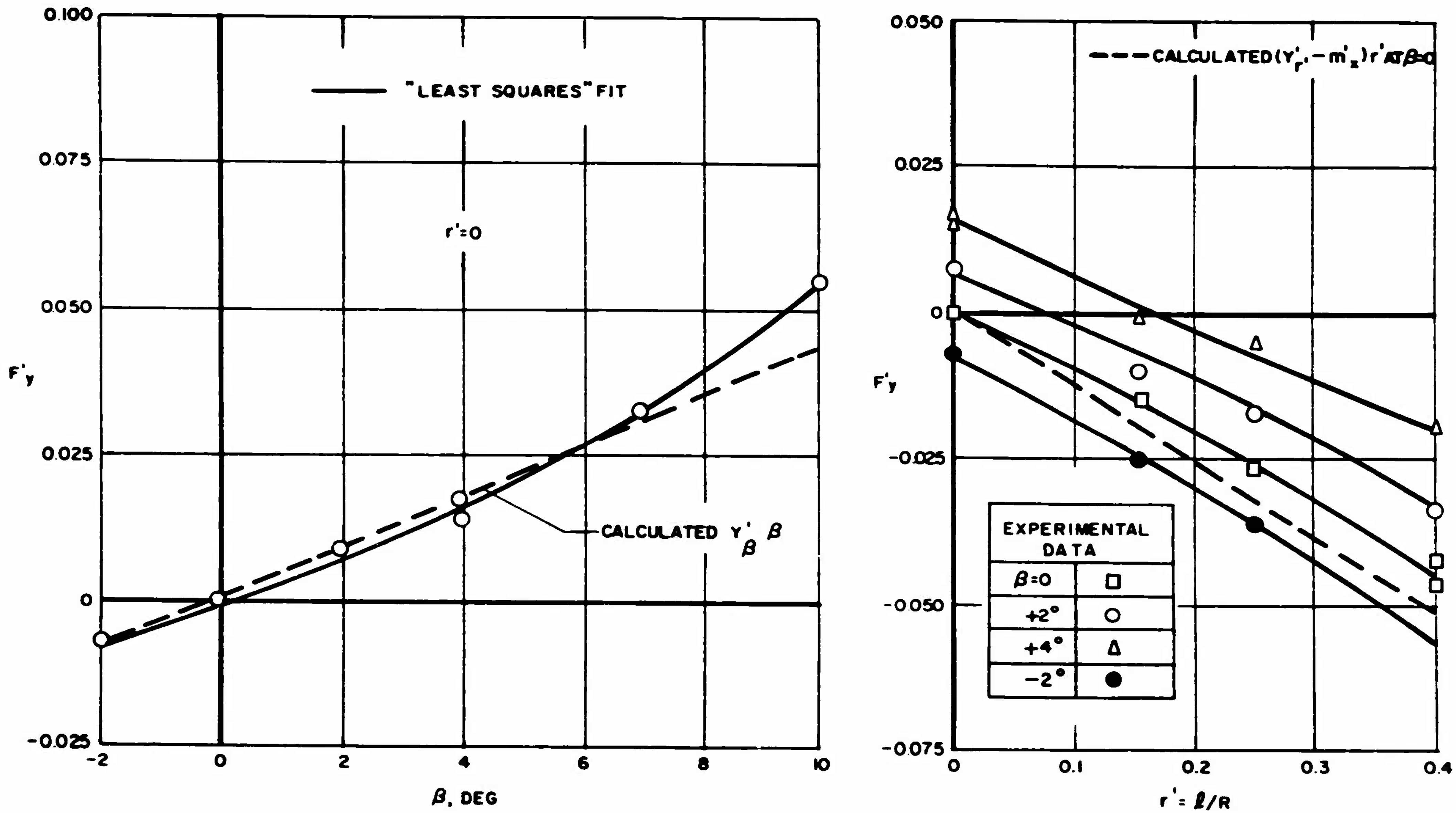


FIGURE B-33. SERIES 60, MODEL 5,0,0. TOTAL LATERAL FORCE COEFFICIENT

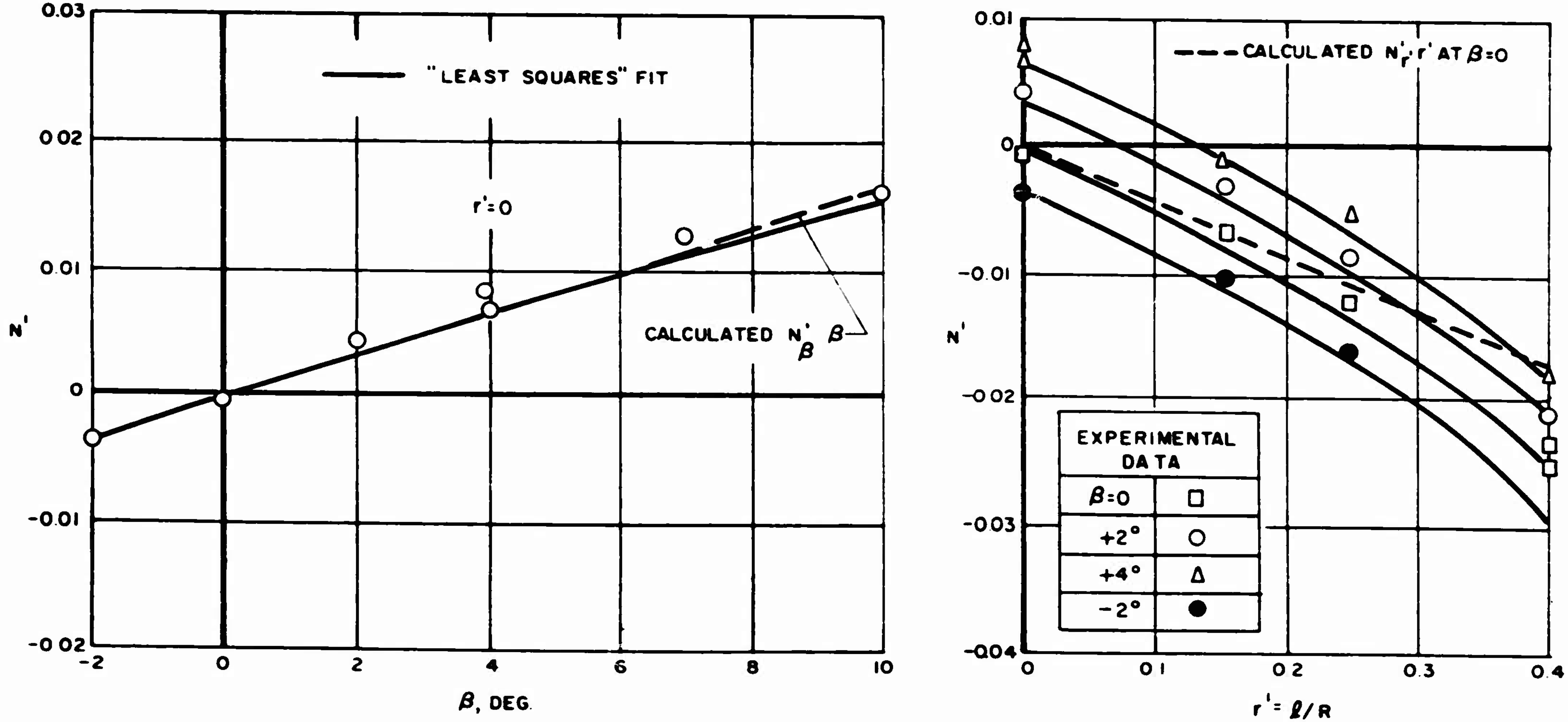


FIGURE B-34. SERIES 60, MODEL 5,0,0. YAWING MOMENT COEFFICIENT

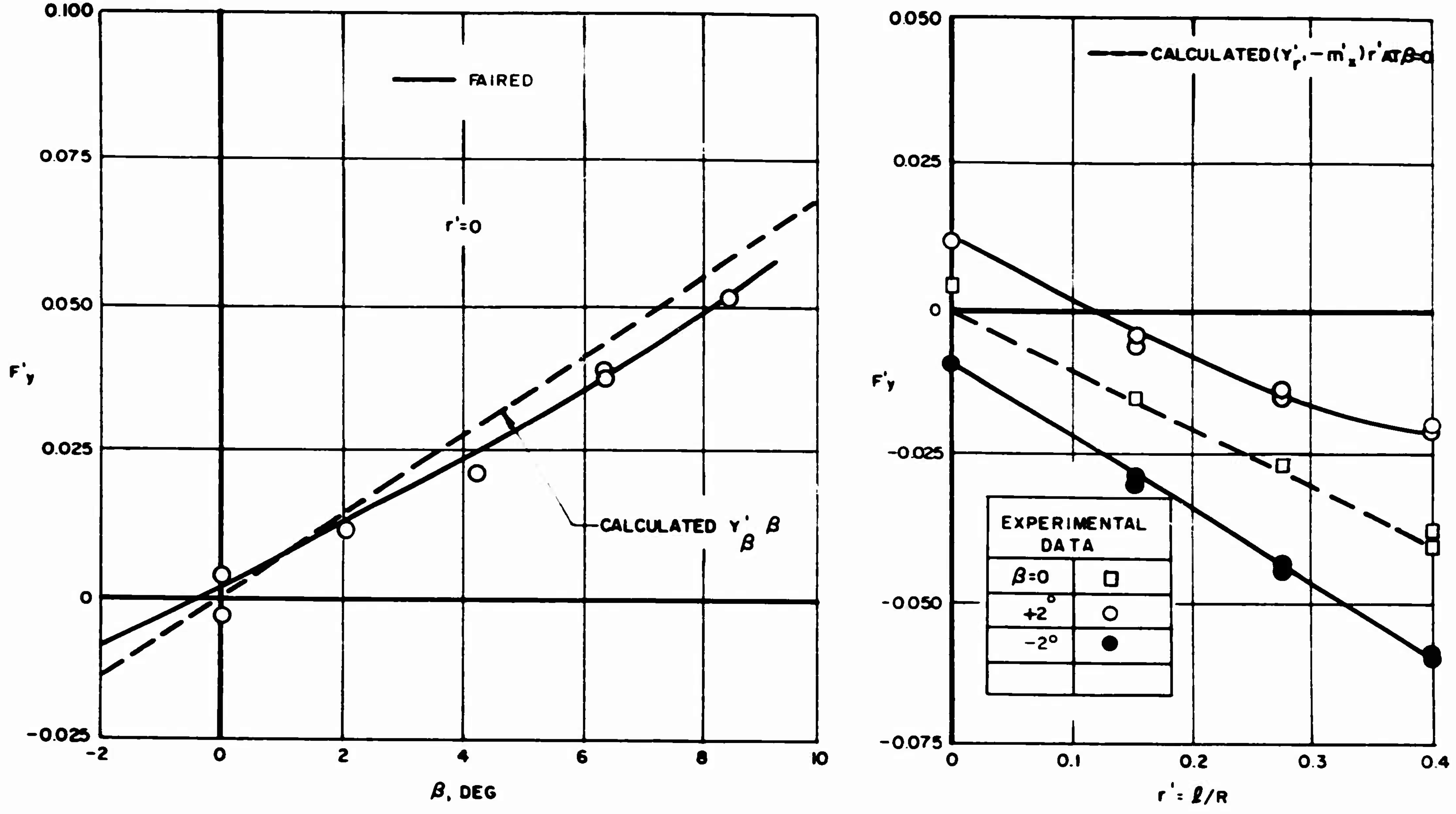


FIGURE B-35. SERIES 60, MODEL 6,0,0. TOTAL LATERAL FORCE COEFFICIENT

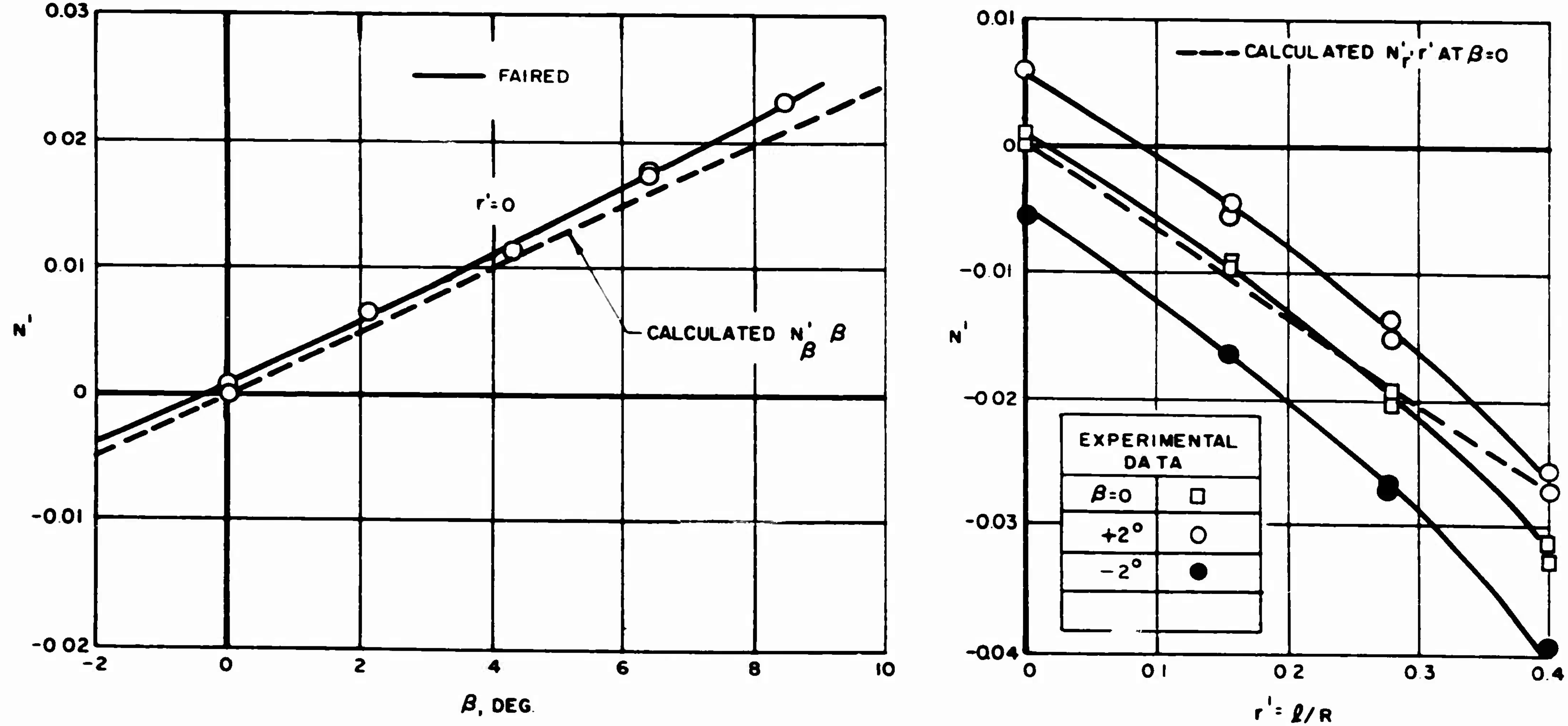


FIGURE B-36. SERIES 60, MODEL 6,0,0. YAWING MOMENT COEFFICIENT

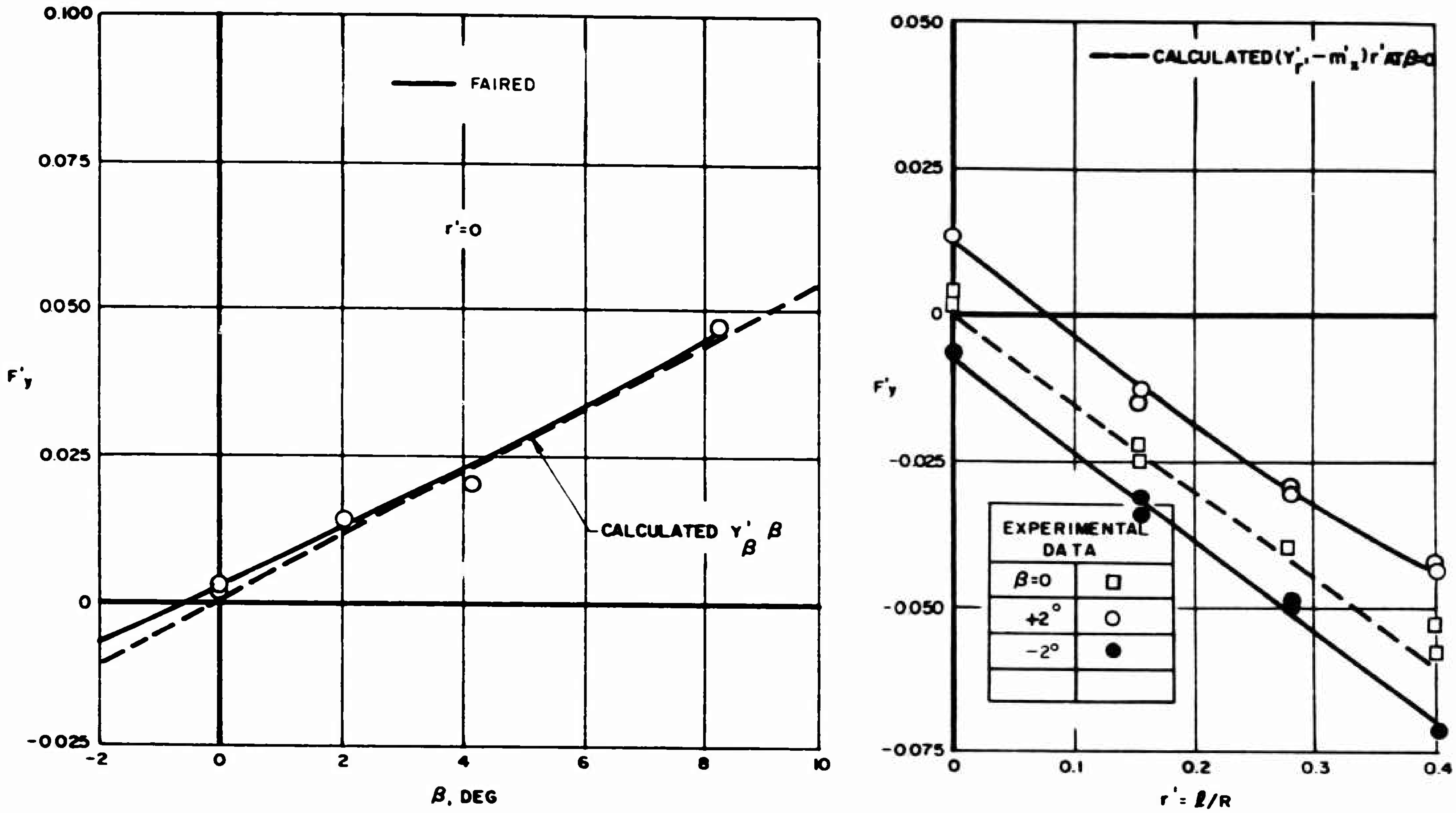


FIGURE B-37. SERIES 60, MODEL 7,0,0. TOTAL LATERAL FORCE COEFFICIENT

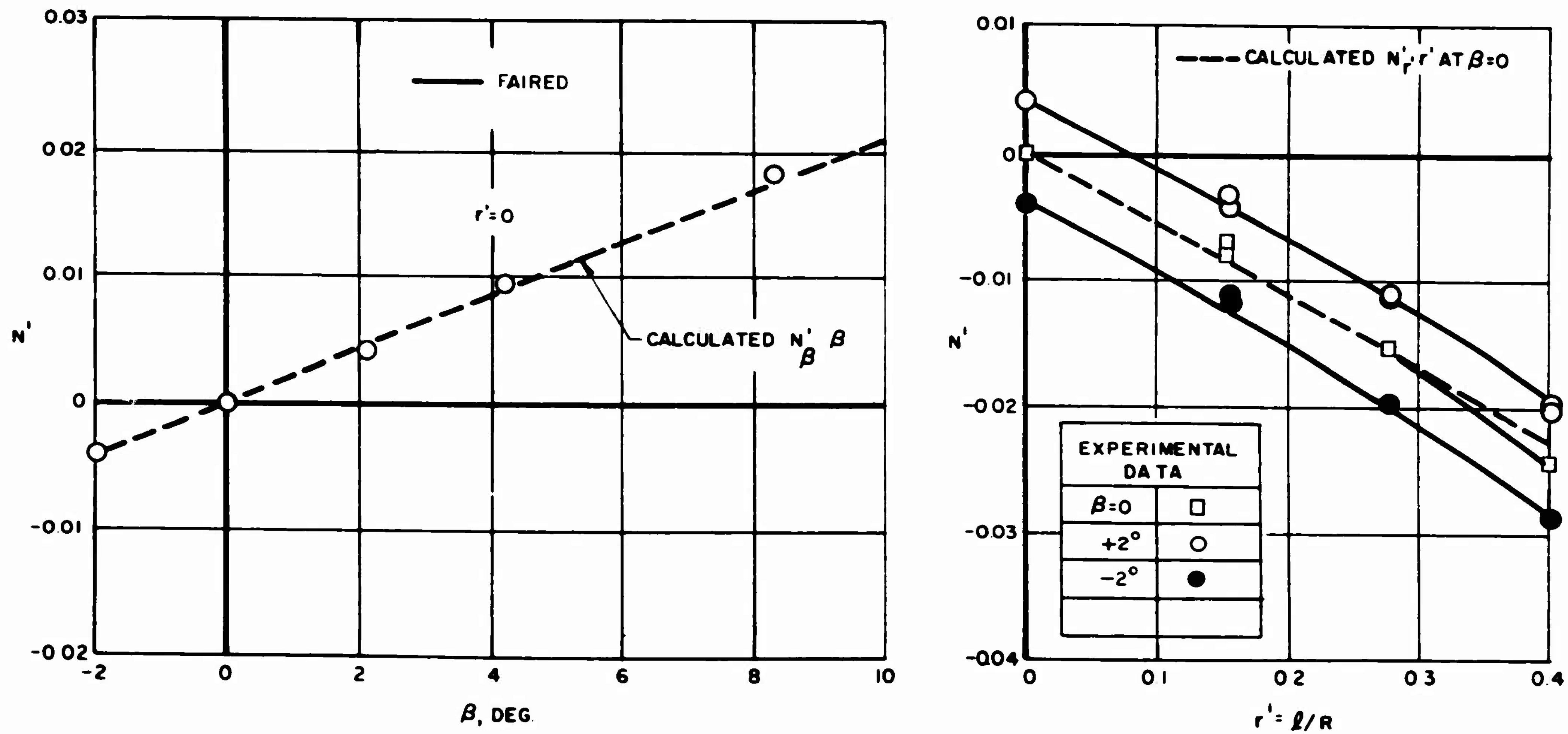


FIGURE B-38. SERIES 60, MODEL 7,0,0. YAWING MOMENT COEFFICIENT

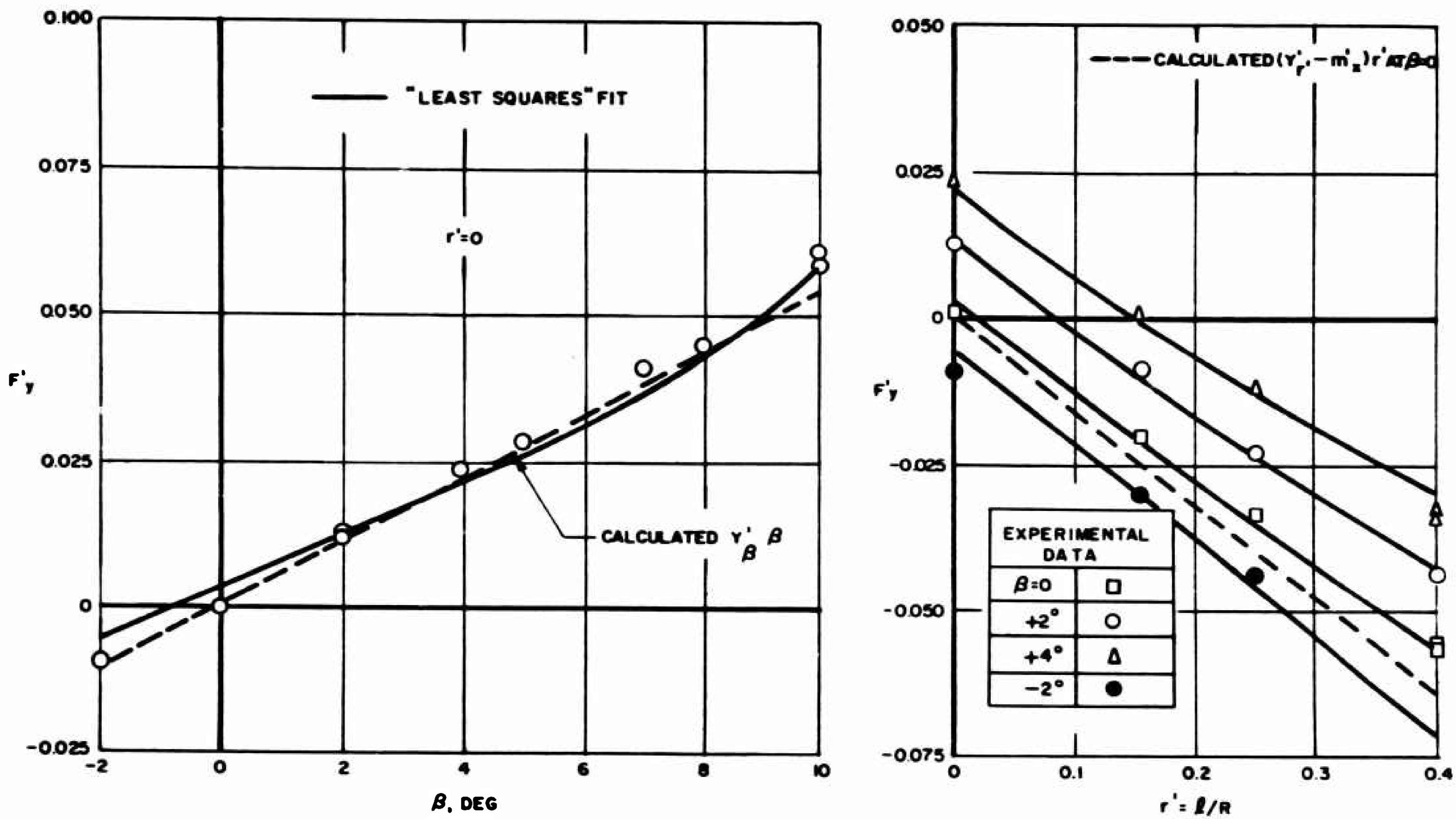


FIGURE B-39. SERIES 60, MODEL 8,0,0. TOTAL LATERAL FORCE COEFFICIENT

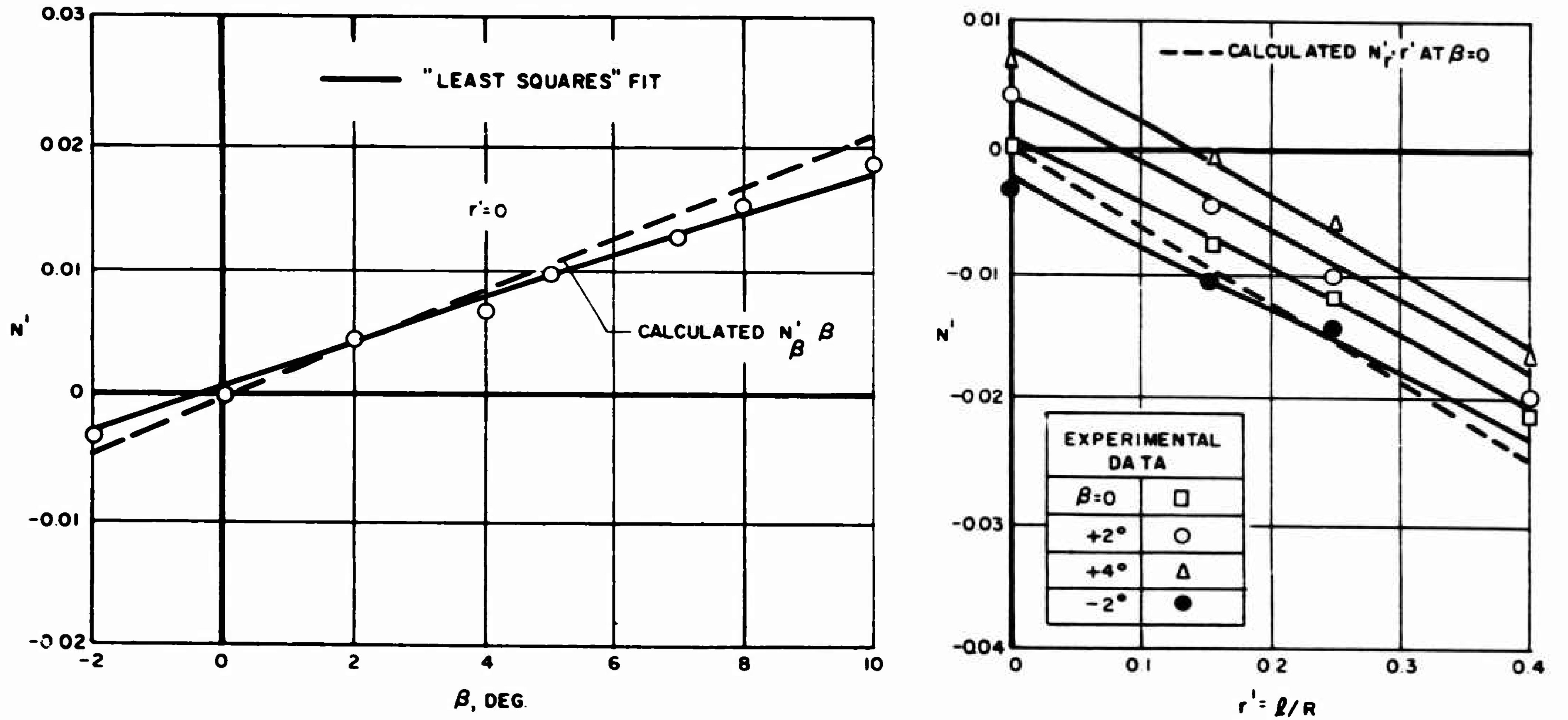


FIGURE B-40. SERIES 60, MODEL 8,0,0. YAWING MOMENT COEFFICIENT

# APPENDIX C

## EXTREME VEE MODIFICATION OF SERIES 60 MODEL 1 DEVELOPED AT THE UNIVERSITY OF MICHIGAN

(Reference 4)

## TABLE C-1

## PERTINENT CHARACTERISTICS OF THE EXTREME VEE MODIFICATION OF SERIES 60 MODEL 1

| | | |
|---|---|---|
| Model | 9,1,1 | 9,0,0 |
| Length $\ell$, ft | 5.0 | → |
| Beam B, ft | 0.667 | → |
| Draft H, ft | 0.267 | → |
| Displacement $\Delta$, lb | 33.10 | → |
| Prismatic coefficient $C_p = 2x_o/\ell$ | 0.614 | → |
| Block coefficient $C_B$ | 0.6 | → |
| LCG/$\ell$, from bow | 0.511 | → |
| B/H | 2.50 | → |
| $\ell$/B | 7.5 | → |
| $\ell$/H | 18.75 | → |
| Rudder span, ft | 0.200 | 0 |
| Rudder chord, ft | 0.105 | 0 |
| <u>Lamb's Coefficients of Accession to Inertia for Equivalent Ellipsoid</u> | | |
| Minor axis/major axis, $2H/\ell$ | 0.107 | → |
| $k_1$ (longitudinal) | 0.022 | → |
| $k_2$ (lateral) | 0.957 | → |
| $k'$ (rotational) | 0.875 | → |
| <u>Other Physical Characteristics</u> | | |
| $m_o'$, mass coefficient | 0.159 | → |
| $m_1'$, longitudinal added-mass coefficient | 0.003 | → |
| $m_2'$, lateral added-mass coefficient | 0.156 | → |
| $m_z'$, rotational added-mass coefficient | 0.143 | → |
| $n_z'$, virtual moment-of-inertia coefficient | 0.019 | → |
| $\bar{x}/\ell$, CG of lateral added mass from LCG | 0.022 | → |
| $x_p/\ell$, center of area of profile from LCG | 0.027 | → |
| $D_o'$ (estimated drag coefficient at $\beta = 0$) | 0.017 | → |
| $\sigma_1$, calculated from theoretical derivatives | -0.62 | -0.17 |
| $\sigma_1$, calculated from experimental rates | -0.55 | -0.17 |

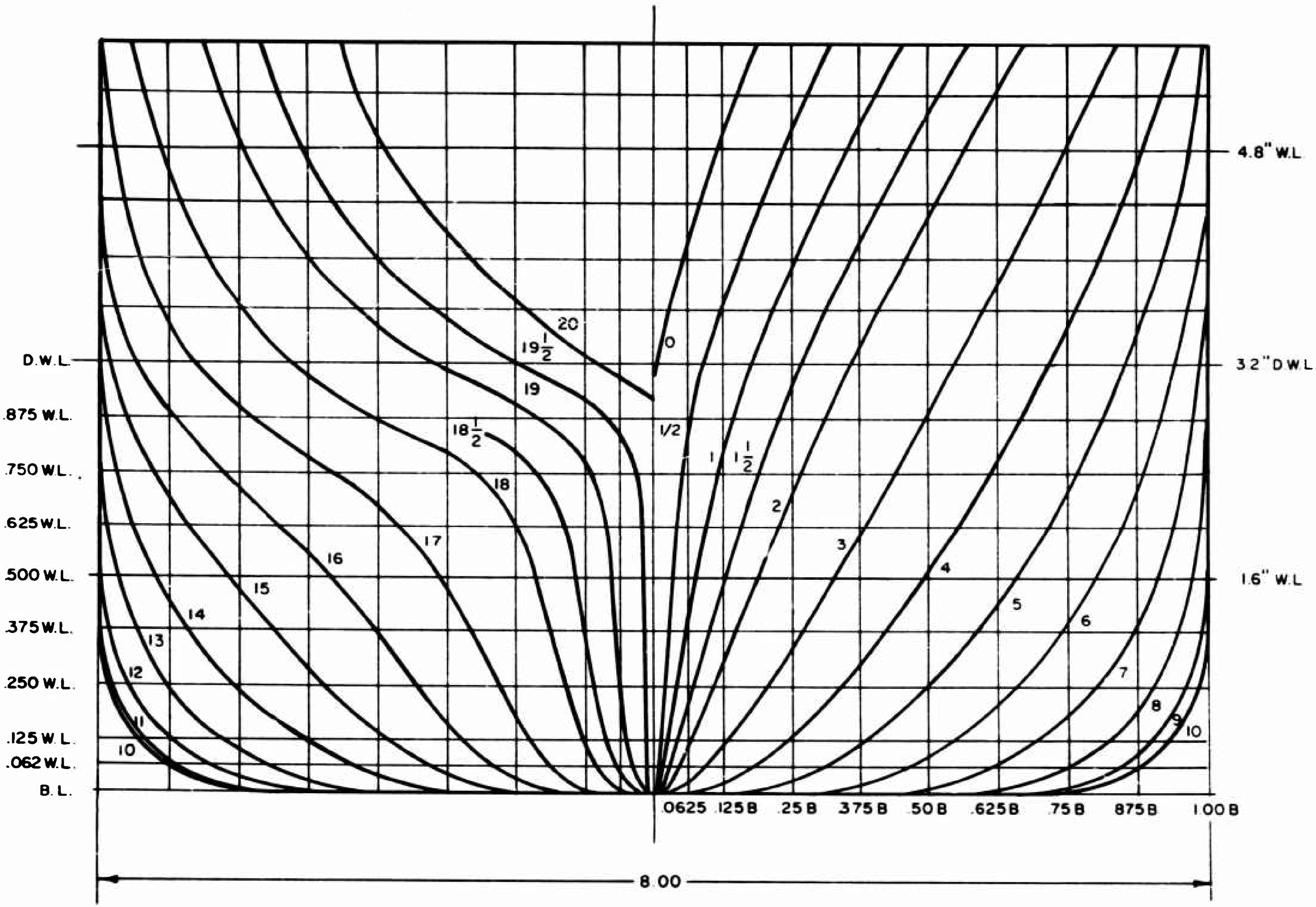


FIGURE C-1. BODY PLAN OF EXTREME VEE MODIFICATION OF SERIES 60.
(MODEL 9)
R-1035

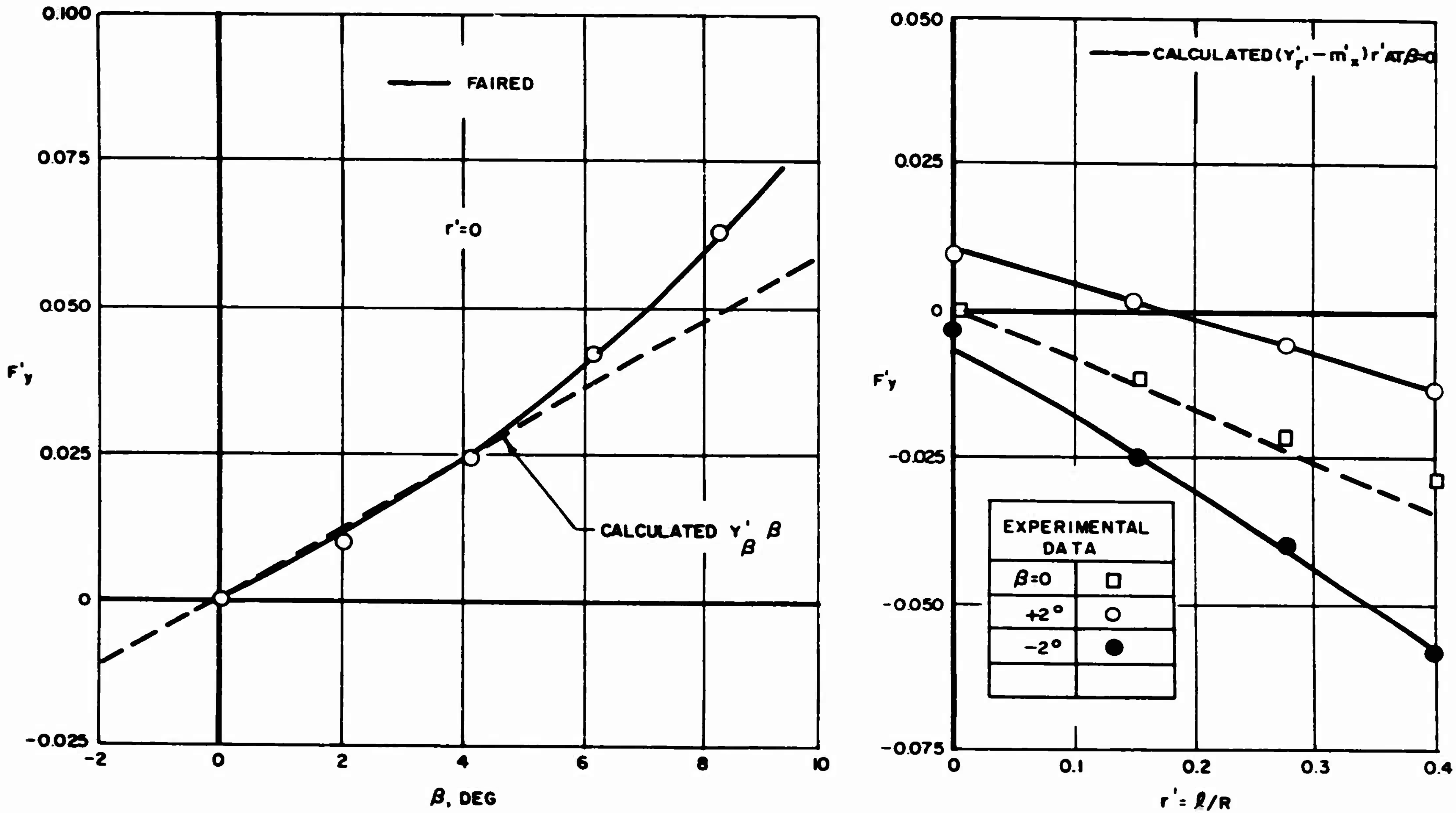


FIGURE C-2. SERIES 60, MODEL 9,1,1. TOTAL LATERAL FORCE COEFFICIENT

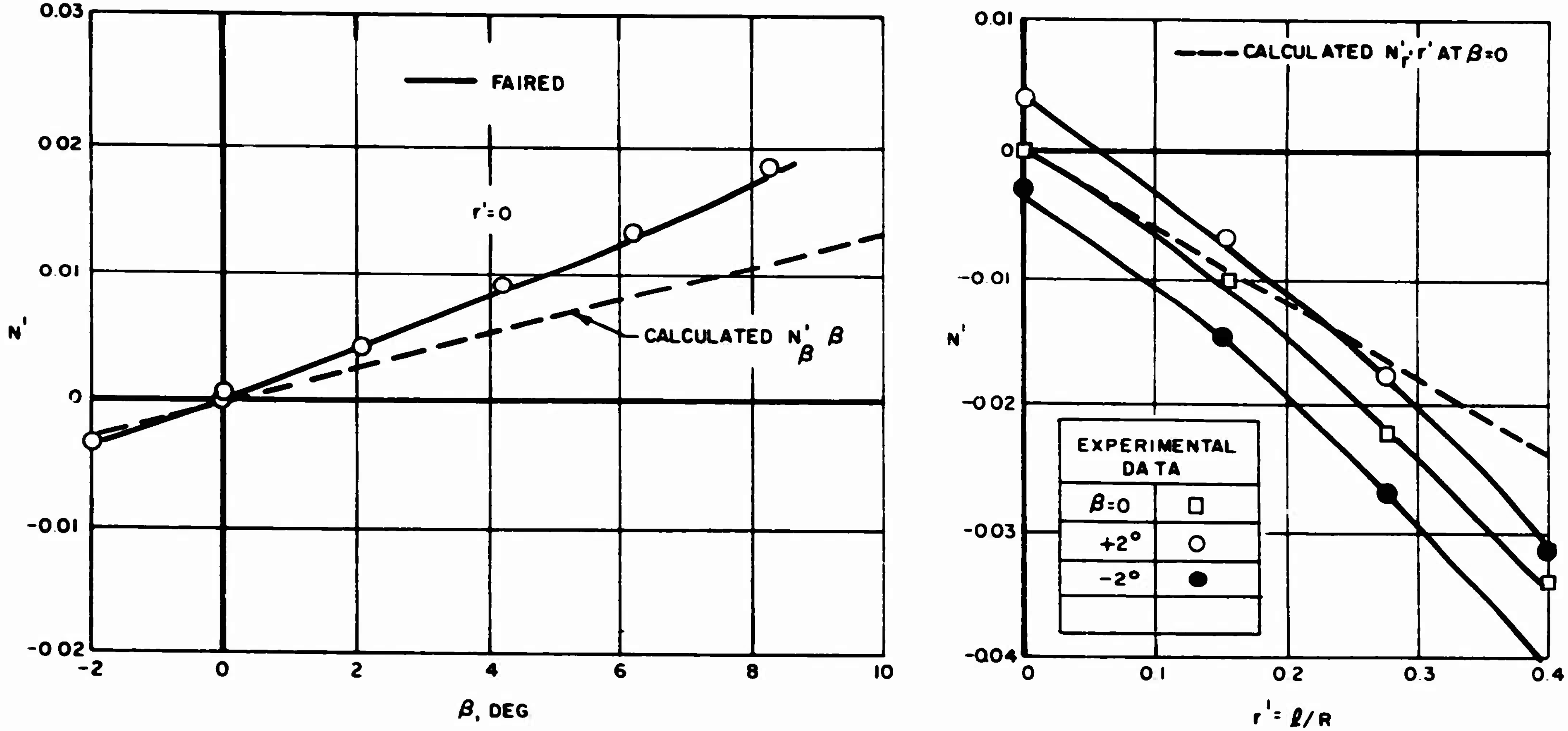


FIGURE C-3. SERIES 60, MODEL 9,1,1. YAWING MOMENT COEFFICIENT

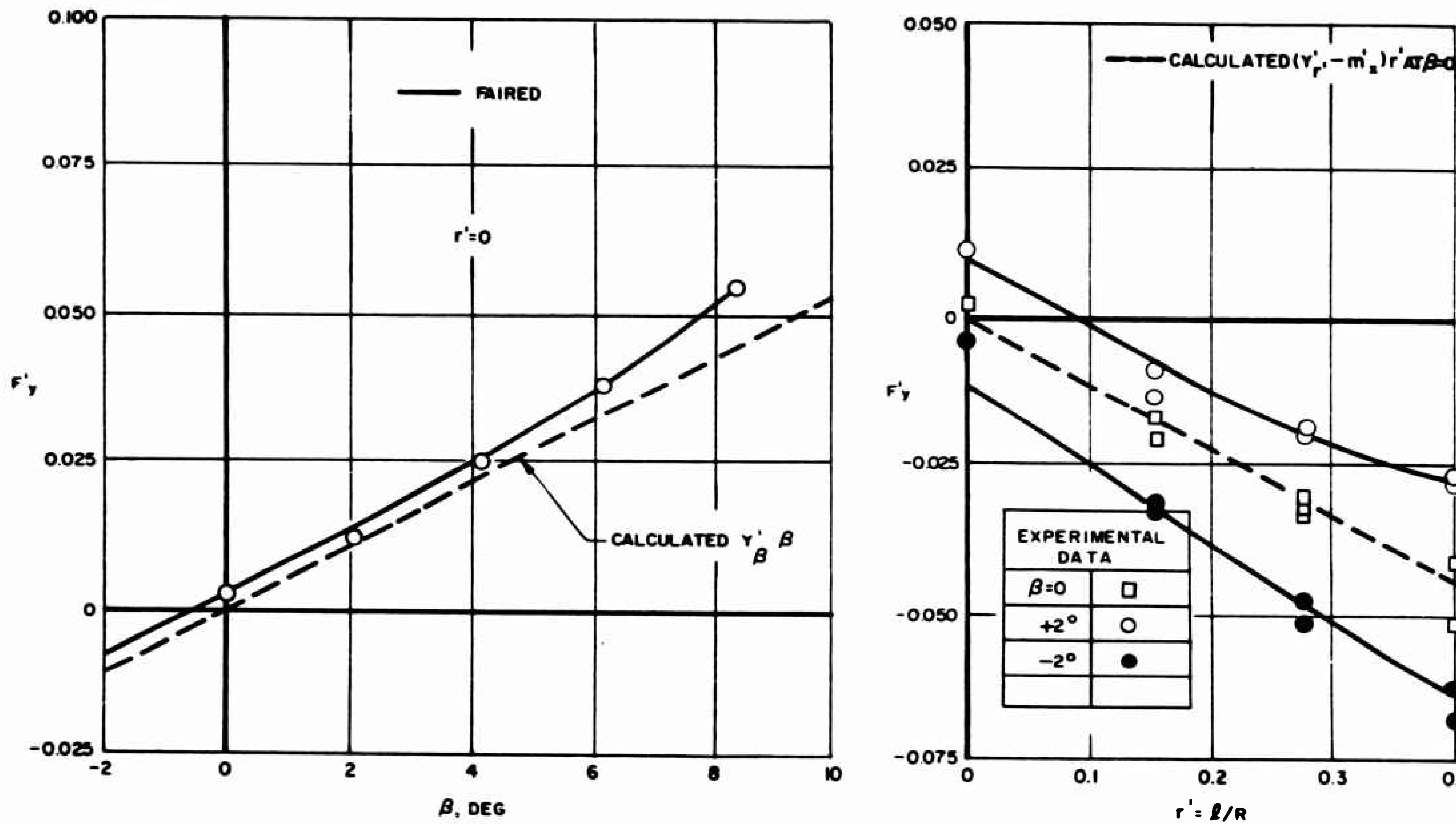


FIGURE C-4. SERIES 60, MODEL 9,0,0. TOTAL LATERAL FORCE COEFFICIENT

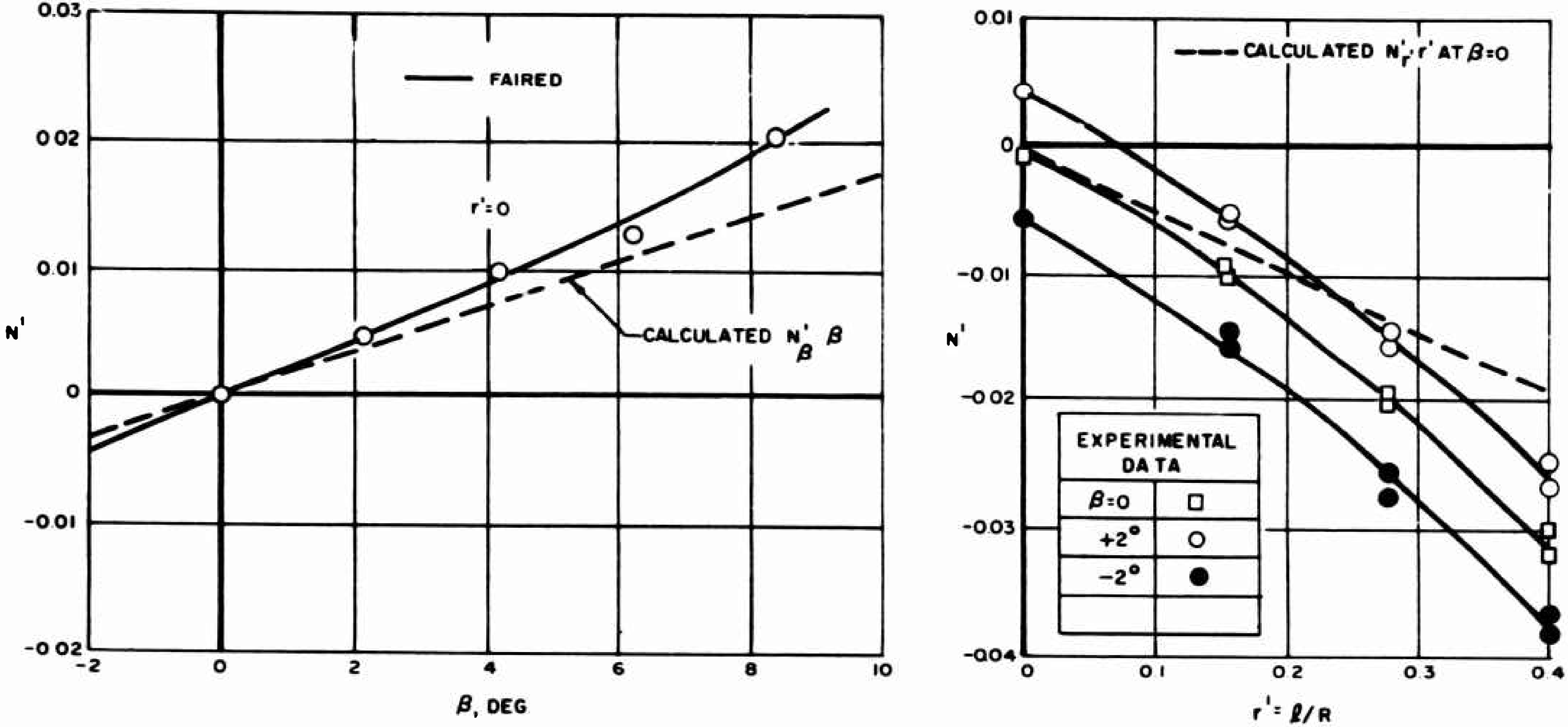


FIGURE C-5. SERIES 60, MODEL 9,0,0. YAWING MOMENT COEFFICIENT

BLANK PAGE

# APPENDIX D

## MARINER CLASS HULL

(Reference 5)

TABLE D-1

PERTINENT CHARACTERISTICS OF THE MARINER CLASS MODEL

| | |
|---|---|
| Length $\ell$ , ft (LWL) | 5.0 |
| Beam B, ft | 0.731 |
| Draft H , ft (mean) | 0.236 |
| Displacement $\Delta$ , lb | 32.6 |
| Prismatic coefficient, $C_p = 2x_o/\ell$ | 0.620 |
| Block coefficient $C_B$ | 0.607 |
| LCG/$\ell$ , from bow | 0.524 |
| B/H | 3.10 |
| $\ell$/B | 6.84 |
| $\ell$/H | 21.19 |

Lamb's Coefficients of Accession to Inertia for Equivalent Ellipsoid

| | |
|---|---|
| Minor axis/major axis, 2H/$\ell$ | 0.094 |
| $k_1$ (longitudinal) | 0.02 |
| $k_2$ (lateral) | 0.96 |
| $k'$ (rotational) | 0.89 |

Other Physical Characteristics

| | |
|---|---|
| $m'_o$, mass coefficient | 0.177 |
| $m'_1$ longitudinal added-mass coefficient | 0.003 |
| $m'_2$ lateral added-mass coefficient | 0.136 |
| $m'_z$ rotational added-mass coefficient | 0.126 |
| $n'_z$ virtual moment-of-inertia coefficient | 0.019 |
| $\bar{x}/\ell$, CG of lateral added mass from LCG | 0.066 |
| $x_p/\ell$, center of area of profile from LCG | 0.058 |
| $D'_o$ (estimated drag coefficient at $\beta = 0$) | 0.014 |

## TABLE D-2

## STABILITY DERIVATIVES FOR THE MARINER CLASS MODEL
(Without Propeller)

| | Theoretical Estimate* | Experimental Range** (Ref. 16) |
|---|---|---|
| $Y'_{\beta}$ | 0.310 | 0.295 to 0.218 |
| $N'_{\beta}$ | 0.068 | 0.066 to 0.122 |
| $Y'_{r'}$ | 0.065 | 0.066 to 0.055 |
| $N'_{r'}$ | -0.059 | -0.050 to -0.037 |
| $m'_{2}$ = lateral added-mass coefficient | 0.136 | 0.114 to 0.151 |
| $n'_{z} - \frac{m'_{o}}{16}$ = added moment-of-inertia coefficient | 0.008 | 0.007 |
| $\sigma_1$ | -0.49 | -0.42 (best)<br>-0.16 (average) |

*Also, as shown on the charts, a reasonable fit to the Davidson Laboratory rotating-arm experimental data.

**Oscillator results nondimensionalized according to the convention adopted in the present paper.

BLANK PAGE

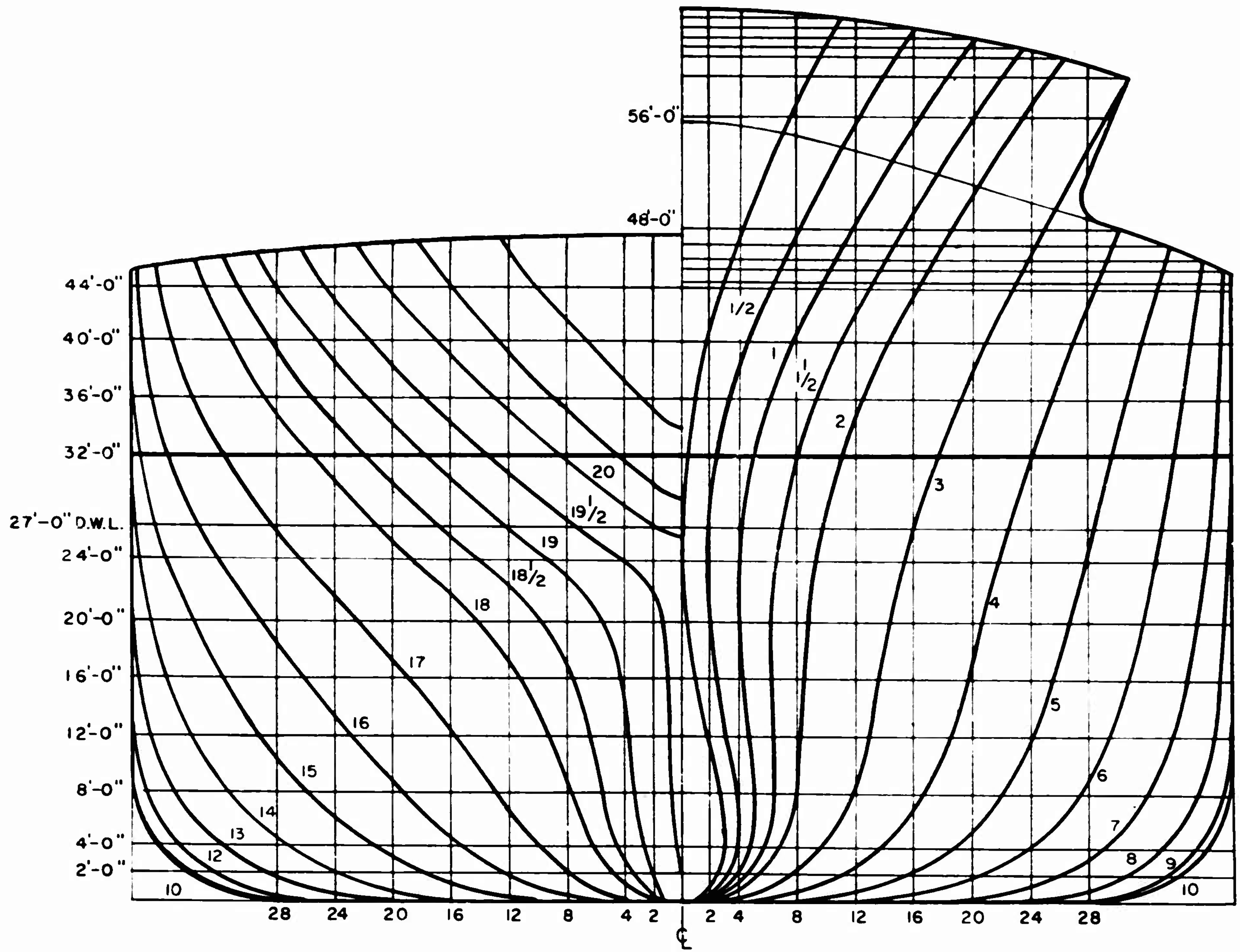


FIGURE D-I. BODY PLAN OF MARINER CLASS MODEL

R-1035

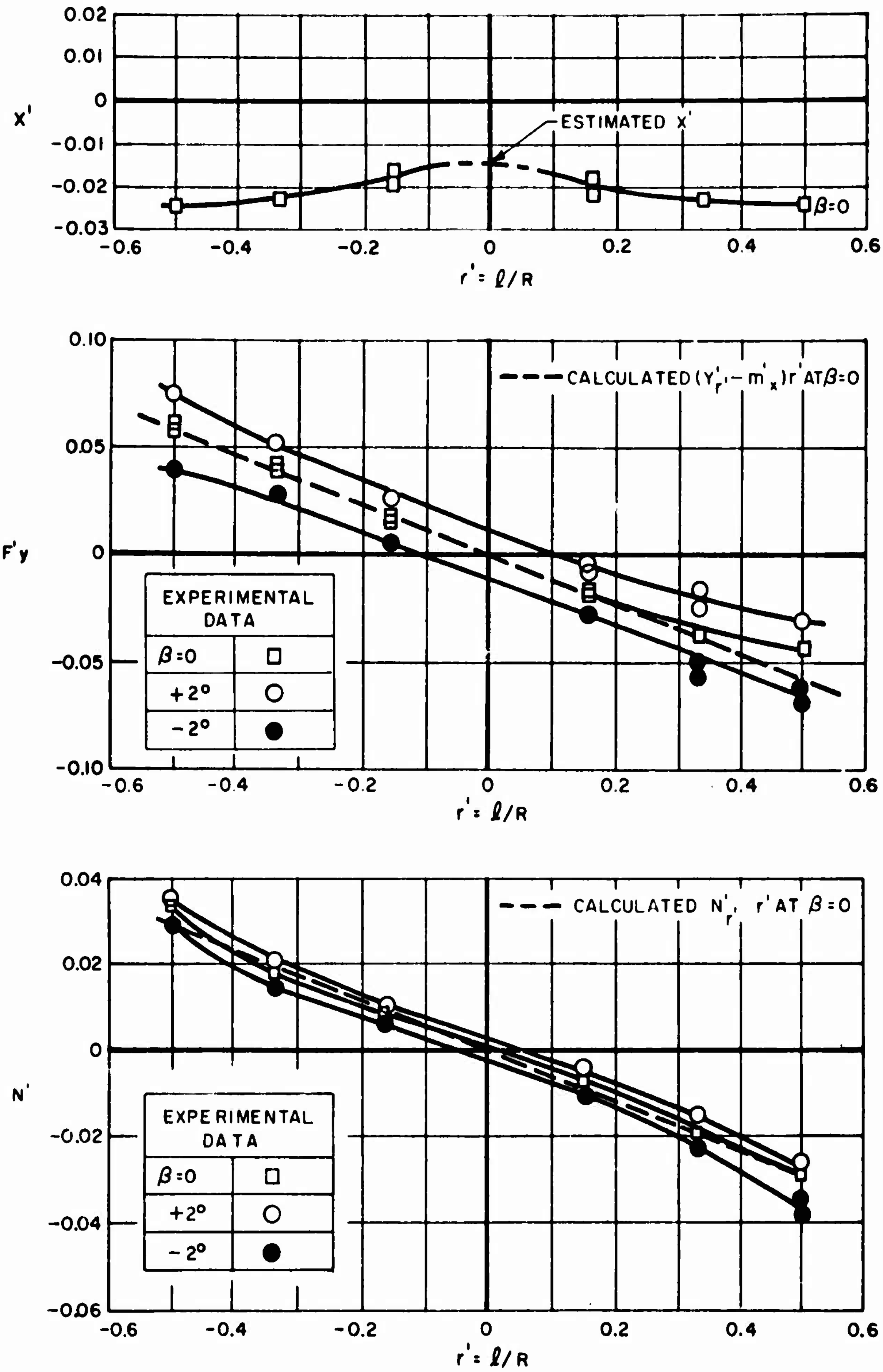


FIGURE D-2. MARINER CLASS. FORCE AND MOMENT COEFFICIENTS VERSUS $r' = \ell/R$

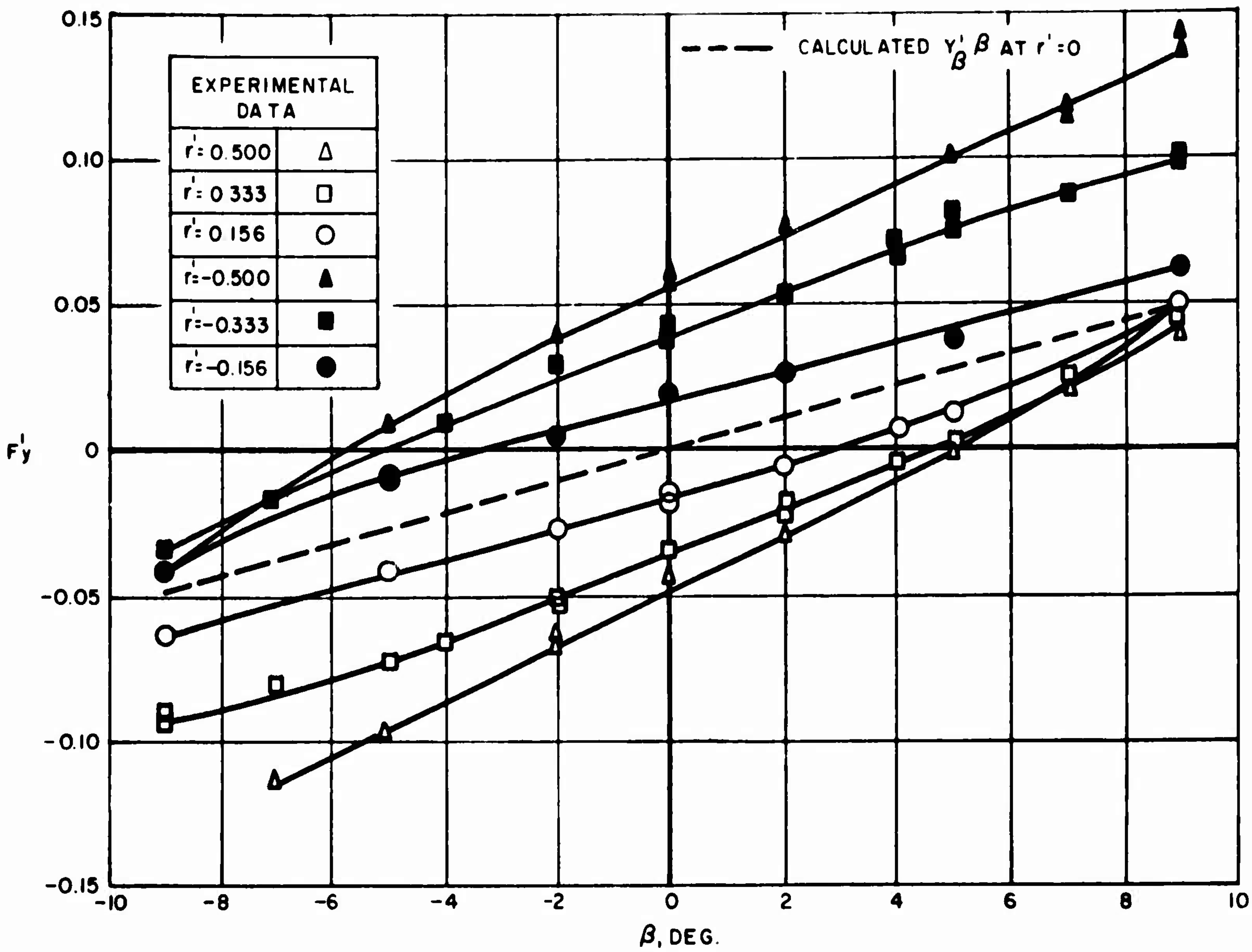


FIGURE D-3. MARINER CLASS. TOTAL LATERAL FORCE COEFFICIENT VERSUS YAW ANGLE $\beta$

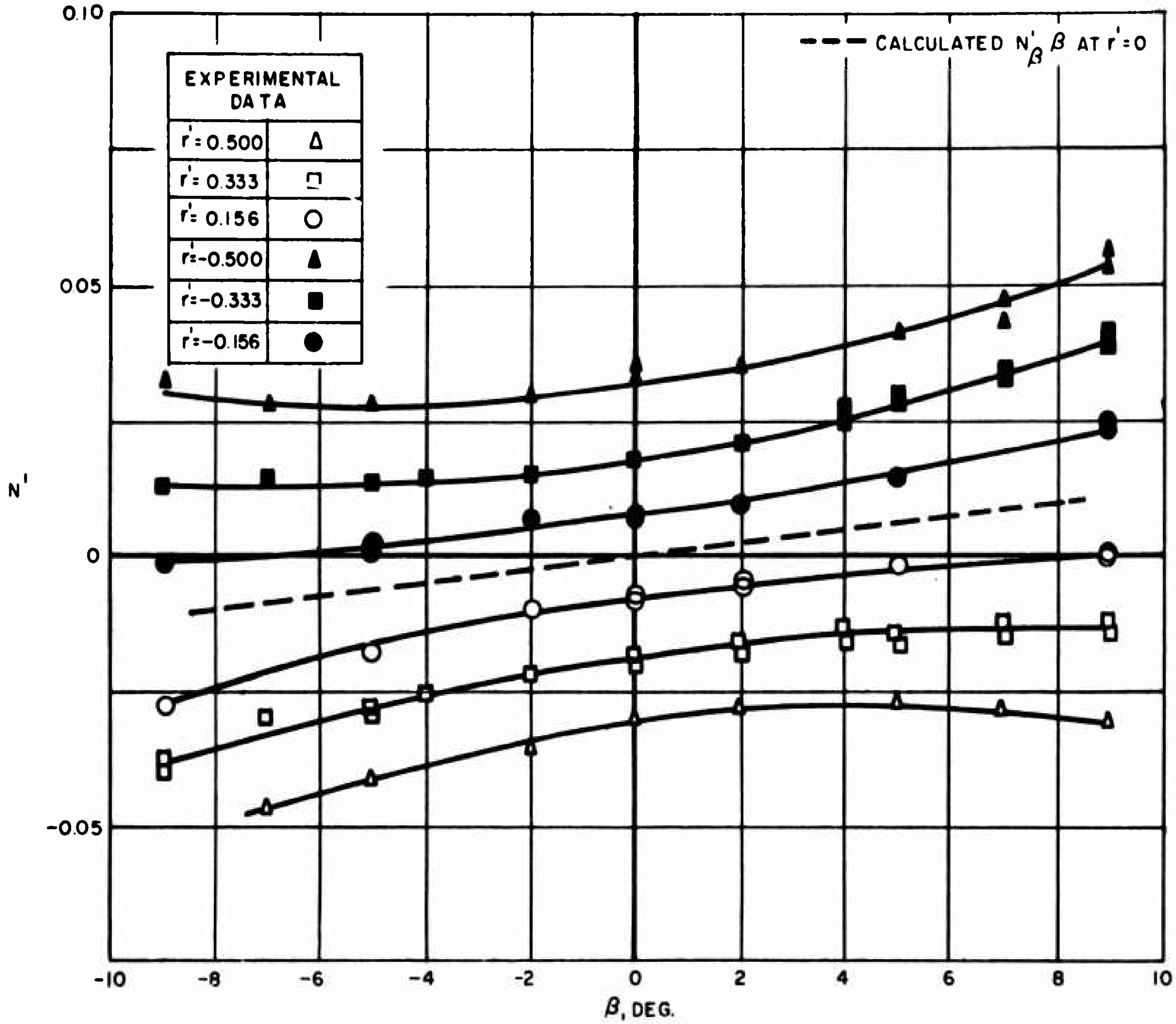


FIGURE D-4. MARINER CLASS. YAWING MOMENT COEFFICIENT VERSUS YAW ANGLE $\beta$

# APPENDIX E

## DESTROYER MODEL

(Reference 6)

TABLE E-1

PERTINENT CHARACTERISTICS OF THE DD692 DESTROYER MODEL

| | |
|---|---|
| Length $\ell$ , ft | 5.710 |
| Beam B, ft | 0.602 |
| Draft H , ft | 0.208 |
| Displacement $\Delta$ , lb | 25.22 |
| Prismatic coefficient, $C_p = 2x_o/\ell$ | 0.643 |
| Block coefficient, $C_B$ | 0.566 |
| LCG/$\ell$ , from bow | 0.522 |
| B/H | 2.90 |
| $\ell$/B | 9.45 |
| $\ell$/H | 27.40 |

Lamb's Coefficients of Accession to Inertia for Equivalent Ellipsoid

| | |
|---|---|
| Minor axis/major axis, 2H/$\ell$ | 0.073 |
| $k_1$ (longitudinal) | 0.015 |
| $k_2$ (lateral) | 0.972 |
| k' (rotational) | 0.920 |

Other Physical Characteristics

| | |
|---|---|
| $m'_o$, mass coefficient | 0.119 |
| $m'_1$ longitudinal added-mass coefficient | 0.002 |
| $m'_2$ lateral added-mass coefficient | 0.087 |
| $m'_z$ rotational added-mass coefficient | 0.082 |
| $n'_z$ virtual moment-of-inertia coefficient | 0.0122 |
| $\bar{x}/\ell$ , CG of lateral added mass from LCG | 0.070 |
| $x_p/\ell$, center of area of profile from LCG | 0.054 |
| $D'_o$, drag coefficient at $\beta$ = 0, U = 2.1 ft/sec | 0.017 |
| $\sigma_1$ stability index | -0.76 |

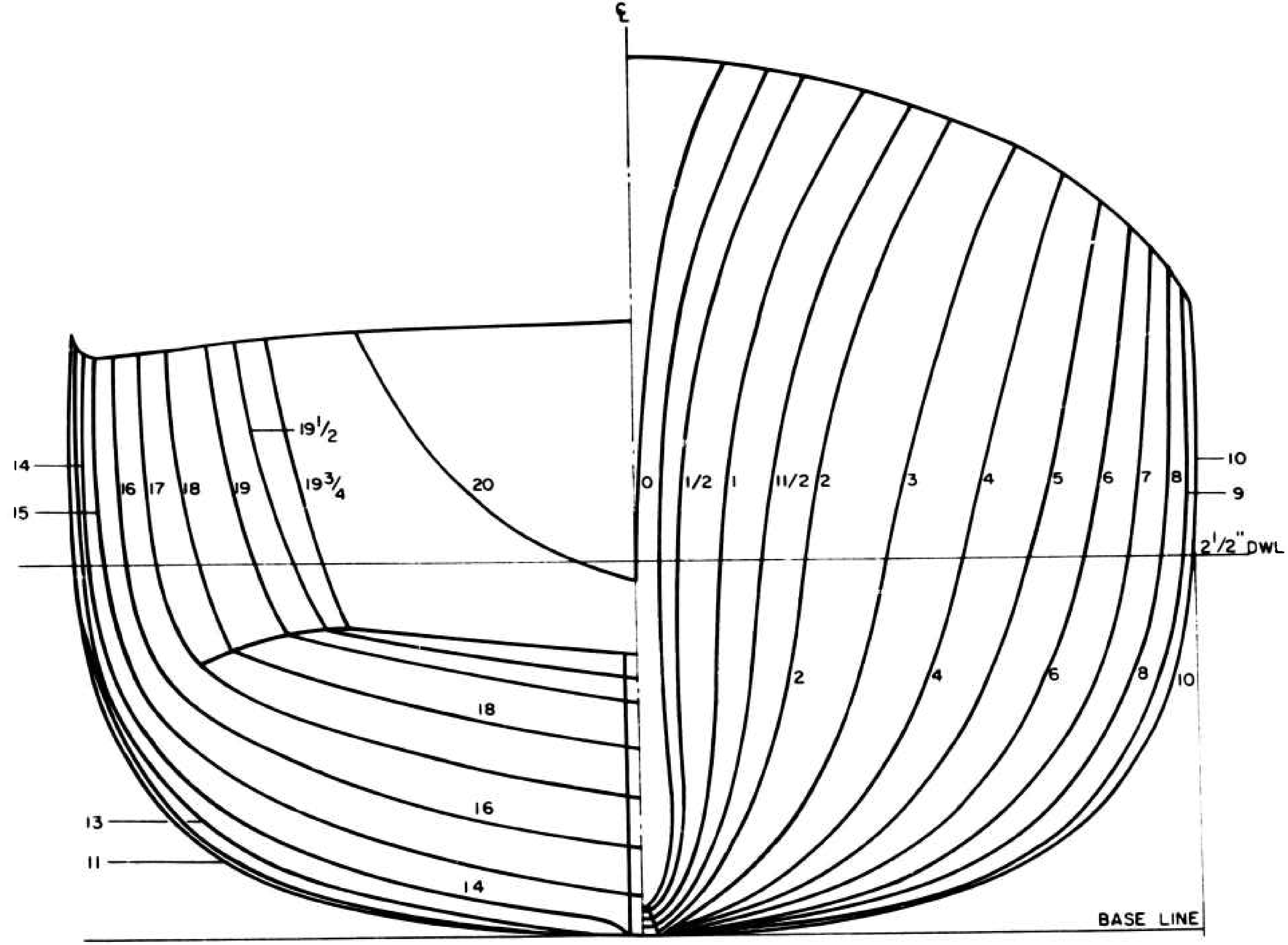


FIGURE E-1. BODY PLAN OF DD 692 DESTROYER MODEL

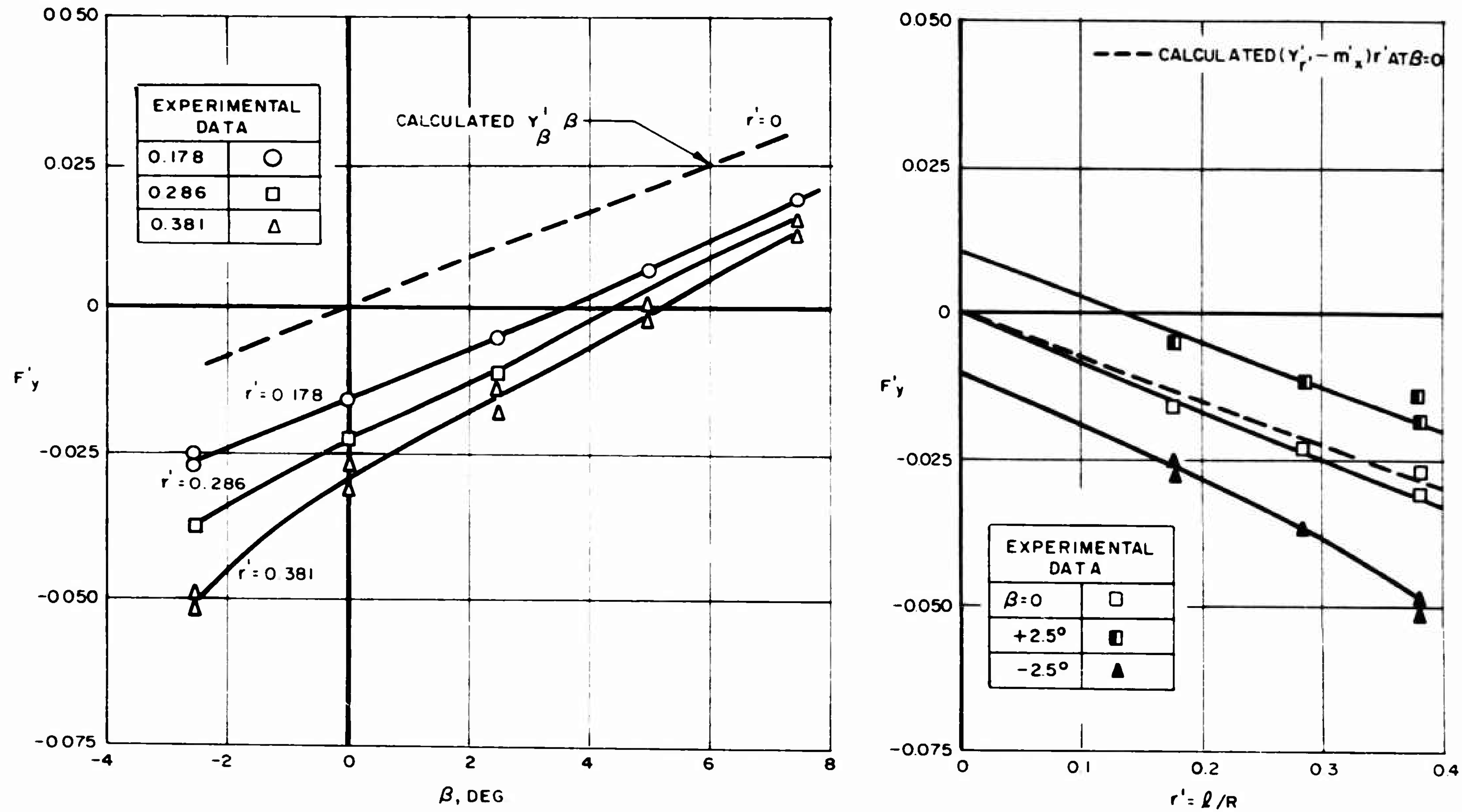


FIGURE E-2. DD 692 DESTROYER. TOTAL LATERAL FORCE COEFFICIENT

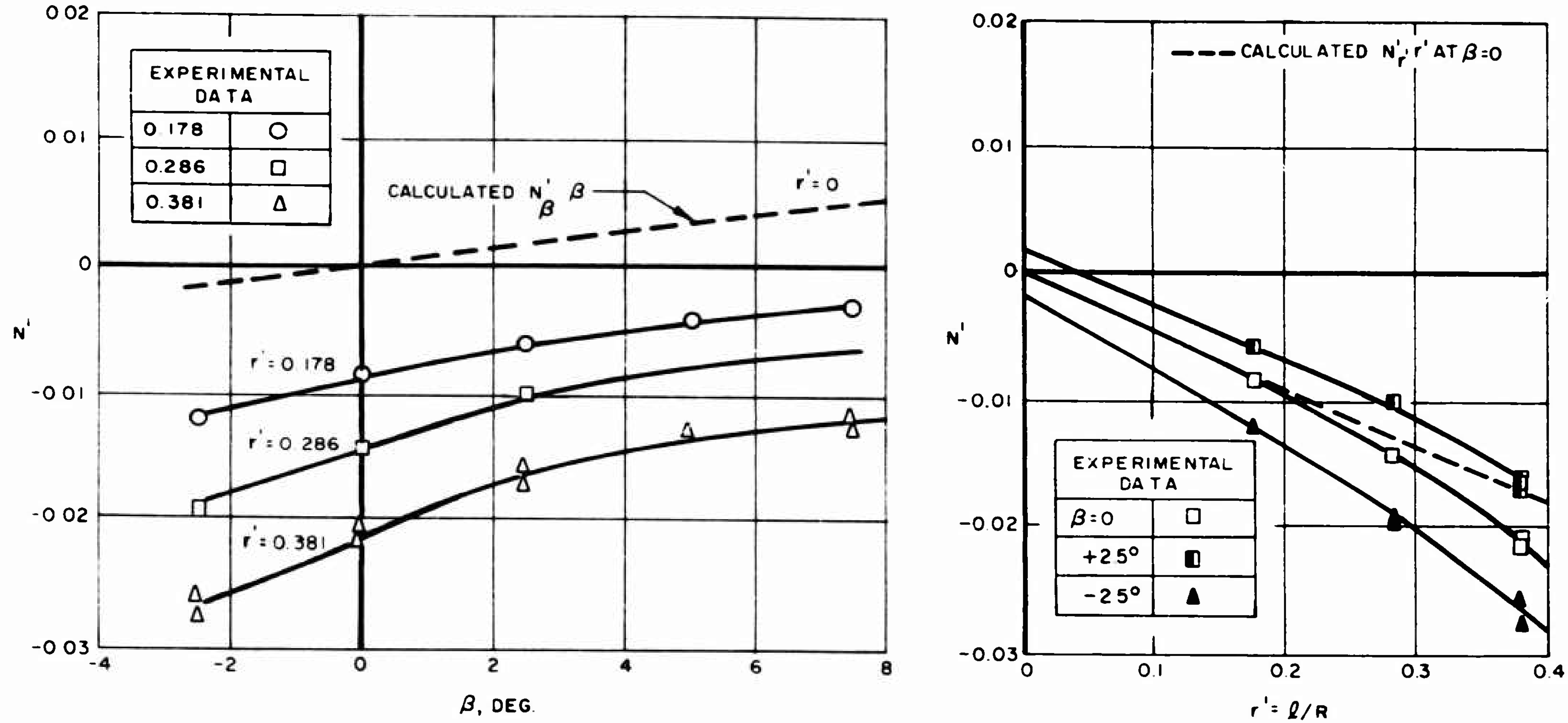


FIGURE E-3. DD 692 DESTROYER. YAWING MOMENT COEFFICIENT

BLANK PAGE

# APPENDIX F

## HOPPER-DREDGE MODELS

(Referencc 7)

TABLE F-1

PERTINENT CHARACTERISTICS OF THE HOPPER-DREDGE MODEL

| Condition | Heavy | Light |
|---|---|---|
| Length $\ell$, ft (LWL) | 4.333 | 4.167 |
| Beam B, ft | 0.721 | 0.721 |
| Draft H, ft | 0.299 | 0.208 |
| Displacement $\Delta$, lb | 41.65 | 32.08 |
| Prismatic coefficient, $C_p = 2x_o/\ell$ | 0.727 | 0.840 |
| Block coefficient $C_B$ | 0.717 | 0.820 |
| LCG/$\ell$, from bow | 0.500 | 0.512 |
| B/H | 2.415 | 3.461 |
| $\ell$/B | 6.00 | 5.78 |
| $\ell$/H | 14.51 | 20.00 |
| **Lamb's Coefficients of Accession to Inertia for Equivalent Ellipsoids** | | |
| Minor axis/major axis, 2H/$\ell$ | 0.138 | 0.100 |
| $k_1$ (longitudinal) | 0.033 | 0.020 |
| $k_2$ (lateral) | 0.936 | 0.960 |
| k' (rotational) | 0.815 | 0.885 |
| **Other Physical Characteristics** | | |
| $m_o'$, mass coefficient | 0.239 | 0.284 |
| $m_1'$, longitudinal added-mass coefficient | 0.008 | 0.006 |
| $m_2'$, lateral added-mass coefficient | 0.237 | 0.171 |
| $m_z'$, rotational added-mass coefficient | 0.207 | 0.158 |
| $n_z'$, virtual moment of inertia | 0.0315 | 0.0311 |
| $\bar{x}/\ell$, CG of lateral added mass from LCG | 0.021 | 0.013 |
| $x_p/\ell$, center of area of profile from LCG | 0.016 | 0.014 |
| $D_o'$ (drag coefficient at $\beta = 0$) | 0.025 | 0.028 |

TABLE F-2

STABILITY INDEX $\sigma_1$ FOR THE HOPPER-DREDGE MODEL

| Condition | Model Speed ft/sec | $\sigma_1$ Theoretical Estimate | Calculated from Measurements (Ref.7) |
|---|---|---|---|
| Heavy | 2.39 | +0.83 | +0.89 |
| | 1.40 | +0.83 | +1.04 |
| Light | 1.80 | +0.60 | +0.82 |

BLANK PAGE

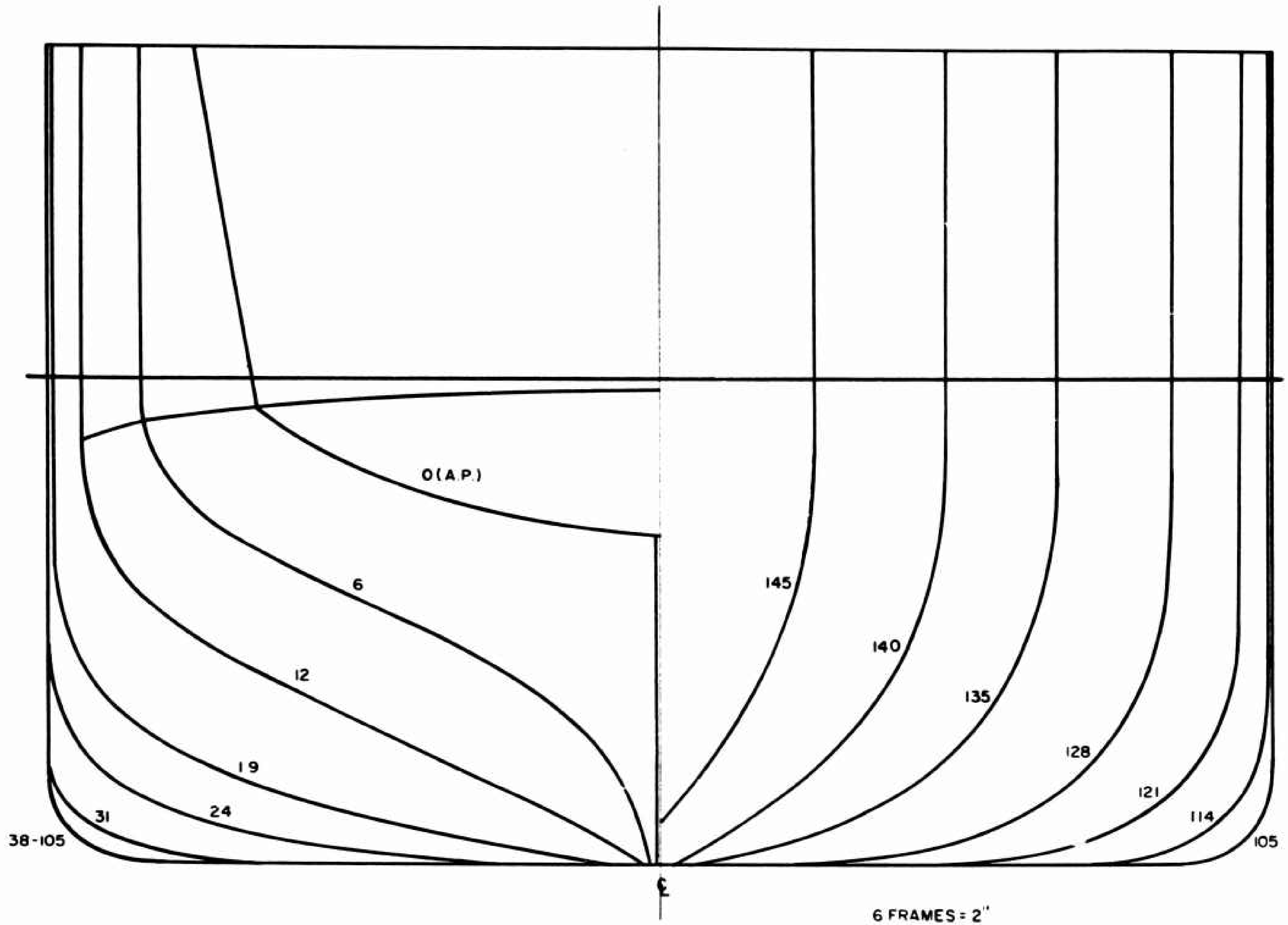


FIGURE F-1. BODY PLAN OF HOPPER DREDGE MODEL

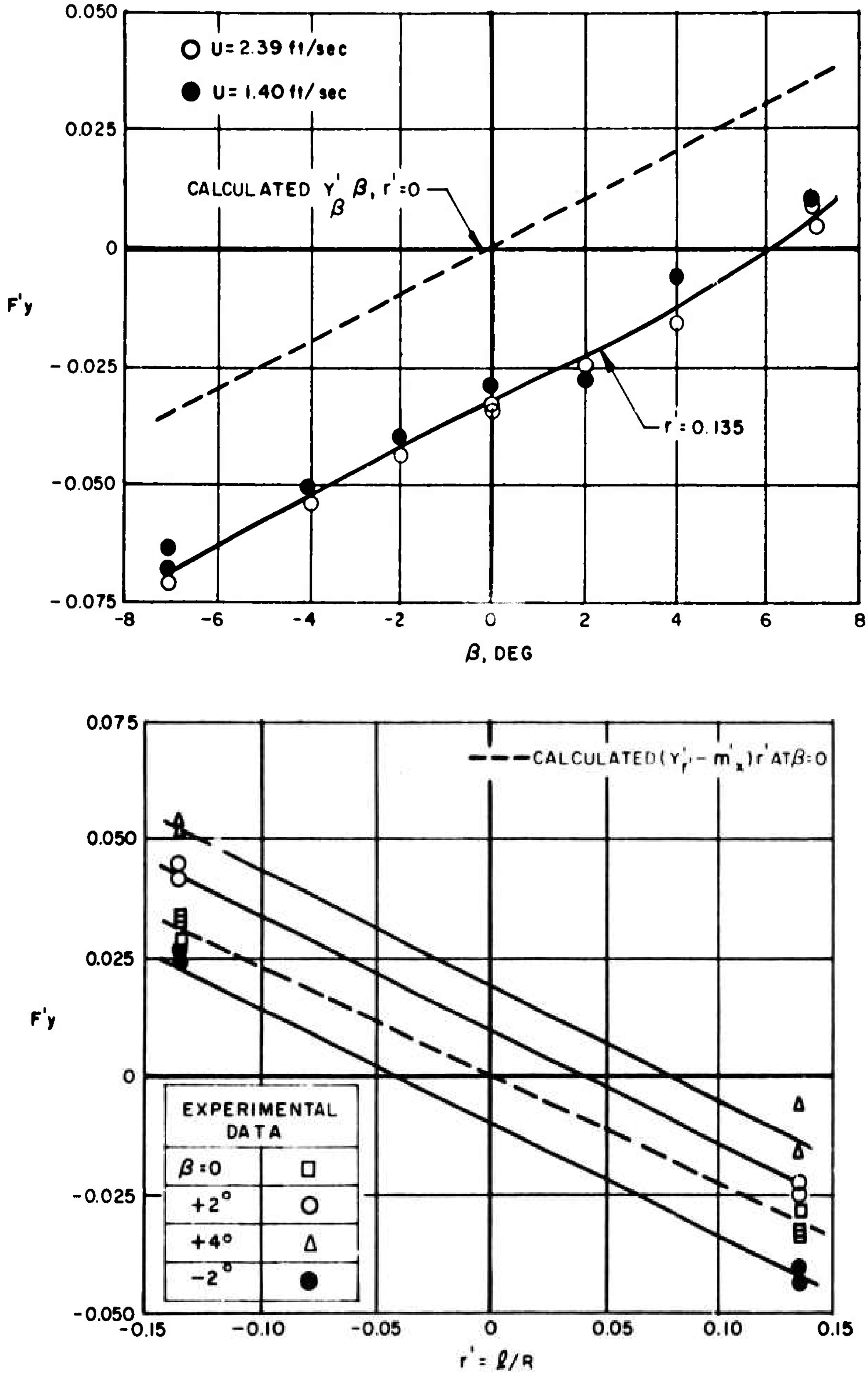


FIGURE F-2. HOPPER DREDGE, HEAVY DISPLACEMENT TOTAL LATERAL FORCE COEFFICIENT

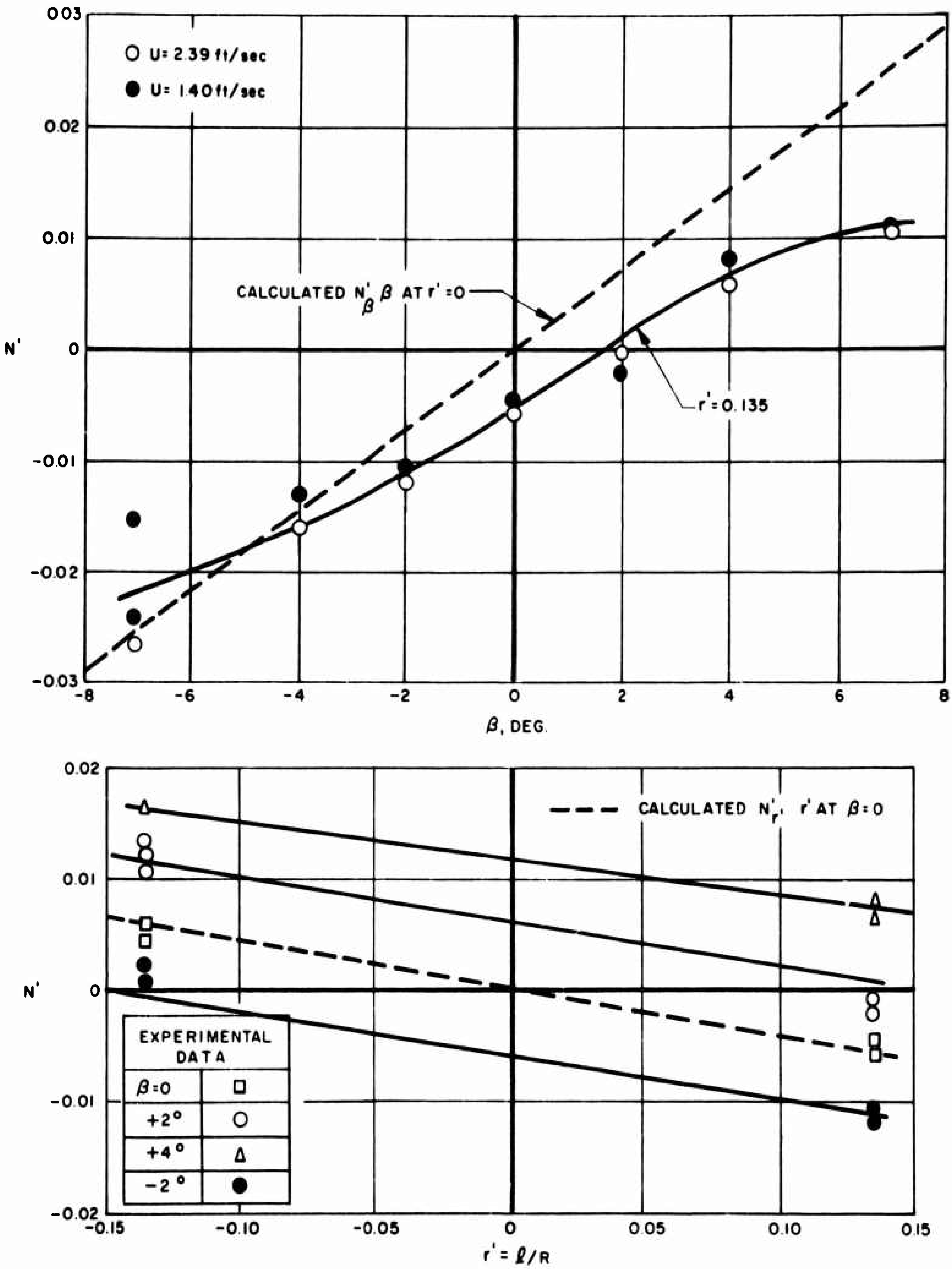


FIGURE F-3. HOPPER DREDGE, HEAVY DISPLACEMENT, YAWING MOMENT COEFFICIENT

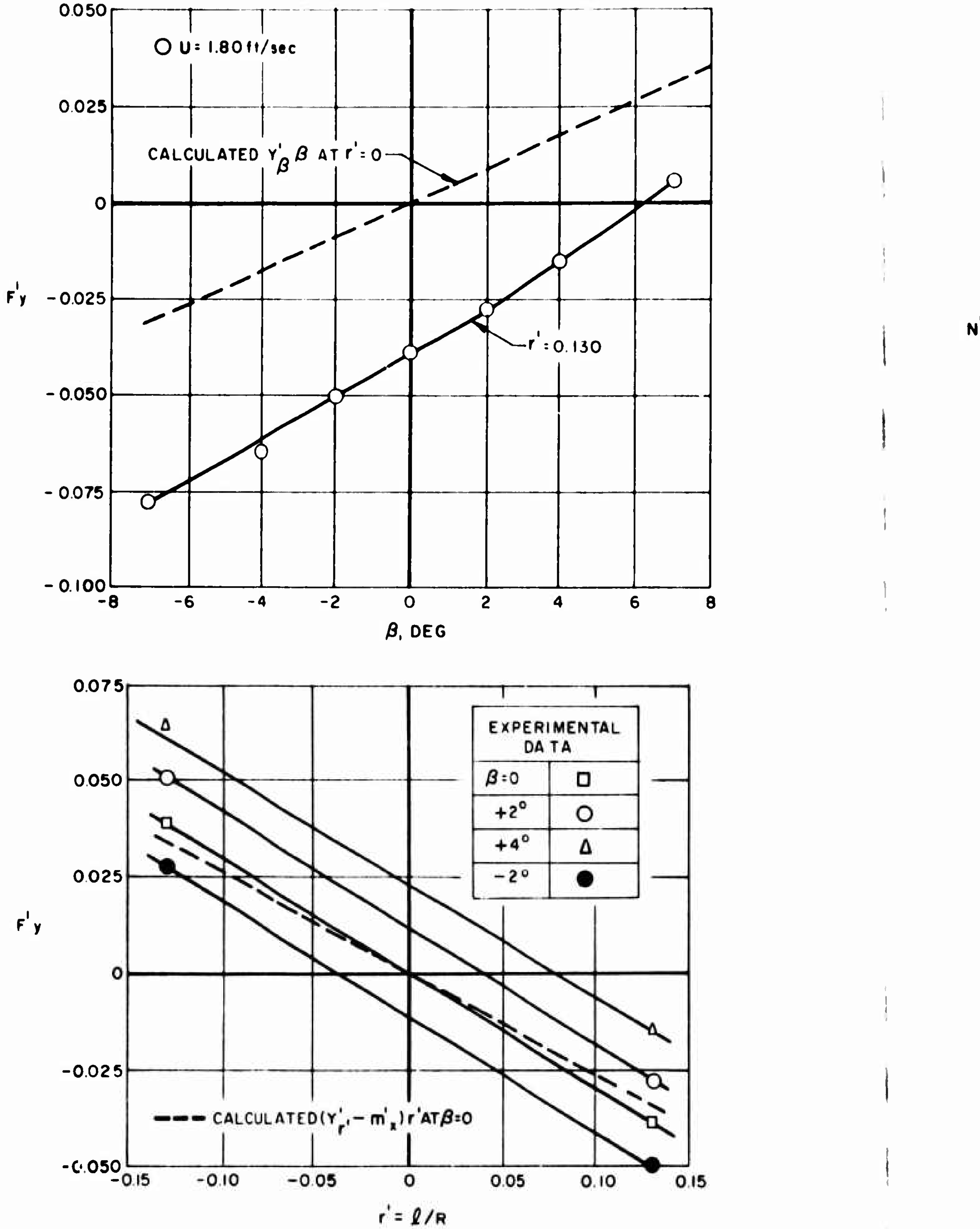


FIGURE F-4. HOPPER DREDGE, LIGHT DISPLACEMENT. TOTAL LATERAL FORCE COEFFICIENT

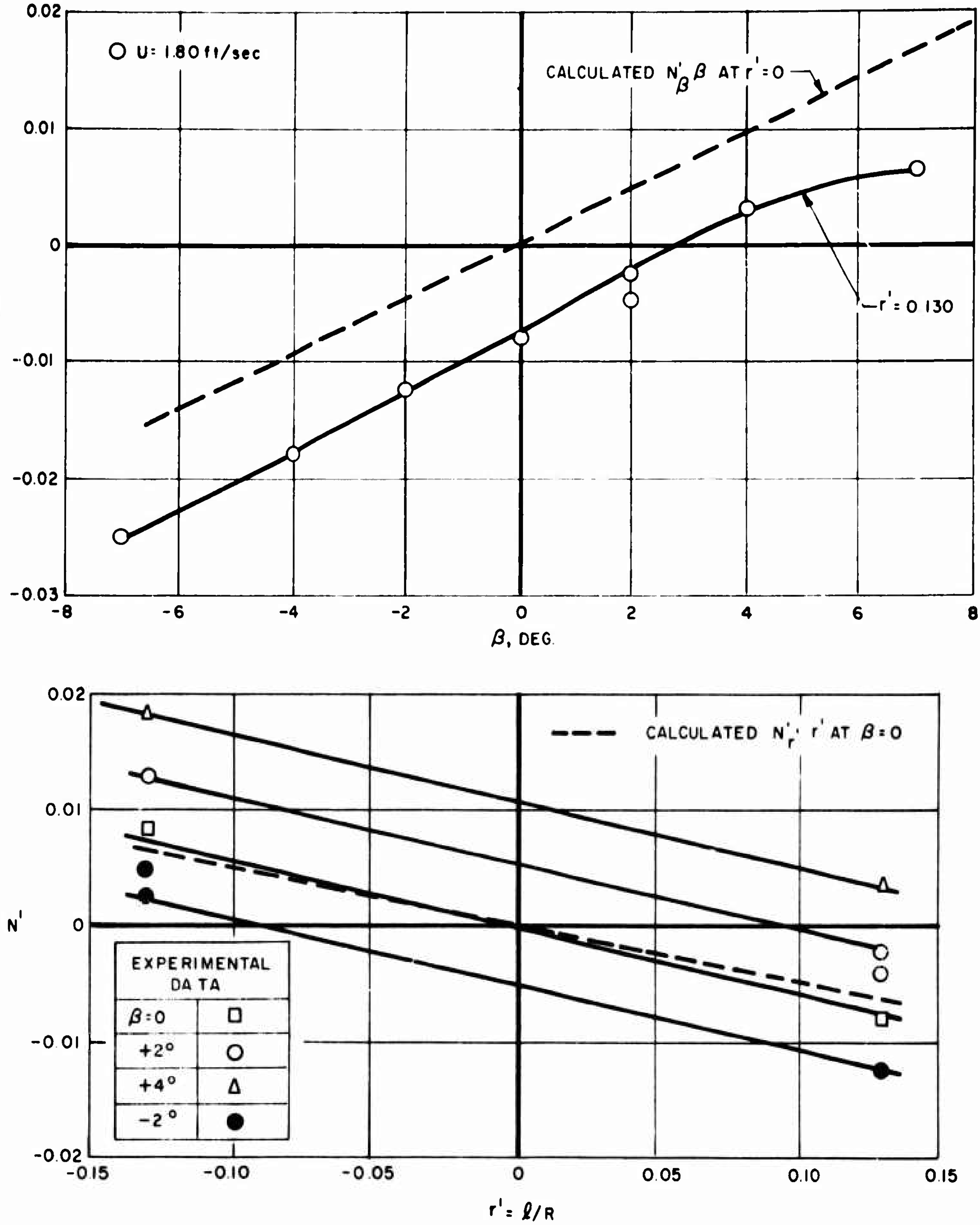


FIGURE F-5. HOPPER DREDGE, LIGHT DISPLACEMENT. YAWING MOMENT COEFFICIENT

BLANK PAGE

DISTRIBUTION LIST

Contract Nonr 263(57)

| Copies | |
|---|---|
| 10 | Chief<br>BUREAU OF SHIPS<br>Department of the Navy<br>Washington 25, D. C.<br>Attn Tech. Info. Br. (Code 335) (3)<br>Res. & Devel. (Code 310) (1)<br>Prelim. Design (Code 420) (1)<br>Prelim. Design (Code 421) (1)<br>Hull Design Br. (Code 440) (1)<br>Scien. & Res. (Code 442) (1)<br>(Code 341B) (1)<br>(Code 345) (1) |
| 75 | Commanding Officer and Director<br>DAVID TAYLOR MODEL BASIN<br>Washington 7, D. C.<br>Attn (Code 513) |
| 20 | DEFENSE DOCUMENTATION CENTER<br>Cameron Station<br>5010 Duke St.<br>Alexandria, Va. 22314 |
| 1 | Chief of NAVAL RESEARCH<br>Fluid Dynamics Branch<br>Department of the Navy<br>Washington 25, D. C.<br>Attn (Code 438) |
| 1 | Commanding Officer<br>OFFICE OF NAVAL RESEARCH<br>Branch Office<br>230 N. Michigan Ave.<br>Chicago 1, Ill. |
| 1 | Commanding Officer<br>OFFICE OF NAVAL RESEARCH<br>207 West 24th St.<br>New York 11, N. Y. |
| 1 | Commanding Officer<br>OFFICE OF NAVAL RESEARCH<br>Branch Office<br>1030 East Green St.<br>Pasadena 1, Calif. |

| Copies | |
|---|---|
| 1 | Commanding Officer<br>OFFICE OF NAVAL RESEARCH<br>Branch Office<br>1000 Geary Street<br>San Francisco 9, California |
| 1 | Commander<br>BOSTON NAVAL SHIPYARD<br>Boston, Massachusetts |
| 1 | Commander<br>CHARLESTON NAVAL SHIPYARD<br>Charleston, South Carolina |
| 1 | Administrator<br>Maritime Administration<br>DEPARTMENT OF COMMERCE<br>Washington 25, D. C.<br>Attn Office of Ship Construction<br>Mr. Vito L. Russo |
| 1 | Office of Technical Services<br>DEPARTMENT OF COMMERCE<br>Washington 25, D. C.<br>Attn Technical Reports Sec. |
| 2 | Chief<br>BUREAU OF WEAPONS<br>Department of the Navy<br>Washington 25, D. C. |
| 1 | Chief<br>BUREAU OF YARDS & DOCKS<br>Department of the Navy<br>Washington 25, D. C.<br>Attn Code D-400 Research Div. |
| 1 | Commander<br>Military Sea Transportation<br>DEPARTMENT OF THE NAVY<br>Washington 25, D. C. |
| 1 | Commander<br>LONG BEACH NAVAL SHIPYARD<br>Long Beach, California |

DISTRIBUTION LIST

Contract Nonr 263(57)

| Copies | |
|---|---|
| 1 | Commander<br>MARE ISLAND NAVAL SHIPYARD<br>Vallejo, California |
| 1 | Director<br>NAT'L AERONAUTICS & SPACE ADM.<br>1512 H Street, N.W.<br>Washington 25, D. C. |
| 1 | Director<br>NATIONAL BUREAU OF STANDARDS<br>Washington 25, D. C.<br>Attn Dr. G. B. Schubauer<br>Fluid Mechanics |
| 1 | Director<br>NATIONAL SCIENCE FOUNDATION<br>1420 H Street, N.W.<br>Washington, D. C. |
| 6 | Director<br>NAVAL RESEARCH LABORATORY<br>Washington 25, D. C.<br>Attn (Code 2021) Library |
| 1 | Commander<br>NEW YORK NAVAL SHIPYARD<br>Brooklyn, New York |
| 1 | Commander<br>NORFOLK NAVAL SHIPYARD<br>Portsmouth, Virginia |
| 1 | Commander<br>PEARL HARBOR NAVAL SHIPYARD<br>Navy #128, Fleet Post Office<br>San Francisco, California |
| 1 | Director<br>PHILADELPHIA NAVAL SHIPYARD<br>Philadelphia, Pennsylvania |
| 1 | Commander<br>PORTSMOUTH NAVAL SHIPYARD<br>Portsmouth, New Hampshire |

| Copies | |
|---|---|
| 1 | Commander<br>PUGET SOUND NAVAL SHIPYARD<br>Bremerton, Washington |
| 1 | Commander<br>SAN FRANCISCO NAVAL SHIPYARD<br>San Francisco, California |
| 1 | U.S. ARMY TRANS. RESEARCH &<br>ENGINEERING COMMAND<br>Fort Eustis, Virginia<br>Attn Marine Transport Div. |
| 2 | U.S. COAST GUARD<br>1300 E Street, N.W.<br>Washington 25, D. C.<br>Attn Sec., Ship Structure<br>Commandant |
| 1 | Superintendent<br>U.S. MERCHANT MARINE ACADEMY<br>Kings Point, L.I., New York<br>Attn Capt. L. McCready, Head<br>Dept. of Engineering |
| 1 | U.S. NAVAL ACADEMY<br>Annapolis, Maryland<br>Superintendent<br>Attn Library |
| 1 | U.S. NAVAL POST GRADUATE SCHOOL<br>Monterey, California<br>Attn Superintendent |
| 1 | Commander<br>U.S. NAVAL PROVING GROUND<br>Dahlgren, Virginia |
| 1 | Commander<br>U.S. NAVAL SHIP REPAIR FACILITY<br>San Diego, California |
| 1 | AERONAUTICAL RESEARCH ASSOCIATES<br>OF PRINCETON, INC.<br>50 Washington Road<br>Princeton, New Jersey<br>Attn Dr. Bernard Paiewonsky |

## DISTRIBUTION LIST

Contract Nonr 263(57)

| Copies | |
|---|---|
| 1 | Mr. Walter J. Blumberg<br>U.S. NAVAL MARINE ENGINEERING LABORATORY<br>Annapolis, Maryland<br>Attn Code 812.8 |
| 1 | CALIFORNIA INST. OF TECHNOLOGY<br>Pasadena 4, California<br>Attn Prof. T. Y. Wu |
| 3 | COLORADO STATE UNIVFRSITY<br>Dept. of Civil Engineering<br>Fort Collins, Colorado<br>Attn Prof. M. Albertson<br>Prof. J. Cermak<br>Prof. L. V. Baldwin |
| 1 | CORNELL AERONAUTICAL LAB., INC.<br>Applied Mechanics Dept.<br>P. O. Box 235<br>Buffalo 21, New York<br>Attn Dr. Irving C. Statler |
| 1 | DARTMOUTH COLLEGE<br>Thayer School of Engineering<br>Hanover, New Hampshire<br>Attn Prof. Sidney Lees |
| 2 | DOUGLAS AIRCRAFT CO., INC.<br>Aircraft Division<br>Long Beach, California<br>Attn Mr. John Hess<br>Mr. A. M. O. Smith |
| 2 | Electric Boat Division<br>GENERAL DYNAMICS CORPORATION<br>Groton, Connecticut<br>Attn Mr. H. E. Sheets<br>Mr. R. J. McGrattan |
| 1 | HYDRONAUTICS, INCORPORATED<br>Pindell School Road<br>Howard County, Laurel, Md.<br>Attn Mr. Phillip Eisenberg |

| Copies | |
|---|---|
| 1 | HYDRO SPACE ASSOCIATES<br>3775 Sheridge Drive<br>Sherman Oaks, California<br>Attn Dr. Leonard Pode |
| 2 | Courant Inst. of Math. Sciences<br>NEW YORK UNIVERSITY<br>25 Waverly Place<br>New York 3, New York<br>Attn Prof. J. Stoker<br>Prof. A. Peters |
| 1 | PENNSYLVANIA STATE UNIVERSITY<br>University Park, Pennsylvania<br>Attn Ordnance Research Lab.<br>Director |
| 1 | Ordnance Research Laboratory<br>PENNSYLVANIA STATE UNIVERSITY<br>P. O. Box 30<br>University Park, Pennsylvania<br>Attn Dr. George F. Wislicenus |
| 1 | ROBERT TAGGART, INC.<br>400 Arlington Blvd.<br>Falls Church, Virginia<br>Attn Mr. Robert Taggart |
| 1 | Dr. Karl E. Schoenherr<br>7053 Western Ave., N.W.<br>Washington, D. C 20015 |
| 1 | SOCIETY OF NAVAL ARCHITECTS AND MARINE ENGINEERS<br>74 Trinity Place<br>New York 6, New York |
| 1 | SOUTHWEST RESEARCH INSTITUTE<br>Dept. of Mechanical Sciences<br>8500 Culebra Road<br>San Antonio 6, Texas<br>Attn Dr. H. Norman Abramson |

DISTRIBUTION LIST

Contract Nonr 263(57)

Copies

2 Iowa Inst. of Hydraulic Research
STATE UNIVERSITY OF IOWA
Iowa City, Iowa
Attn Prof. H. Rouse, Director
Prof. L. Landweber

1 Maritime College
STATE UNIVERSITY OF NEW YORK
Fort Schuyler
New York 65, New York
Attn Engineering Dept.
Prof. J. J. Foody

1 MASS. INST. OF TECHNOLOGY
Cambridge 39, Massachusetts
Attn Prof. J. E. Kerwin
Dept. of Naval Arch. &
Marine Engineers

1 MASS. INST. OF TECHNOLOGY
Cambridge 39, Massachusetts
Attn Dr. E. Covert
Aerophysics Laboratory

1 MASS. INST. OF TECHNOLOGY
Cambridge 39, Massachusetts
Attn Dr. H. L. Moses
Gas Turbine Laboratory

2 MASS. INST. OF TECHNOLOGY
Cambridge, Massachusetts 02139
Attn Dept. of Naval Arch. &
Marine Engineers
Prof. L. Troost, Head
Prof. Philip Mandel

2 NEW YORK UNIVERSITY
University Heights
New York 53, New York
Attn Dept. of Oceanography
Prof. W. J. Pierson, Jr.

1 TECHNICAL RESEARCH GROUP, INC.
Route 110
Melville, L.I., New York
Attn Dr. Jack Kotik

Copies

3 UNIVERSITY OF CALIFORNIA
Berkeley 4, California
Attn College of Engineering
Prof. H. A. Schade
Prof. J. Johnson
Prof. J. V. Wehausen

1 UNIVERSITY OF ILLINOIS
College of Engineering
Dept. of Theoretical &
Applied Mechanics
Urbana, Illinois
Attn Prof. J. M. Robertson

1 UNIVERSITY OF MARYLAND
College Park, Maryland
Attn Institute for Fluid Dynam
and Applied Mathematics

2 UNIVERSITY OF MICHIGAN
Dept. of Naval Arch. & Marine
Engineers
Ann Arbor, Michigan
Attn Prof. R. B. Couch, Head
Dr. Finn C. Michelsen

2 UNIVERSITY OF MINNESOTA
St. Anthony Falls Hydraulic Lab
Minneapolis 14, Minnesota
Attn Prof L. G. Straut

1 VIDYA
1450 Page Mill Road
Palo Alto, California
Attn Dr. A. H. Sacks

1 VIRGINIA POLYTECHNIC INST.
Blacksburg, Virginia
Attn Librarian

1 WEBB INST. OF NAVAL ARCHITECTUR
Crescent Beach Road
Glen Cove, L. I., New York
Adminstrator
Attn Technical Library

1 WOODS HOLE OCEANOGRAPHIC INST.
Woods Hole, Massachusetts
Attn Dr. C Iselin

amics
s

# BLANK PAGE

ab.

URE

•

DAVIDSON LABORATORY Report 1035 (UNCLASSIFIED) Sept. 1964

ESTIMATION OF STABILITY DERIVATIVES AND INDICES OF VARIOUS SHIP FORMS, AND COMPARISON WITH EXPERIMENTAL RESULTS

By Winnifred R. Jacobs

BuShips Fundamental Hydromechanics
Research Program (S-R009-01-01) Administered by DTMB
Contract Nonr 263(57) DL Project 2803/063

The analytical method of Ref. 1 for estimating stability derivatives, and hence stability on course, which combines Albring's empirical modifications of simplified flow theory with low aspect-ratio wing theory, is extended to take into consideration the effects on course stability of higher aspect-ratio fins as well. The method, which had

(over)


DAVIDSON LABORATORY Report 1035 (UNCLASSIFIED) Sept. 1964

ESTIMATION OF STABILITY DERIVATIVES AND INDICES OF VARIOUS SHIP FORMS, AND COMPARISON WITH EXPERIMENTAL RESULTS

By Winnifred R. Jacobs

BuShips Fundamental Hydromechanics
Research Program (S-R009-01-01) Administered by DTMB
Contract Nonr 263(57) DL Project 2803/063

The analytical method of Ref. 1 for estimating stability derivatives, and hence stability on course, which combines Albring's empirical modifications of simplified flow theory with low aspect-ratio wing theory, is extended to take into consideration the effects on course stability of higher aspect-ratio fins as well. The method, which had

(over)

DAVIDSON LABORATORY Report 1035 (UNCLASSIFIED) Sept. 1964

ESTIMATION OF STABILITY DERIVATIVES AND INDICES OF VARIOUS SHIP FORMS, AND COMPARISON WITH EXPERIMENTAL RESULTS

By Winnifred R. Jacobs

BuShips Fundamental Hydromechanics
Research Program (S-R009-01-01) Administered by DTMB
Contract Nonr 263(57) DL Project 2803/063

The analytical method of Ref. 1 for estimating stability derivatives, and hence stability on course, which combines Albring's empirical modifications of simplified flow theory with low aspect-ratio wing theory, is extended to take into consideration the effects on course stability of higher aspect-ratio fins as well. The method, which had

(over)

DAVIDSON LABORATORY Report 1035 (UNCLASSIFIED) Sept. 1964

ESTIMATION OF STABILITY DERIVATIVES AND INDICES OF VARIOUS SHIP FORMS, AND COMPARISON WITH EXPERIMENTAL RESULTS

By Winnifred R. Jacobs

BuShips Fundamental Hydromechanics
Research Program (S-R009-01-01) Administered by DTMB
Contract Nonr 263(57) DL Project 2803/063

The analytical method of Ref. 1 for estimating stability derivatives, and hence stability on course, which combines Albring's empirical modifications of simplified flow theory with low aspect-ratio wing theory, is extended to take into consideration the effects on course stability of higher aspect-ratio fins as well. The method, which had

(over)

BLANK PAGE

been applied in the earlier report to a family of eight hulls of 0.5 block coefficient, is tested further by application to eight Series 60 forms differing in block coefficient as well as in beam, draft, and displacement — with and without rudders; to an extreme vee modification of a Series 60 model; and to three other forms — a Mariner Class model, a destroyer, and a hopper dredge. Comparison with experimental results shows that the values of stability derivatives and indices determined by the analytical method are of the right orders of magnitude and indicate correct trends. Application to a variety of ship forms has demonstrated that the method can predict relative effects of changes in the geometry of a ship form, as well as the effects of changes in skeg and rudder area.

Keywords: Hydrodynamics, Maneuvering, Controllability

been applied in the earlier report to a family of eight hulls of 0.5 block coefficient, is tested further by application to eight Series 60 forms differing in block coefficient as well as in beam, draft, and displacement — with and without rudders; to an extreme vee modification of a Series 60 model; and to three other forms — a Mariner Class model, a destroyer, and a hopper dredge. Comparison with experimental results shows that the values of stability derivatives and indices determined by the analytical method are of the right orders of magnitude and indicate correct trends. Application to a variety of ship forms has demonstrated that the method can predict relative effects of changes in the geometry of a ship form, as well as the effects of changes in skeg and rudder area.

Keywords: Hydrodynamics, Maneuvering, Controllability

been applied in the earlier report to a family of eight hulls of 0.5 block coefficient, is tested further by application to eight Series 60 forms differing in block coefficient as well as in beam, draft, and displacement — with and without rudders; to an extreme vee modification of a Series 60 model; and to three other forms — a Mariner Class model, a destroyer, and a hopper dredge. Comparison with experimental results shows that the values of stability derivatives and indices determined by the analytical method are of the right orders of magnitude and indicate correct trends. Application to a variety of ship forms has demonstrated that the method can predict relative effects of changes in the geometry of a ship form, as well as the effects of changes in skeg and rudder area.

Keywords: Hydrodynamics, Maneuvering, Controllability

been applied in the earlier report to a family of eight hulls of 0.5 block coefficient, is tested further by application to eight Series 60 forms differing in block coefficient as well as in beam, draft, and displacement — with and without rudders; to an extreme vee modification of a Series 60 model; and to three other forms — a Mariner Class model, a destroyer, and a hopper dredge. Comparison with experimental results shows that the values of stability derivatives and indices determined by the analytical method are of the right orders of magnitude and indicate correct trends. Application to a variety of ship forms has demonstrated that the method can predict relative effects of changes in the geometry of a ship form, as well as the effects of changes in skeg and rudder area.

Keywords: Hydrodynamics, Maneuvering, Controllability

BLANK PAGE